

Elucidating the molecular function of CLUH in mammalian system

Inaugural-Dissertation

zur

**Erlangung des Doktorgrades
der Mathematisch-Naturwissenschaftlichen Fakultät
der Universität zu Köln**



**vorgelegt von
Jie (Jane) Gao
aus China
Köln 2015**

Berichterstatter

Prof. Dr. Elena Rugarli

Prof. Dr. Aleksandra Trifunovic

Tag der Mündlichen Prüfung: 04 May 2015

To my dear father, mother and husband
致我亲爱的父母与丈夫

Table of Contents

Abstract	7
1 Introduction	8
1.1 Mitochondria	9
1.1.1 Origin of mitochondria	9
1.1.2 Mitochondrial genome	9
1.1.3 Brief introduction of the mitochondrial function	11
1.2 Biogenesis of nuclear encoded mitochondrial proteins	15
1.2.1 Coordination between nucleus and mitochondria to ensure appropriate protein expression	15
1.2.2 Regulation of nuclear encoded mitochondrial proteins	17
1.2.3 Mitochondrial post-translational versus co-translational protein targeting and import.	17
1.2.4 The targeting and sorting sequence of mitochondrial proteins	19
1.2.5 TOM and the sorting machinery	21
1.3 mRNA localisation	22
1.3.1 mRNA localisation is an ubiquitous phenomenon	22
1.3.2 mRNA localisation to mitochondria	25
1.3.3 PUF3p	26
1.4 CLUH	28
1.4.1 Clu mutant leads to mitochondrial clustering and abnormal mitochondrial morphology	28
1.4.2 Clu mutants of multicellular organism display growth defects	30
1.4.3. Primary structure and the molecular function of Clu	32
2 Aim of the Thesis	36
3 Material and Method	37
3.1 Cell biology	38
3.1.2 Cell culture	38
3.1.3 Long-term galactose experiment	38
3.1.4 Short-term galactose and acetoacetate treatment	39
3.1.5 Bezafibrate treatment	39

3.1.6 RNA interference	40
3.1.7 Immunofluorescence and imaging	40
3.2 Molecular biology	42
3.2.1 Polymerase chain reaction (PCR) and agarose gel electrophoresis.....	42
3.2.2 Gel extraction, DNA extraction, DNA digestion and ligation	43
3.2.3 Bacterial transformation and colony selection	43
3.2.4 Generation of CLUH-FLAG and CLUH deletion HEK 293T cell lines.....	44
3.2.5 Crosslinking immunoprecipitation (CLIP) and RNA immunoprecipitation	45
3.2.6 RNA extraction	46
3.2.7 Reverse transcription and quantitative real-time PCR	46
3.2.8 RNA sequencing and analysis.....	48
3.3 Biochemistry	49
3.3.1 Protein extraction for western blot analysis	49
3.3.2 Protein quantification and preparation	49
3.3.3 SDS-PAGE, western blot analysis and quantification	50
3.3.4 Cell fractionation.....	51
3.3.5 Sucrose gradient and polysome profiling.....	52
3.3.6 Metabolic labeling and biotinylation of the newly synthesised proteins.....	53
3.4 Obtaining mouse tissues.....	53
3.5 Statistical analysis	54
4 Results	55
4.1 CLUH is coregulated with genes encoding mitochondrial proteins and involved in translation.....	56
4.2 CLUH is an RNA binding protein.....	57
4.3 CLUH preferentially binds to mRNAs encoded in the nucleus for mitochondrial proteins	59
4.4 Global analysis of the mRNAs bounds by CLUH	61
4.5 The mRNA of the cytosolic protein astrin is bound by CLUH.....	71
4.6 CLUH affects the protein level of its mRNA targets	71
4.7 CLUH overexpression upregulates the protein level of some of its targets	73
4.8 Global cytosolic translation is unaffected in the absence of CLUH	74
4.9 Translation of CLUH targets is affected	77

4.10 Localisation of CLUH.....	79
4.11 CLUH level in response to galactose and acetoacetate treatment.....	83
4.12 CLUH protein level is reduced in PGC-1 α deficient MEFs.....	88
4.13 CLUH levels in mouse liver during development and aging	90
4.14 Identification of the function of CLUH protein domains	92
5 Discussion	100
5.1 Elucidation of the molecular function of CLUH unravels the cause of Clu mutant phenotypes.....	101
5.2 Identification of the molecular function of CLUH could be a support for co-translational import	106
5.3 CLUH affects the levels of protein encoded by target mRNAs	107
5.4 Regulation of CLUH	109
5.4.1 Effect of galactose treatment on CLUH.....	109
5.4.2 CLUH level during acetoacetate	112
5.4.3 CLUHs level during different life stages in mouse liver.....	113
5.5 Conclusions	114
Zusammenfassung.....	115
Reference.....	117
Appendix	126
List of Abbreviations.....	138
Acknowledgement.....	139
Eidesstattliche Erklärung.....	141
Curriculum Vitae.....	142

Abstract

The mitochondrial proteome is composed of both mitochondrial and nuclear encoded proteins. Restructuration of mitochondrial proteome is often required upon on change in nutrient availabilities and stress conditions. To facilitate this process, the nuclear and mitochondrial genome must coordinate their protein expression in a well-concerted manner. Additional factors are present to mediate the coordination. These factors are diverse in function ranging from energy sensing to translation of the specific nuclear encoded mitochondrial proteins.

Clu is a well-conserved cytosolic protein, however its molecular function remains unknown. A small fraction of Clu is observed outside of mitochondria in *Drosophila*. Clu mutant of multicellular organisms display phenotypes of growth defect, failure to respond to stress and early death. However these phenotypes are absent from single cellular organisms. Nevertheless, all Clu mutants have clustered mitochondria and this leads to the speculation that CLUH and mitochondria are functionally closely related.

In this study, we analysed the genes that coregulate with human and murine *CLUH/Cluh*, respectively, and identified two main clusters of genes: nuclear encoded mitochondrial genes and cytosolic translation related genes. After this, we identified the molecular function of human CLUH as an mRNA binding protein by using crosslinking immunoprecipitation (CLIP). By comparing the mRNAs enriched by CLUH to control IgG, we discovered that CLUH binds specifically to mRNAs of nuclear encoded mitochondrial proteins (NEMP). Among the mRNAs bound by CLUH, we found enrichments for genes involved in branched-chain amino acid degradation, mitochondrial dysfunction, TCA cycle, oxidative phosphorylation and fatty acid α -oxidation. Subsequently, we showed that CLUH is a positive translation regulator of its target mRNAs, because in the absence of CLUH, translation of its target mRNAs appeared to be reduced. However, general translation was not affected in the absence of CLUH. Furthermore, we found a reduction of CLUH in PGC-1 α null mouse embryonic fibroblasts (MEFs), which indicates that CLUH expression might be under the transcriptional control of PGC-1 α . Together, we conclude that CLUH might be important for the biogenesis of its target proteins under influence of cellular metabolism.

1 Introduction

1.1 Mitochondria

1.1.1 Origin of mitochondria

Mitochondria were first observed and described with various names as early as the 1800s, when the German histologist Richard Altmann proposed that this cellular granule to be autonomous and forming colonies in the cytoplasm in his book “Die Elementarorganismen”. It took another seven decades to discover the existence of DNA in mitochondria (mtDNA) (Nass and Nass 1963) and another two decades to find the evidence that mtDNA is not originated from the host genome via invagination during evolution (Farrelly and Butow 1983). Altogether, these evidences strongly support the endosymbiotic theory, which explains that mitochondria arose as a result of either a singular or multiple events of fusion of α -proteobacterium and eukaryotic progenitor (Macklin 1927). To many respects, these original endosymbiotic events mark the rise of the eukaryotes since a nucleus-bearing living eukaryotes completely devoid of mitochondria has yet to be discovered (Williams, Hirt et al. 2002; Chan, Slotboom et al. 2005; van der Giezen and Tovar 2005). This cooperation allowed the expansion of eukaryotes due to the acquisition of the super energy-producing “plant”. Along the course of evolution, mitochondria have lost and transferred most of their genes to the nucleus (Adams and Palmer 2003) and mitochondria only retain a skeletal genome, relatively small compared to the bacterial ancestor and encoding only components of the mitochondrial translation machinery and of the oxidative phosphorylation (OXPHOS).

1.1.2 Mitochondrial genome

In human, the circular mtDNA is composed of only 16,569 base pairs. Despite the comparatively small size of this genome (only 1/3000th of the size of our smallest chromosome 21), mutation, deletion and depletion of mtDNA can lead to severe diseases. Human mitochondrial genome encodes for 37 genes including 22 tRNAs, two rRNAs and 13 polypeptides. The mtDNA is a double stranded molecule with cytosine-rich light strand and a guanine-rich heavy strand (Anderson, Bankier et al. 1981).

Unlike the nuclear genome, multiple copies of mtDNAs can be found per mitochondrion as a result of regulated replication and this condition is referred as polyploidy. Despite the existence of DNA repair systems in plant and mammalian mitochondria (Boesch, Ibrahim et al. 2009; Boesch, Ibrahim et al. 2010), high rate of mutations still occurs and leads to heteroplasmy (Dianov, Souza-Pinto et al. 2001). In such case, mitochondria will host a heterogeneous mix of healthy and mutated genomes, the specific threshold at which mutated genome exceeds the wildtype genome can determine the onset of mitochondrial dysfunction (Wong 2007). Since mtDNAs are maternally inherited, this condition can be prevented through three parents *in vitro* fertilisation or mitochondrial replacement therapy, in which the resulting embryo contains the nuclear genetic material from two parents and mitochondrial genetic material from a healthy female donor (Klitzman, Toyne et al. 2015).

mtDNA is not naked, instead, multiple copies are packed by proteins and form nucleoid structures. This is in contrast to the nucleosome, where DNA wraps around the histone complex (Table 1) (Taylor and Turnbull 2005). Nucleoids are not free floating in the matrix but associate with the inner mitochondrial membrane (Wang and Bogenhagen 2006; Holt, He et al. 2007). It is estimated that one nucleoid is capable of packing 5-7 copies of the mtDNA (Iborra, Kimura et al. 2004). The exact composition of the nucleoids as well as the very nature of the molecule or complex tethering the mtDNA to the mitochondrial inner membrane (IM) is still debated today (Kukat and Larsson ; Holt, He et al. 2007). The mtDNA copy number is subjected to tight regulation and failures to maintain the desired copy numbers lead to mtDNA depletion syndromes (MDS) (Macmillan and Shoubridge 1996; Choi, Kim et al. 2001; Blokhin, Vyshkina et al. 2008; Xing, Chen et al. 2008). MDS can be caused by mutations in both nuclear and mitochondrial genomes.

Mitochondria are not only involved in the aforementioned diseases but also have a possible role in the aging process. Indeed, the original Harman theory of aging postulated that the accumulation of free radical damage over time ultimately led to cellular aging (Harman 1956). While this theory became widely accepted, it has been challenged by work done on the mutator mice, in this model, aging and mutation load were studied in mice deficient in mtDNA repair mechanisms but free radicals did not

correlate with accumulation of mutations and aging (Trifunovic, Wredenberg et al. 2004).

Table 1: comparison between the human nuclear and mitochondrial genome (Taylor and Turnbull 2005)

Characteristic	Nuclear genome	Mitochondrial genome
Size	~3.3 x 10 ⁹ bp	16,569 bp
Number of DNA molecules per cell	23 in haploid cells; 46 in diploid cells	Several thousand copies per cell (polyploidy)
Number of genes encoded	~20,000–30,000	37 (13 polypeptides, 22 tRNAs and 2 rRNAs)
Gene density	~1 per 40,000 bp	1 per 450 bp
Introns	Frequently found in most genes	Absent
Percentage of coding DNA	~3%	~93%
Codon usage	The universal genetic code	AUA codes for methionine; TGA codes for tryptophan; AGA and AGG specify stop codons
Associated proteins	Nucleosome-associated histone proteins and non-histone proteins	No histones; but associated with several proteins (for example, TFAM) that form nucleoids
Mode of inheritance	Mendelian inheritance for autosomes and the X chromosome; paternal inheritance for the Y chromosome	Exclusively maternal
Replication	Strand-coupled mechanism that uses DNA polymerases α and δ	Strand-coupled and strand-displacement models; only uses DNA polymerase γ
Transcription	Most genes are transcribed individually	All genes on both strands are transcribed as large polycistrons
Recombination	Each pair of homologues recombines during the prophase of meiosis	There is evidence that recombination occurs at a cellular level but little evidence that it occurs at a population level

*Table modified from REF. 171 © (1999) John Wiley and Sons. TFAM, mitochondrial transcription factor A; rRNA, ribosomal RNA.

1.1.3 Brief introduction of the mitochondrial function

Mitochondria are present in virtually all eukaryotic cells, with the notable exception of the erythrocytes, which are also devoid of nuclei, Golgi and endoplasmic reticulum in mammals. They constantly undergo fusion and fission events to assist in content exchanges and protect against stresses (Chan 2006). Mitochondria are compartmentalised by two membranes composed of phospholipid bilayers (Figure 1): the two membranes, namely the outer membrane (OM) and inner membrane are separated by the intermembrane space (IMS) while the compartment enclosed by IM is referred as the matrix. IM infolds into the matrix and forms cristae. Cristae structure alters according to the respiratory state of mitochondria and apoptosis (Hackenbrock 1966; Scorrano, Ashiya et al. 2002; Frezza, Cipolat et al. 2006; Yamaguchi, Lartigue et

al. 2008). The OM is not considered as a potent membrane barrier due to the presence of a large, pore forming complex, the porin or voltage dependant anion channel (VDAC) which allows for the passive diffusion of molecules under 5000 kDa (Scheffler 2007). In contrast, the IM harbors many carriers and uniporters that selectively transport molecules such as ADP/ATP, Pi, NAD⁺/NADH, H⁺, Ca²⁺, Fe²⁺, Cu⁺, Zn²⁺, pyruvate, amino acids and many more (Kunji 2004). It is estimated that 39 carriers with different functions are present in the IM. Moreover, it also provides sites for the complexes of OXPHOS for ATP production.

The function of mitochondrial proteins are extremely diverse, including ATP production, type II fatty acid synthesis, fatty acids and amino acids oxidation, pyrimidine biosynthesis, calcium homeostasis, iron-sulfur cluster synthesis, urea cycle, ROS and heat production, apoptosis and viral defense response. Here I will only focus on pathways involved in direct ATP production (Scheffler 2007).

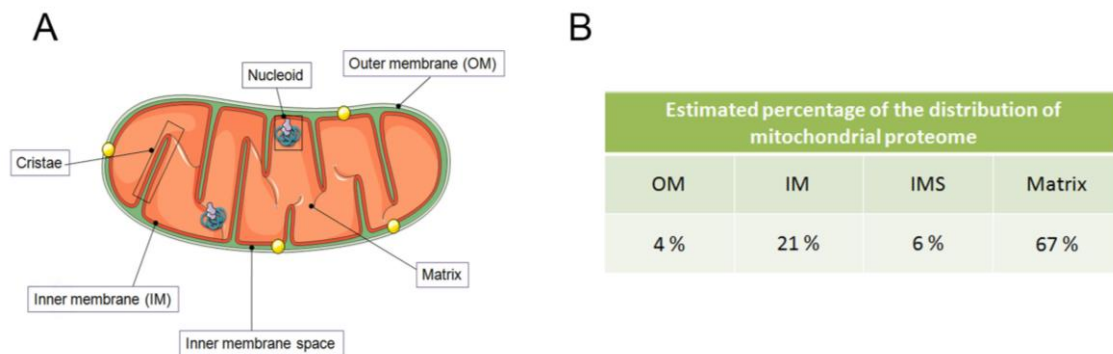


Figure 1: Mitochondrial compartment and proteome distribution (A) Schematic illustration of a mitochondrion. (B) Estimation of protein distribution across the compartments of mitochondrion, data extracted from Distler, 2008).

TCA cycle

Tricarboxylic acid cycle or TCA cycle is central for metabolism. It is in this pathway that the substrates derived from carbohydrates, fats and proteins are interconnected. TCA cycle utilises acetyl-CoA to form diverse metabolic chemicals, such as NADH, FADH₂, ATP (GTP), ubiquinone and other precursors. NADH and FADH₂ are then conveyed to the OXPHOS to create a proton gradient that generates ATP. The cycle

itself is generally controlled by the end product of each reaction. All protein components of the TCA cycle are encoded by the nuclear genome.

The TCA cycle provides many metabolites and precursors for the cellular activities. Oxaloacetate and α -ketoglutarate can be taken from the cycle by cataplerotic reaction to form amino acids, or they can be put back directly into the cycle by anaplerotic reactions. Glutamine, when provided externally, is transported into the matrix and converted to glutamate and subsequently α -ketoglutarate, and enters the TCA cycle. At the end of TCA cycle, oxaloacetate can be taken to yield aspartate and asparagine or alternatively, oxaloacetate is redirected to gluconeogenesis. Acetyl-CoA is essential to form fatty acid, ketone bodies, and cholesterol, while acetyl-CoA can be replenished back from these metabolites. The cycle is also important in providing acetyl-group required for post-translational modification. Succinyl-CoA from TCA cycle can combine with glycine to form δ -aminolevulinic acid (ALA). This is the initial reaction for heme synthesis and is catalysed by the mitochondrial ALA synthase.

Oxidative phosphorylation

OXPPOS is a metabolic process where ATP is produced from ADP and P_i by transferring electrons from NADH and $FADH_2$ to O_2 . This process requires the participation of the electron transport chain (ETC) and ATP Synthase (complex V), both are made up by nuclear and mitochondrial encoded proteins (Figure 2). The ETC is composed of four complexes, collectively known as oxidoreductases, which couple electron transport with translocation of protons across the IM to IMS (apart from complex II, which does not possess proton pumping activity).

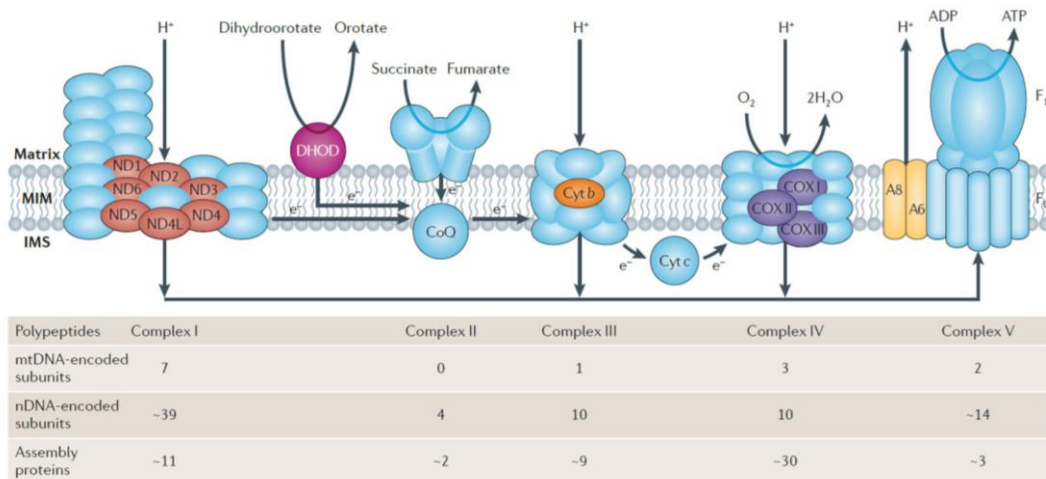


Figure 2: Distribution of nuclear encoded (nDNA, blue, except for DHOD) and mitochondrial encoded protein (other colours) in the OXPHOS in human (Schon, DiMauro et al. 2012)

Complex I, also known as NADH-ubiquinone oxidoreductase is the largest in size with 45 core subunits and an enormous amount of assembly factors, it forms an L shape complex in the IM (Diaz, Kotarsky et al. 2011). In this step, the electron carrier NADH generated from TCA cycle is oxidized to NAD^+ , generating four protons across the membrane. It is also the major source of reactive oxygen species inside mitochondria (Murphy 2009).

Complex II (succinate:ubiquinoneoxidoreductase, or succinate dehydrogenase) is the simplest complex of the ETC with only four subunits which are exclusively nuclear encoded in mammals. The two largest subunits SDHA and SDHB locate on the peripheral of the IM. Complex II also takes part in TCA cycle to facilitate conversion of succinate to fumarate. The resulting electrons are then transferred directly through complex II to ubiquinone in the ETC.

Complex III or ubiquinone-cytochrome c oxidoreductase, also known as cytochrome c reductase is another major source of reactive oxygen species production in mitochondria. Mammalian complex III consists of 11 subunits, however only three are functionally important since they are the only components of the bacterial counterparts, they are: cytochrome b (mtDNA encoded) cytochrome C_1 and the Rieske iron-sulfur protein.

Complex IV, the cytochrome c oxidase, catalyses the final electron transfers to H₂O with O₂ as the electron acceptor. It contains 13 subunits, three of the largest subunits are encoded by the mitochondrial genome (COX I, II and III) however around 30 factors are required for the assembly of this complex.

Complex V or ATP synthase utilises the proton gradient generated in the IMS to catalyse the phosphorylation of ADP to ATP. Complex V is a lollipop-like structure with a “head” facing the matrix and its “neck” inserted in the IM. The “head” is named F₁-ATP synthase and is made up of nine subunits: 3 α , 3 β , 1 γ , 1 δ , and 1 ϵ . The neck is F₀-synthase and consists of a subunit c-ring and a, b, d, F6 and the oligomycin sensitivity-conferring protein (OSCP). There are also other subunits associated with F₀: e, f, g and A6L. Two of the F₀ subunits are encoded by mtDNA: *ATP6* (a) and *ATP8* (A6L) (Anderson, Bankier et al. 1981) (Jonckheere, Smeitink et al. 2012)

Complexes I, III and IV are found to form specific respirasome (complex I + III + IV) and/or supercomplexes (complex I + III, complex III + IV) (Dudkina, Sunderhaus et al. 2008; Lapuente-Brun, Moreno-Loshuertos et al. 2013) while ATP synthase can dimerise and form long oligomeric chains. Moreover because of such formation, assembly of one complex can affect the other: for instance, complex I disassembles in the absence of complex III and IV (Scheffler 2007).

1.2 Biogenesis of nuclear encoded mitochondrial proteins

1.2.1 Coordination between nucleus and mitochondria to ensure appropriate protein expression

Because of the coexistence of nuclear and mitochondrial genomes, concerted coordination is required for the expression of nuclear and mitochondrial encoded proteins. For example, the OXPHOS houses nearly 80 subunits with only 13 being encoded in the mitochondria (Figure 2A). It is estimated that about 1500 proteins are present in a given mitochondrion depending on the sample type, purification method and detection sensitivity (Calvo and Mootha 2010). Moreover, mitochondrial protein expression pattern is tightly controlled in specific cell types depending on the metabolic

demand (Figure 3A and B) (Calvo and Mootha 2010) Therefore, mitochondria and nucleus need to constantly communicate with each other to monitor protein expression.

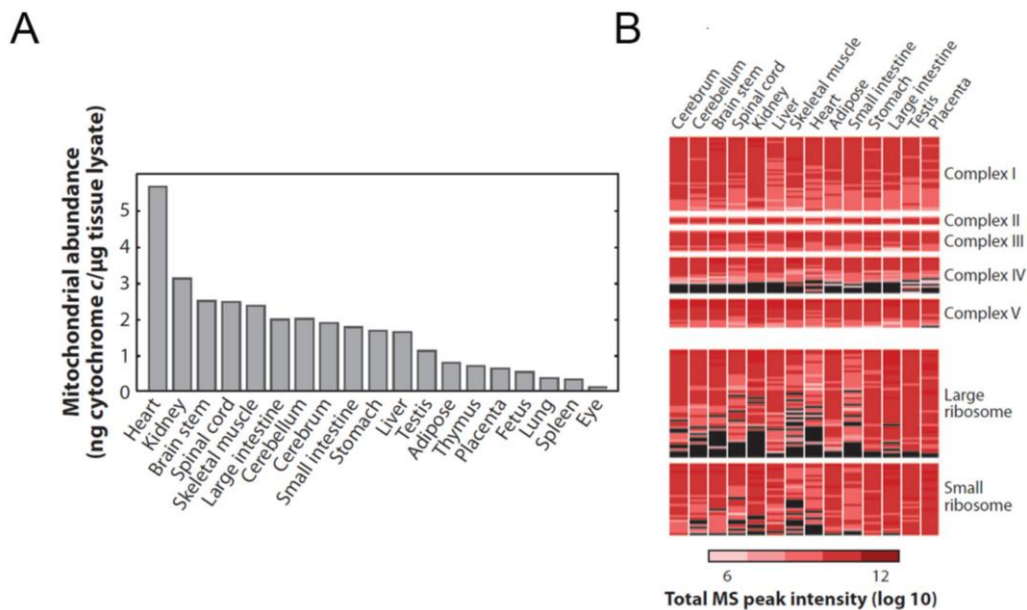


Figure 3: Mitochondrial proteome. (A) Mitochondrial abundance in tissues (B) Expression profile of the subunit of protein complexes in different tissues. Black indicates lack of detection whereas red is the level of abundance (Calvo and Mootha 2010).

There is an enormous amount of factors involved in the cross-talk processes, residing or shuttling in between mitochondria, cytosol and the nucleus. If we take the example of ATP production, mitochondrial function is monitored in terms of metabolites (pyruvate, NADH and ATP) derived from glycolysis, TCA cycle and the OXPHOS, respectively. During fasting, in the liver, the increase of pyruvate is coupled with an increased ratio of $\text{NAD}^+ : \text{NADH}$, this subsequently leads to post-translational upregulation of Sirt1 (a NAD^+ dependent deacetylase) in the nucleus (Rodgers, Lerin et al. 2005). In the meantime the ratio of AMP: ATP or ADP levels are monitored by AMP-activated protein kinase (AMPK) in the cytosol. When AMP:ATP ratio increases, AMPK is phosphorylated and induces a cascade of changes (Mihaylova and Shaw 2011). AMPK phosphorylation and Sirt1 activation can lead to the upregulation of the master

transcriptional coactivator: peroxisome proliferators-activated receptor γ coactivator 1-alpha (PGC-1 α). Consequently, this triggers the transcription induction of NEMPs such as OXPHOS components (Puigserver, Wu et al. 1998; Nunnari and Suomalainen 2012).

1.2.2 Regulation of nuclear encoded mitochondrial proteins

PGC-1 was first identified as a cold inducible activator of uncoupling protein 1 (UCP-1), which is important for energy dissipation in the brown fat cells. Under normal condition, PGC-1 is expressed in the heart, kidney, brown fat and brain but at very low level in lung, muscle, liver, white fat, testis and spleen (Puigserver, Wu et al. 1998). PGC-1 expression can be induced in the liver under fasting or diabetic condition (Yoon, Puigserver et al. 2001) or cold shock in brown fat and slow-twitch skeletal muscles (Puigserver, Wu et al. 1998). It interacts with various transcription factor partners, to name a few: peroxisome proliferator-activated receptor γ (PPAR γ), thyroid hormone receptor (TR), retinoic acid receptor (RA), estrogen receptors (Puigserver, Wu et al. 1998), PPAR α (Vega, Huss et al. 2000), PPAR β (Wang, Lee et al. 2003), nuclear respiratory factor 1 and 2 (Wu, Puigserver et al. 1999) and estrogen-related receptors α (ERR α) (Huss, Kopp et al. 2002; Schreiber, Knutti et al. 2003). Depending on the combination of the complexes, different set of genes can be activated: ERR α , PPAR α , PPAR γ and NRF-1, which regulates the transcription of genes involved in mitochondrial fatty acid beta-oxidation and oxidative phosphorylation and mtDNA transactions (Scarpulla 2002). All nuclear encoded proteins are translated in the cytosol, however whether they are localised to mitochondria before or after translation is still under debate, this is especially true for the NEMPs.

1.2.3 Mitochondrial post-translational versus co-translational protein targeting and import.

Two main mitochondrial protein targeting/import models exist (Figure 4): post-translational (Neupert and Herrmann 2007) and co-translational (MacKenzie and Payne 2007). In the former, the NEMPs are translated in the cytosol, unfolded by chaperons,

imported via the translocases of the outer membrane (TOM complex) and sorted to their respective destination. This mode of protein localisation and import to mitochondria relies on the presence of mitochondrial targeting signals which is also a determinant for mitochondrial protein sorting after passing TOM (Chacinska, Koehler et al. 2009). The mRNA, in this case, does not participate in the event of protein targeting to mitochondria. Evidences supporting post-translational import include: (1) Many precursor proteins can be made and imported into isolated mitochondria by *in vitro* protein import assays (Harmey, Hallermayer et al. 1977). (2) Not all nuclear encoded mRNAs are associated with mitochondria, many are present in the cytosol and associate with free polysomes (Marc, Margeot et al. 2002). (3) The order of protein translation dictates that all proteins have to be translocated from the N-terminal in co-translational model. This is challenged by protein with a non-canonical C-terminal targeting and sorting sequence.

On the other hand, the co-translational model suggests that localisation of mRNAs to the vicinity of mitochondria prior to their translation. After translation, the peptide emerges from the ribosome exit tunnel of the ribosome and is “captured” and “pulled” through the TOM complex. Therefore, in this case, mRNA targeting to mitochondria precedes protein localisation and is important for mitochondrial biogenesis. This model is supported by increasing evidence of (1) A fraction of NEMP mRNAs localise in the vicinity of mitochondria (Marc, Margeot et al. 2002). (2) Mitochondrial targeting sequence is not necessary to be a determinant for mitochondrial localisation of some proteins (Mukhopadhyay, Ni et al. 2004). In fact mRNA localisation is not only observed in mitochondria but also in peroxisomes and ER (Marc, Margeot et al. 2002; Pyhtila, Zheng et al. 2008; Zipor, Haim-Vilmovsky et al. 2009). When translation elongation is inhibited, ribosomes accumulate on the surface of mitochondria. Moreover the signal peptides are believed to be translated during mRNA transport and acting as a guide for path finding to the proper destination. Tom20, part of the TOM complex can mediate localisation of some mRNAs (Eliyahu, Pnueli et al. 2010; Kilchert and Spang 2011). It is, of course, possible that in nature, the two models coexist. Localisation of mRNAs and localisation of mRNA to mitochondria will be discussed further in the next chapter.

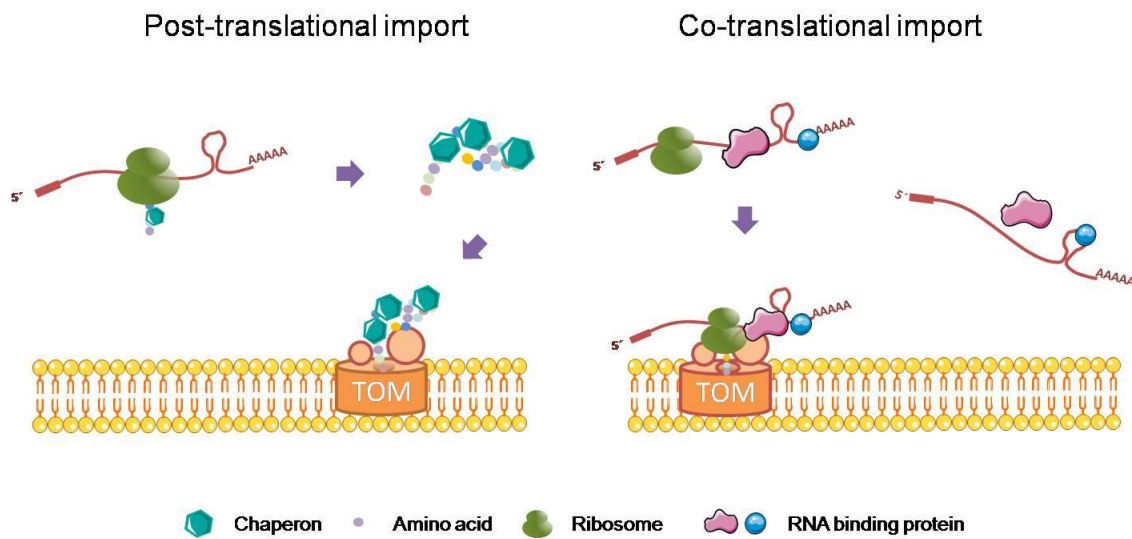


Figure 4: Protein targeting models. In post-translational model, protein targeting relies on the presence of mitochondrial targeting signals whereas co-translational model requires the targeting of mRNAs to the vicinity of mitochondria followed by localised translation.

1.2.4 The targeting and sorting sequence of mitochondrial proteins

The function of a protein dictates its conformation and location. Newly synthesised proteins must be sorted and folded correctly by the virtue of the other proteins as well as the intrinsic targeting signal that the new proteins possess (Table 2) (Chacinska, Koehler et al. 2009).

The best-known mitochondrial targeting sequence (MTS) is the cleavable amphipathic α -helix presequence at the N-terminal of a protein. This sequence can be up to 100 amino acids and is cleaved off by the matrix processing peptidase (MPP) after import. Therefore, it is used by most of matrix proteins. For some IM proteins, a hydrophobic segment is present after the amphipathic α -helix. This segment can halt further translocation of the preprotein and remains as a part of the mature protein. In contrast to some IMS proteins, the mature protein is formed after translocating through the IM, followed by cleavage by MPP in the matrix as well as cleavage of the hydrophobic IM insertion by inner membrane peptidase (Table 2 A).

None of the OM proteins possesses any of the aforementioned features mainly because they do not translocate the IM and reach the matrix, however large number of IM

proteins and IMS proteins do not have any cleavable targeting sequence. The targeting sequence of OM proteins can be found at the N-terminus, internal or the C-terminus (Table 2B) based on the topology of the proteins: α -helices with N-terminal, internal domain or C-terminal insertion into the membrane or β -barrel conformation. The IM contains many multi-spanning transmembrane metabolite carriers that harbor multiple intrinsic α -helix targeting signals. A number of IM proteins contain a presequence like structure with positively charged α -helices after hydrophobic stretch (Table 2B). IMS proteins embody mitochondrial intermembrane space signal (MISS) with a cysteine residue that can be recognised and sorted (Table 2C) (Chacinska, Koehler et al. 2009).

Table 2: Targeting and sorting signals present in nuclear encoded mitochondrial proteins (Chacinska, Koehler et al. 2009).

A	Presequences and variations	Imported via	Destination of proteins
	Presequence Amphipathic α helix Typically cleaved after import	TOM TIM23 PAM	Matrix
	Presequence + uncleaved hydrophobic anchor (sorting signal)	TOM TIM23 (PAM)	Inner membrane
	Presequence + cleaved hydrophobic sorting signal (bipartite presequence)	TOM TIM23 (PAM)	Intermembrane space
B	Noncleavable signals of hydrophobic proteins		
	β signal	TOM SAM	Outer membrane (β -barrel)
	Signal-anchor sequence	Mim1	Outer membrane (α -helical)
	C tail anchor	?	Outer membrane (α -helical)
	Internal signal	(TOM) (SAM)	
	Multiple internal signals	TOM Tim9-Tim10 TIM22	Inner membrane (metabolite carrier)
	Presequence-like internal signal (after hydrophobic region)	TOM TIM23	Inner membrane
C	Internal signal for intermembrane space		
	Cysteine-containing signal	TOM MIA	Intermembrane space

1.2.5 TOM and the sorting machinery

TOM complex is the entry gate of almost all nuclear encoded mitochondrial proteins. TOM is composed of 7 subunits: two receptors TOM70 and TOM20 and the general import core TOM40 (forms oligomeric β -barrel), TOM22, TOM7, TOM6 and TOM5 (Figure 5) (Model, Meisinger et al. 2008). TOM20 and TOM70 are the initial contact sites for preprotein with presequence and IM proteins, respectively. They are also important for the localisation of mRNAs in co-translational import model together with TOM7 (Eliyahu, Pnueli et al. 2010; Gadir, Haim-Vilmovsky et al. 2011). After the initial contact, the preproteins are then transferred to TOM22, TOM5, translocated through TOM40 to bind to the IMS domain of TOM22. From this point onward, preproteins are sorted to OM via the SAM (sorting and assembly machinery), to the IMS via MIA (mitochondrial intermembrane space assembly), to the IM via TIM 22 (transloase of the inner mitochondrial membrane) and to the matrix via TIM23 (Figure 5).

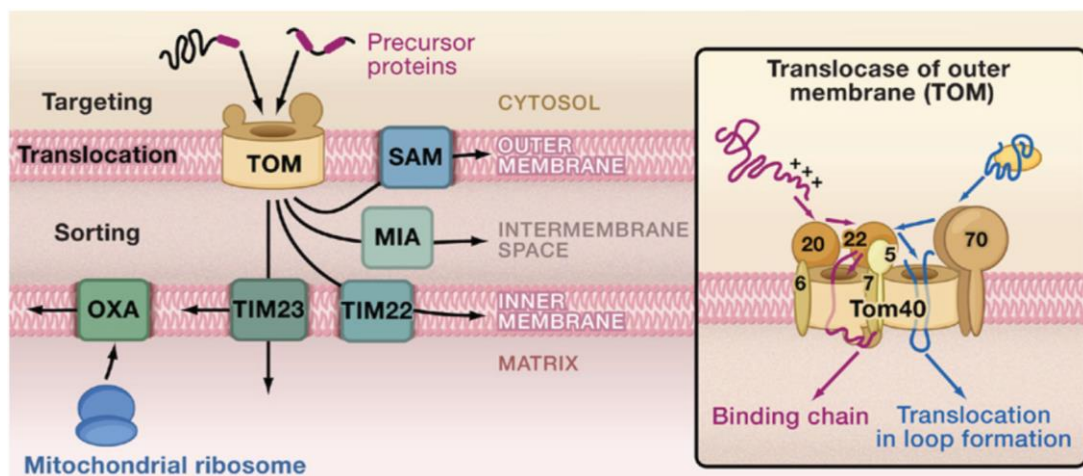


Figure 5: Mitochondrial protein sorting pathways. After entry through TOM, the precursor proteins are sorted into different compartments. OXA is the insertase of mitochondrial encoded IM protein (Chacinska, Koehler et al. 2009).

1.3 mRNA localisation

1.3.1 mRNA localisation is an ubiquitous phenomenon

mRNA localisation in the cell is evolutionarily conserved from single cell organism to multicellular systems and serves as a mean of stimuli-controlled local translation. This regulation ensures that the right amount of proteins can be made at the right time, in the right place with right conformation and post-translational modifications. In yeasts, to ensure that the daughter cells cannot switch mating types, *ASH 1* mRNA is transported to the daughter bud via myosin and actin prior to fission (Long, Singer et al. 1997). Tightly controlled compartmentalisation of mRNAs is observed during early *Drosophila* embryogenesis (Lecuyer, Yoshida et al. 2007). The mRNA of cytoskeletal elements: actin, vimentin and tubulin have been shown to localise to cell extremities, perinuclear and peripheral cytoplasm, respectively in chicken embryonic myoblasts and fibroblasts (Lawrence and Singer 1986). In highly polarised and specialised cell types such as neurons, many different types of mRNAs are found to be localised to direct the growth of axons (Zivraj, Tung et al. 2010) and dendrites (Kleiman, Banker et al. 1990).

Normally, functionally related mRNAs are bundled and translated coordinately and therefore can be efficiently controlled (Gerber, Herschlag et al. 2004; Keene 2007). This precise local translational control is favored over directly transporting protein, because (1) One mRNA can be translated to the exact desired amount of proteins according to demand. (2) Local translation provides rapid response to local demand when compared to protein localisation. (3) During protein transport, cellular stress could impose undesired damage to the protein. (4) For some hydrophobic membrane proteins, it can be energetically favorable to insert the protein while being translated to avoid misfolding and aggregation.

mRNA localisation is different from transport and it can be seen as a final step following the transportation of mRNA. mRNA protein complexes (mRNPs) are composed of mRNA, mRNA binding proteins or other associating proteins and proteins that connect the mRNP complex to cytoskeleton via motor proteins (Gagnon and Mowry 2011). As soon as the mRNAs are transcribed and spliced, they are sorted according to their destination with different protein compositions (i.e. RNP granules).

These granules are distinct from both stress or P granules in composition and function even though, general translation is halted in all cases (Anderson and Kedersha 2006; Anderson and Kedersha 2009).

Transport of mRNAs to their final destination is a result from two factors: the *cis*-acting RNA sequence and the *trans*-acting proteins (RNA binding proteins or RBP) that bind to the mRNAs.

Cis-acting RNA sequences, also known as "zipcodes", lie within the mRNAs and dictate the direction of transport, they could be in the 3'-UTR (for example, *ASH 1* and *β -actin*) (Bassell, Zhang et al. 1998; Chartrand, Meng et al. 1999), 5'-UTR (*kor*, mRNA of kappa opioid receptor) (Tsai, Bi et al. 2007), and even within the protein coding sequence (mRNA target of FMRP, loss of function mutation causes fragile X syndrome) (Darnell, Van Driesche et al. 2011). The coding message can be hidden either in a short or long stretch of nucleotides or multiple units scattered through the sequence. It can also be coded in its secondary structure. Different signals may even be employed at different stages of mRNA transport and localisation (Hervé, Mickleburgh et al. 2004). One representative of such complexity is the localisation of the mRNA of myelin basic protein (MBP) to myelin: it is firstly transported to the oligodendrocytes via a 21-nucleotide sequence in the 3'-UTR (RNA transport signal), followed by localisation to myelin compartment via a long stretch of nucleotides in 3'-UTR that forms a stable secondary structure (the RNA localisation region) (Ainger, Avossa et al. 1997). Another example is that the *bicoid* mRNA localisation to the anterior pole in *Drosophila* embryo requires two different *cis*-acting elements for early and late localisation and formation of double stranded helical structure to achieve the anchorage in the anterior cytoplasm (Ferrandon, Koch et al. 1997).

Trans-acting proteins are the other factor that dictates the transport and localisation of mRNAs. They bind to the *cis*-acting elements of the mRNAs, their binding or association depends on the life cycle of an mRNA: transport, localisation or anchorage. In cultured HeLa cells, approximate 860 proteins have been identified as RNA binding proteins, the actual number, however might be even more due to the stringent threshold of the analysis (Castello, Fischer et al. 2012). To complicate the matters further, one RBP is able to bind to hundreds of different mRNAs (Gerber, Herschlag et al. 2004) and

one RNA can be bound by numerous RBPs. For example, Staufen recognises the loop structure formed by two strands of different RNAs in the zipcode, its target mRNAs include *prospero* and *bicoid* in flies. The association between Staufen and its target mRNAs is location specific: anterior to the anchoring of *bicoid*, and posterior to the localisation of *oskar* (St Johnston, Beuchle et al. 1991; Ferrandon, Koch et al. 1997). Therefore, it is reasonable to extrapolate that the RNA granules are extremely dynamic structures that change in time, space and cellular stresses. It is believed that during transport, mRNA translation is inhibited and mRNA is stabilised/protected and only become activated when reaching its destination (Abaza and Gebauer 2008; Besse and Ephrussi 2008).

Proper localisation of mRNAs in either polarised or less polarised cells is an essential feature to determine the morphogenesis and development. However, mRNAs are also localised to different organelles (Weis, Schleiff et al. 2013). For example, the mRNAs for secretory, integral proteins and some cytosolic proteins are localised to the ER prior to complete translation, the signal recognition particle (SRP) pathway. After the release of mRNP into the cytosol, the complex is bound by ribosomes and a small length of polypeptide (signal peptide) is translated. Together this forms ribosome mRNA-nascent polypeptide complexes (RNCs) that can be recognised by the SRP. At the ER, SRP receptor recognises RNC-SRP, RNC stalks at the translocation channel and continues the translation while the nascent chain is “pulled” inside of the ER (Figure 6A) (Nicchitta, Lerner et al. 2005). However this classical co-translational model is also challenged by other models where the *cis*-acting element is important for localisation to the surface of ER instead of the SRP (Figure 6B).

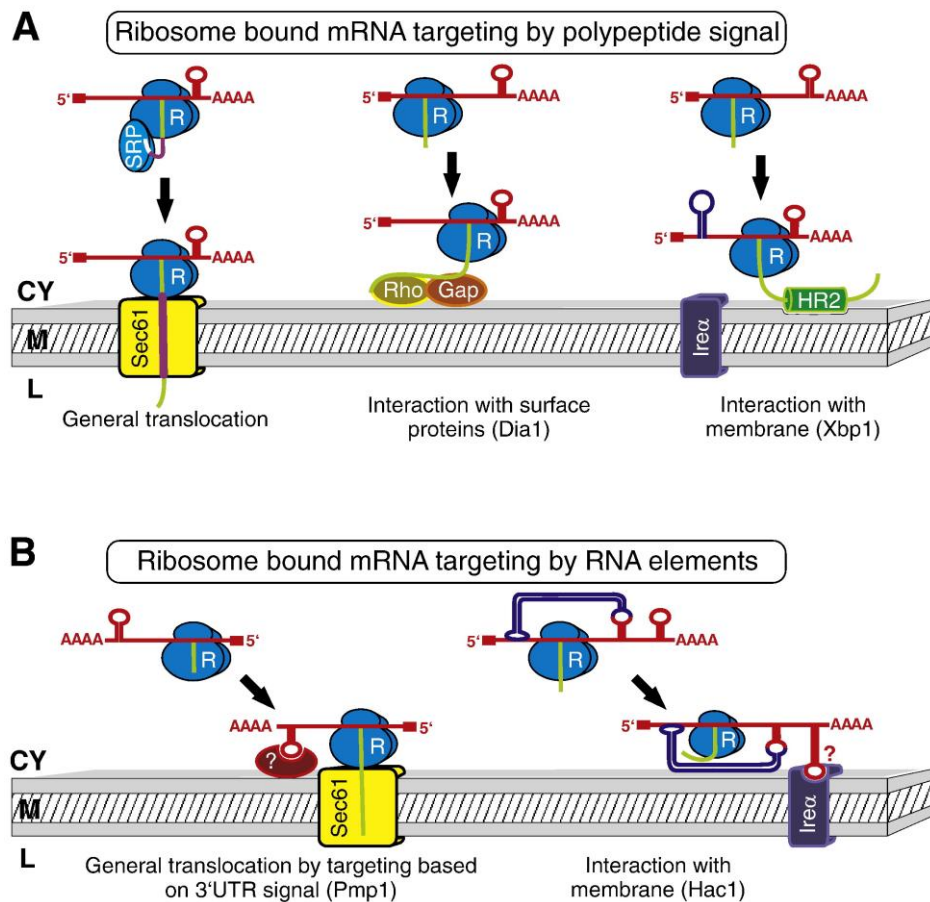


Figure 6: mRNA localisation to the ER. (A) Three forms of mRNA localisation mediated by the signal peptide. (B) mRNA localisation imposed by the *cis*-acting element of the mRNA together with ribosomes (Weis, Schleiff et al. 2013).

1.3.2 mRNA localisation to mitochondria

This brings us to the question of whether a similar mRNA localisation pathway also occurs in the mitochondria. The vast majority of the work on mRNA localisation to mitochondria was carried out in yeast owing to ease in manipulation, however this is also observed in mammalian cells (Matsumoto, Uchiumi et al. 2012; Gehrke, Wu et al. 2015). First of all, ribosomes are found to locate on the surface of mitochondria (Kellems and Butow 1972; Keyhani 1973). Secondly, about 500 mRNAs were estimated to reside close to mitochondria. Furthermore, the authors show that the localised mRNAs are likely to be ancient with bacterial origins (Marc, Margeot et al. 2002; Saint-Georges, Garcia et al. 2008). The association of mRNA in the vicinity of mitochondria requires the presence of protein import machinery, the *cis*-acting

sequences and the RBP (Eliyahu, Pnueli et al. 2010; Gadir, Haim-Vilmovsky et al. 2011). The best-studied mRNA binding protein involved in localisation of NEMP mRNA is the yeast PUF3p.

1.3.3 PUF3p

The yeast PUF3p is one of the six PUFs (Pumilio and FBF) with known RNA binding domains. Members of this family are well conserved from yeast to human and can recognise the specific sequence at the 3'-UTR in order to regulate mRNA localisation, translation and stability (Wickens, Bernstein et al. 2002). Yeasts contain five PUFs, *Drosophila*, one, mammals, two. The RNA binding motif of RBP and the RNA signature for binding of the targets are also well conserved (Wickens, Bernstein et al. 2002). The RNA binding domain of PUF proteins are PUM-HD-type which forms an arc-like shape that can interact with both RNA and protein (Zamore, Williamson et al. 1997; Zhang, Gallegos et al. 1997). Members of this protein family display different functions, they can either suppress or activate translation or involved in targeting mRNA to subcellular localisation/organelle (Murata and Wharton 1995; Sonoda and Wharton 1999). In *Drosophila*, PUMILIO can repress the translation of *hunchback* during early embryogenesis. Yeast Puf6p can regulate both localisation and translation of *ASH1* for mating type switching while Puf5p can affect the localisation of *PEX14* to peroxisomes (Wreden, Verrotti et al. 1997; Zipor, Haim-Vilmovsky et al. 2009).

Puf3p binds preferentially to approximately 162 mRNAs of NEMPs in yeast to facilitate localisation and co-translational import. The protein products of these mRNAs are involved in mitochondrial protein synthesis, structural components of the ribosome, tRNA ligases, OXPHOS and translational regulators (Huh, Falvo et al. 2003; Gerber, Herschlag et al. 2004). Puf3p is also found to be a component of P-body under stress (Lee, Dudley et al. 2009; Eliyahu, Pnueli et al. 2010). In the absence of Puf3p, the target mRNAs mislocate (Olivas and Parker 2000; Saint-Georges, Garcia et al. 2008; Eliyahu, Pnueli et al. 2010). Puf3p associate with mitochondria via binding to Mdm12, the component of ER-mitochondria encounter structure (Garcia-Rodriguez, Gay et al. 2007).

One would expect that Puf3p could be important for mitochondrial biogenesis regarding its molecular function, however in reality, it is more complicated. Mitochondrial biogenesis and Puf3p reduction occur at the same time, and both overexpression and deletion lead to impairment in respiratory growth (Gerber, Herschlag et al. 2004; Garcia-Rodriguez, Gay et al. 2007; Saint-Georges, Garcia et al. 2008; Eliyahu, Pnueli et al. 2010). Puf3p activity is dependent on the carbon source without alteration in transcript or protein level. (Gerber, Herschlag et al. 2004; Foat, Houshmandi et al. 2005). Furthermore, Puf3p is essential for the growth of TOM20 mutant yeast in glycerol. In the absence of TOM20, *puf3* mRNA increases and so is its protein level, however Puf3p associates less with the mitochondria (Eliyahu, Pnueli et al. 2010). Moreover mitochondria in $\Delta puf3$ are fragmented and aggregated with impaired anterograde movement (Garcia-Rodriguez, Gay et al. 2007). Based on these observations, it is suggested that Puf3p exists as two pools: mitochondrial and non-mitochondrial. Puf3p on mitochondria localises and tethers the mRNAs to mitochondria. Non-mitochondrial Puf3p locates in the cytoplasm and may inhibit translation when mitochondrial biogenesis is not required (Garcia-Rodriguez, Gay et al. 2007; Quenault, Lithgow et al. 2011).

It is worth remembering that Puf1p also localises to mitochondria and facilitates the association of mitochondria to Arp2/3 complex of actin in yeast (Moreau, Madania et al. 1996). There are two Pumilio homolog (*PUM1* and *PUM2*) in human (Spasov and Jurecic 2002; Galgano, Forrer et al. 2008). *PUM2* knockout mice displays smaller testis but without obvious effect on fertility (Xu, Chang et al. 2007). The mRNA targets of *PUM1* shares little similarity to Puf3p or Pumilio and is not enriched for NEMP (Gerber, Herschlag et al. 2004; Gerber, Luschnig et al. 2006; Morris, Mukherjee et al. 2008) despite the conservation of the protein binding domain and RNA motif. There is no protein with similar role to Puf3p that has been identified so far in mammalian system. Furthermore, it is unclear if mRNA localisation to mitochondria occurs at all in the mammalian system.

1.4 CLUH

1.4.1 Clu mutant leads to mitochondrial clustering and abnormal mitochondrial morphology

Clu stands for clustered mitochondria and is well conserved from amoeba to human (see the gene and protein annotations in Table 3). For the sake of simplicity, all homologs mentioned below will be referred as Clu when general function is introduced. Its name originated from the phenotype of mitochondrial clustering after *clu* is deleted. CluA was first identified in 1992 as an unconventional myosin in *Dictyostelium* because of its cross-reactivity with the antiserum specific for myosin-IC (Zhu and Clarke 1992). However it neither possesses any myosin like activity nor shares significant homology to myosin (Zhu, Hulen et al. 1997).

Table 3: Annotation of *clu* genes and proteins in different organisms.

Organism	Gene	Protein	Amino acid
<i>Dictyostelium discoideum</i>	<i>cluA</i> ID: 8628948	CluA XP_629429	1320
<i>Saccharomyces cerevisiae</i>	<i>CLU1, TIF31</i> ID: 855025	Clu1p, p135 NP_013725	1277
<i>Arabidopsis thaliana</i>	<i>AT3G52140</i> <i>noxy38</i> NM_001203139.1	Tetratricopeptide repeat (TPR) containing protein, FREINDLY, NP_001190068	1419
<i>Drosophila melanogaster</i>	<i>Clueless</i> ID: 36793	Clueless NP_611095.1	1448
<i>Mus musculus</i>	<i>Cluh</i> ID:74148	CLUH NP_001074627	1353
<i>Homo sapiens</i>	<i>CLUH</i> ID:23277	CLUH NP_056044.3	1347

In *Dictyostelium*, when *cluA* is deleted, mitochondria cluster at the cell center while peroxisomes and ER remain morphologically unchanged (Zhu and Clarke 1992; Fields, Arana et al. 2002). Disruption of microtubules or actin filaments, does not affect the distribution of existing mitochondria (i.e. mitochondria that were already transported to the positions) (Fields, Arana et al. 2002). Mitochondria within the cluster are free to undergo deformation and rearrangement, however, individual mitochondrion appears to

have constrained movement. Half of the *CluA* mutants are multinucleated, indicating a failure in cytokinesis.

Yeast mitochondria in *clu1Δ* cells were condensed and accumulated on one side of the cell. However, the inheritance of functional mitochondria to daughter was not affected. No multinucleated cells were observed in yeast mutants. Interestingly, yeast Clu1p (sharing only 50 % similarity in primary structure to CluA) can correct the cytokinetic defect in *Dictyostelium cluA⁻* cells to wildtype level. However it can only partially rescue the mitochondrial clustering phenotype in *cluA⁻* cells: Clu1p complemented mitochondria were dispersed in the cytoplasm but in the form of small aggregates (Fields, Conrad et al. 1998). The *Arabidopsis* homolog friendly mitochondria (*FMT*, also known as *noxy 38* or *friendly*) also gave rise to clustered mitochondria (Logan, Scott et al. 2003; Vellosillo, Aguilera et al. 2013; El Zawily, Schwarzlander et al. 2014). However only a portion of total mitochondria were clustered, others resemble mitochondria in the wildtype cells. Consistent with the observation in *Dictyostelium*, other organelles in *Arabidopsis* mutant are not affected morphologically (El Zawily, Schwarzlander et al. 2014). Importantly, two *fnt* mutations were studied and both led to aggregated (clustered) mitochondria. *Fnt* mutant identified by Logan and colleague contains G-to-A mutation of the first base of the second intron and this result in almost complete absence of the respective transcript. In contrast, Vellosio and colleague's *noxy38* mutant contains G-to-A transition in the last nucleotide of intron 22. This transcript is translated into a truncated protein (1053 amino acids) without the TPR domains (see more information of this domain later).

In *Drosophila clueless* mutants, mitochondria clustered in the anterior region of germline stem cells, mitotic germline stem cells, old germ cells, stage 5 nurse cells, somatic follicle cells and neuroblast cells (Cox and Spradling 2009; Sen, Damm et al. 2013). Mitochondrial clusters were present in microtubule plus end (Cox and Spradling 2009). Moreover, the electron microscope (EM) data showed swollen mitochondria with loss of cristae in the 3-days old flight muscles and ovaries. Sperm from sterile male mutants was immobile and the spermatide mitochondria derivative was irregular and swollen. Most interestingly, the fly mutant with double heterozygous *park* (gene associates with Parkinson's) and *clu* leads to clustered mitochondria suggesting that

these two proteins genetically interact. The clustering phenotype of mitochondria was also observed in mouse, monkey and human cells (Gao, Schatton et al. 2014).

Analyses were conducted to understand mitochondrial clusters. The EM images of mitochondria from *cluA*⁻ cells displayed interconnection between neighboring mitochondria. This observation suggests a failure of mitochondrial fission at a very late stage (Fields, Arana et al. 2002). However, interconnected mitochondria were not observed in the other organisms. The clustered mitochondria in *Arabidopsis* did not have interconnected OM between mitochondria (Logan, Scott et al. 2003; El Zawily, Schwarzlander et al. 2014). However, electron dense regions were observed between individual mitochondrion within a cluster of the mutant.

The cytoskeleton in all Clu mutants appeared to be intact and functional (Zhu and Clarke 1992; Fields, Arana et al. 2002; Cox and Spradling 2009). Moreover mitochondrial transport was unaffected (Cox and Spradling 2009; El Zawily, Schwarzlander et al. 2014). Deletion of Clu did not affect the transport and accumulation of mitochondria to Balbiani bodies (Balbiani body is a collection of organelles, mRNA and inclusions present in the early oocyte of all animals, it is normally close to the nucleus.). In *friendly* mutant, small mitochondrial aggregates as well as individual mitochondrion could be transported on actin. Altogether, these evidences indicate that mitochondrial clustering phenotype is independent of cytoskeletal alteration and defects in mitochondrial transport. It is postulated that the clustering phenotype might be caused by prolonged association between mitochondria (El Zawily, Schwarzlander et al. 2014).

1.4.2 Clu mutants of multicellular organism display growth defects

Clu function is not essential for single cellular organisms. *Dictyostelium cluA*⁻ mutant displayed a moderate reduction for growth that could be caused by unequal distribution of mitochondria after cell division (Zhu, Hulen et al. 1997). Yeast *clu1*Δ mutants showed no defect in growth in non-fermentable media (glycerol, lactate and ethanol), glucose media, heat and osmotic stress (Fields, Conrad et al. 1998). No signs of failure in cell wall synthesis or mitochondrial membrane potential were observed in yeast. It

was not even considered to be an essential gene in yeast, since *TIF31* mutant could still grow at temperatures higher or lower than 30°C (Vornlocher, Hanachi et al. 1999).

Arabidopsis Friendly mutant leaves were smaller, shorter and more rounded than the wildtype (El Zawily, Schwarzlander et al. 2014). The length and width of root were significantly reduced and this might due to increased cell death. Along with this, the mutant root displayed increased number and size of acid vacuoles (El Zawily, Schwarzlander et al. 2014). Interestingly, the *noxy38* mutant was more susceptible to pathogen invasions (Velloso, Aguilera et al. 2013).

Despite the clustering phenotype during development, the fly *clueless* mutants strived to adulthood. However, there was a prolonged larval development. At the end, only 40 % of the pupae can manage to eclose (Sen, Damm et al. 2013). These flies then developed phenotypes similar to *park* and *pink1* mutants: short lifespan, small size, uncoordination, sterility, flight muscle defects (wings up and down) and problems with utilising larval fat body in the new adults (Cox and Spradling 2009) (Goh, Zhou et al. 2013). Clu was highly expressed in neuroblasts but functionally dispensable (Goh, Zhou et al. 2013; Sen, Damm et al. 2013). In Clu mutant neuroblasts, mitochondria were not evenly segregated into the daughter cells. However, this did not have any impact on cell development or mitochondrial numbers.

Little is known regarding the function of *clu1* in *C. elegans*, however genomic RNAi studies revealed that *clu-1* mutant is embryonic-lethal (6 %, 24 hours recovery after soaking the worms with RNAi) (Maeda, Kohara et al. 2001). Interestingly, mitochondria are not clustered in *C. elegans* (Logan, Scott et al. 2003). However, it is not clear if the above RNAi data on *C. elegans* can be correlated.

1.4.3. Primary structure and the molecular function of Clu

The structure and molecular functions of Clu proteins are unknown, however provisional bioinformatics studies show that all Clu homologs share similar domains arrangement: CLU_N domain also known as TIF31-like, GSKIP domain, CLU domain, eIF_p135 (or Clu_central) domain and finally the TRP domain (Figure 7).

The nomenclature of TIF31 and eIF_p135 domain was based on the finding of Vornlocher *et al.* that TIF31 co-purified with eukaryotic translation initiation factor eIF3 (Vornlocher, Hanachi *et al.* 1999). However, deletion of TIF31 affected neither the function of eIF3 nor the global cytosolic translation. Moreover, TIF31 is neither always associated with eIF3 complex nor identified in eIF3 complex in human or plant (Browning, Gallie *et al.*). Consequently, Clu is not considered as part of the core eIF-3 complex despite its interaction with p33 (or TIF35, eIF3G, an essential eIF3 subunits) in yeast. There is no evidence so far that Clu plays any roles in translation.

The TPR motif contains degenerate sequences and proteins with these repeats act as scaffolds for the assembly of multicomplexes or protein-protein interactions. As mentioned before, truncated FMT protein without the TPR domains can lead to mitochondrial clustering phenotype. Moreover, FRIENDLY protein is subjected to post-translational modification, it contains two acetylation sites Lys-1022 and Lys-1029 which is located in between eIF_p135 and TPR domains (Finkemeier, Laxa *et al.* 2011; El Zawily, Schwarzlander *et al.* 2014). The acetylation status of FRIENDLY might be involved in mitochondrial clustering and other functions.

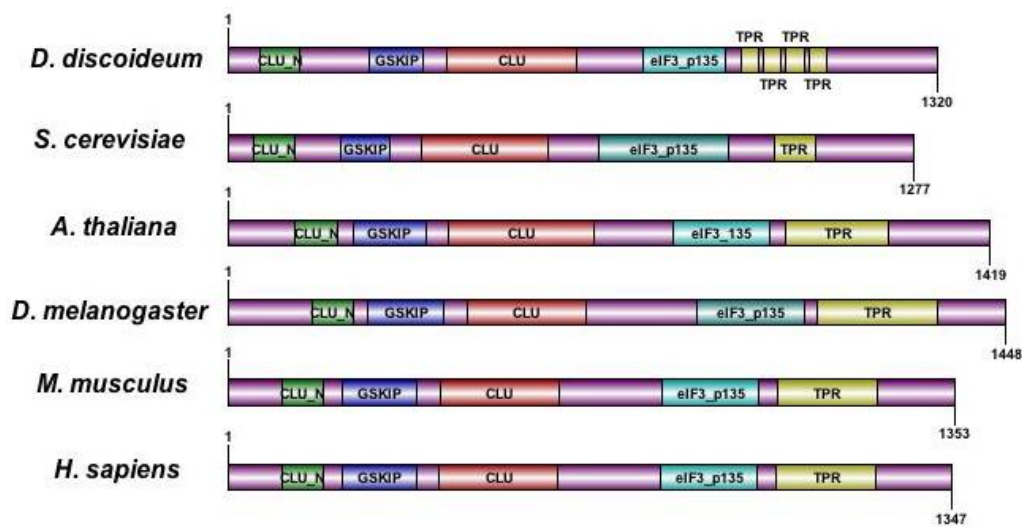


Figure 7: Illustration of the predicted protein domain of CLUH. CLU_N domain is also known as TIF31-like, eIF_p135 domain is also known as CLU-central. Protein domain information obtained from NCBI Conserved domains and InterPro from EMBL-EBI (for GSKIP domain). Protein domains are annotated with DOG (Ren, Wen et al. 2009).

It is also interesting to note that the mRNA level of *cluA* is elevated from the vegetative stage to the developing stage of the cell (Zhu, Hulen et al. 1997).

Clu locates in the cytoplasm as discrete puncta / granule (Fields, Conrad et al. 1998; Fields, Arana et al. 2002; Cox and Spradling 2009; Gao, Schatton et al. 2014). Some Clueless particles were observed outside of mitochondria, while some other associated with microtubules. However it is not clear if Clueless particles, mitochondria and microtubules colocalise (Cox and Spradling 2009). The ovary microtubule network in *clueless* mutants remained undisrupted. Deletion of Clu in flies and mammalian cells led to reductions of a subset of mitochondrial proteins (Cox and Spradling 2009; Gao, Schatton et al. 2014).

Transcriptome studies of Clu mutants indicated mitochondrial dysfunction. Gene expression study of the mild *clueless* mutant (with low expression level of Clu) showed downregulation of genes involved in reactive oxygen species protecting agents, DNA repair, apoptosis regulator and fatty acid production regulator. Some candidate metabolic genes involved in amino acid/fatty acid transporter, putative choline transporter and putative aminoadipate-semialdehyde were upregulated (Cox and Spradling 2009). Transcriptome analysis in *Arabidopsis* indicates alteration in genes

involved in protein synthesis, degradation, photosynthesis, photosynthetic light reaction, abiotic stress, redox and TCA cycle (El Zawily, Schwarzlander et al. 2014).

Biochemical analysis of the mutants in different organisms also suggests defects in mitochondria. In *Arabidopsis*, mutation induced the upregulation of the alternative oxidase pathway without affecting the average oxygen uptake (Velloso, Aguilera et al. 2013; El Zawily, Schwarzlander et al. 2014). AOX directs reduction of oxygen with the electrons donated from ubiquinol. Therefore, it reduced the total electron flow to complex III and the eventual production of ATP. Similarly, *clueless* adult mutants displayed severely reduced level of ATP as well as aconitase activity. However both phenotypes were absent in the mutant larvae.

Investigation of the neuroblasts of *Clueless* mutant showed that Clu was important for the asymmetric cell division of neuroblasts. Neuroblast asymmetric cell division generates one big daughter neuroblast cell and another small ganglion mother cell. These two cells inherit different materials including cell fate determinants Numb and Miranda. Numb and Miranda are positioned to the basal cortex of neuroblasts before mitosis. After cell division, they are inherited by ganglion mother cell. Positioning of the cell fate determinants is achieved by phosphorylation conducted by the Par complex. Par complex is composed of atypical protein kinase C (aPKC), Defective 6 (Par6) and Bazooka. In interphase, Par6 and aPKC are associated with lethal giant larvae (Lgl). It is proposed that aPKC/Baz/Par6 (active) complex is in equilibrium with aPKC/Lgl/Par6 (inactive) complex in the apical cortex to direct the phosphorylation of cell fate determinants Miranda and Numb. Phosphorylation of these proteins results in exclusion of their apical position. Interestingly, a small portion of neuroblast mutant cells displayed mislocalised Miranda during metaphase. Clu was mainly if not exclusively present in the neuroblasts throughout asymmetric cell division (Goh, Zhou et al. 2013; Sen, Damm et al. 2013). In addition, Clu coimmunoprecipitated with aPKC and Baz but not Lgl. *Lgl* mutant also led to mislocalisation of Miranda and Numb to a large extent and mislocalisation could be rescued by depleting *clu* or *park*. The author concluded that the function of *park* and *clu* is likely to be independent from mitochondrial function during neurogenesis (Goh, Zhou et al. 2013). However according to Sen and colleagues, the number of neuroblasts in *clu* mutant were comparable to the wildtype and neurons

can differentiate properly. Therefore it is still unclear why neuroblasts require high expression level of Clu.

In spite of mitochondrial clustering phenotype, Clu is a cytosolic protein and might be located in close proximity to mitochondria (Cox and Spradling 2009). The relationship between clu and mitochondria remains to be elucidated.

2 Aim of the Thesis

Mitochondria are indispensable organelles to support the normal function of cells in all eukaryotic systems, including mammals. The status of mitochondria in response to metabolic alteration and signaling is vital for cell survival. It is well established that mitochondrial biogenesis requires concerted coordination between the nuclear and mitochondrial genomes. This process demands the participation of armies of factors: transcriptional regulators, transcriptional factors, mRNA export of nucleus, mRNA transport and localisation, translation, post-translational modification, protein folding, and protein import to mitochondria.

Accumulated evidences in different organisms indicate the important relationship between Clu and mitochondria. Clu is a well-conserved cytosolic protein with a similarly conserved peculiar mitochondrial clustering phenotype, yet its function remains to be elucidated. Despite being a cytosolic protein, Clu is proposed to be involved in regulating mitochondrial position in response to physiological changes. A small portion of Clu is observed in close proximity to mitochondria. It can affect the protein levels of OXPHOS while genetically interacting with *Park* in *Drosophila*. In yeast, Clu copurifies with eIF3, however it is not an essential components of the cytosolic translation machinery.

The aim of this project is to investigate the molecular function of CLUH in mammalian system in order to address the following questions: (1) what is the molecular function of CLUH? (2) What is the relationship between CLUH and mitochondria? (3) How is CLUH regulated transcriptionally and in respect to cellular alterations?

3 Material and Method

All chemicals used in this study were purchased from Merck, Sigma-Aldrich, Serva or Roth unless stated otherwise.

3.1 Cell biology

3.1.2 Cell culture

Mouse embryonic fibroblasts (MEFs) and HeLa cells were cultured in DMEM (Life Technologies, 11960085), supplemented with 10 % FCIII (HyClone, FetalCloneIII, SH30109.03, Life Technologies), 2 % penicillin-streptomycin (Life Technologies, 151401232), and 2 mM L-glutamine (Life Technologies, 25030024). NSC34 cells (Cashman, Durham et al. 1992) were cultured in DMEM, supplemented with 10 % defined FBS (Life Technologies, SH30070.03), 2 % penicillin-streptomycin, and 2 mM L-glutamine.

HEK 293T cells were maintained in media containing DMEM, 7.5 % tetracycline-free fetal bovine serum (Biochrom AG, S0115), 1 mM sodium pyruvate (Life Technologies, 1136-070), 1x non-essential amino acids (Life Technologies, 1140-035), 2 mM L-glutamine and 1.5 mg/ml of hygromycin (Invivogen, ant-hm-5) and 150 µg/ml of blasticidin (Invivogen, ant-bl-5b). 1 µg/ml of tetracycline (dissolved in ethanol) was used to induce protein expression.

PGC-1 α MEFs were kindly provided from Dr. Tina Wenz. The embryos were collected at E12.5, and immortalized using the classic 3T3 protocol. PGC-1 α knockout mice were obtained by breeding PGC-1 α floxed (<http://jaxmice.jax.org/strain/009666.html>) with a full body Cre-deletor mouse line.

Cluh knockout MEFs were prepared by Dr. Henriette Hansen.

3.1.3 Long-term galactose experiment

The scheme of the galactose experiment is provided below (Figure 8). In general, HeLa cells were cultured in galactose media containing DMEM (glucose free, Life Technologies,

11966-025), 10 % dialysed serum (Life Technologies, 26400-036) 1 mM sodium pyruvate; 6 mM galactose and 2 % penicillin-streptomycin). Galactose media were changed every 24 hours.

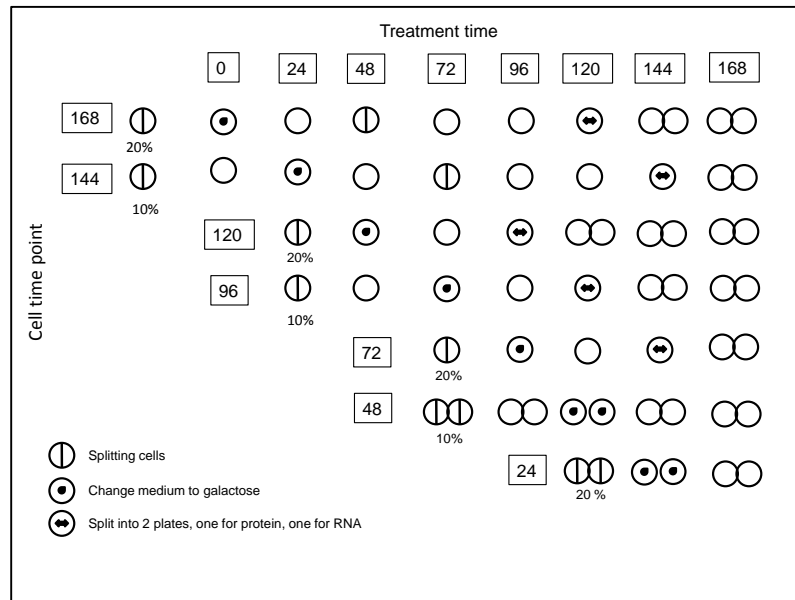


Figure 8: Experimental scheme of long-term galactose treatment.

3.1.4 Short-term galactose and acetoacetate treatment

The treatment was performed by Dr. David Pla-Martin. Briefly, 400,000 of MEF cells were plated on P60 plates and incubated in complete DMEM for overnight. The media was replaced with media containing galactose or acetoacetate (glucose free DMEM, 10% dialysed FBS, 100 mM acetoacetate (Sigma-Aldrich, 164100-50G) and 2 % penicillin-streptomycin).

3.1.5 Bezafibrate treatment

The treatment was conducted in MEFs as illustrated below (Figure 9). Bezafibrate solution (B7273, sigma) was prepared by dissolving 0.199 g of bezafibrate in 2 ml of DMSO (100%) for a final concentration of 275 mM. MEFs were treated with a final concentration

of 550 μM (10 μl for 5 ml of complete media) and 0.2 % DMSO was added to the control MEFs.

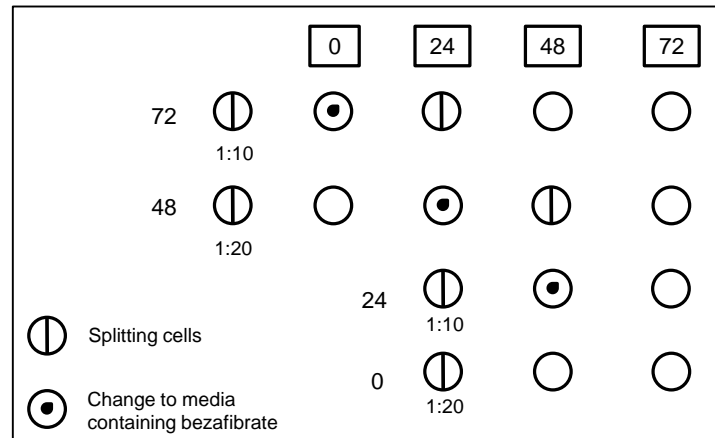


Figure 9: Experimental scheme of bezafibrate treatment.

3.1.6 RNA interference

NSC34 were grown to 70-80 % confluence. Either one or all three siRNAs (Table 4) against murine *Cluh* (Life Technologies) were transfected in a 1:1:1 ratio (final concentration was 100 nM) using Lipofectamine® 2000 (Life Technologies, 11668). Cells were collected for experiment 72 hours after the transfection.

Table 4: Oligos used in RNA interference for NSC34 cells

Oligo	Sequence
oligo1	5'-CAUGGACCGUGAGGAUACUUGUCAU-3'
oligo2	5'-CCUCGGUCAUGCUGUUGAAUGGUGA-3'
oligo3	5'-CCGAAUCCAUGUGCGUCAUGUCAGA-3'

3.1.7 Immunofluorescence and imaging

Cells were washed twice with PBS and fixed with 4 % paraformaldehyde pH7.4 in PBS for 30 min at RT or with ice-cold methanol for 20 min at -20°C. Cells were then permeabilised

with 0.2 % Triton X-100 in PBS for 10 min at RT. Cells were blocked in 10 % pig serum in PBS for 10 min and subjected to primary antibodies diluted in PBS including 1 % pig serum for 2 h at RT (See Table 5 for the information of primary antibodies). Afterwards, cells were washed in PBS and incubated in secondary antibodies diluted in PBS and 1 % pig serum for 1 h at RT (See Table 6 for the information of secondary antibodies). Cells were then washed twice with PBS for 5 min, followed by DAPI staining (1:2,000 in PBS, Sigma-Aldrich, D9542-5MG) for 5 min and mounted with Fluorsave (Calbiochem, 345789). Images were taken with an epifluorescence microscope Imager.M2m (Zeiss) using an ApoTome module with 63x 1.4 NA oil immersion objective lens. The software AxioVision Version 4.8 2.0 was used for Image acquisition. Images represent a single-plane with a thickness of 0.250 μm .

Table 5: Primary antibodies used for immunofluorescence

Primary Antibody	Dilution
CLUH 06, Novus Biologicals, NB100-93306	1:500
COX1, Life Tecnologies, A6403	1:1000
FLAG Sigma-Aldrich, F3165	1:5000
TOM20, Santa Cruz, sc-11415	1:500

Table 6: Secondary antibodies used for immunofluorescence

Secondary Antibody	Dilution
AlexaFluor 594, Donkey anti-rabbit	1:500
Life Technologies, A-21207	
AlexaFluor 488, Chicken anti-mouse	1:500
Life Technologies, A-21200	
TRITC	1:200
Dako, R0156	
FITC	1:200
Dako, F0479	

3.2 Molecular biology

3.2.1 Polymerase chain reaction (PCR) and agarose gel electrophoresis

Full length human CLUH was cloned from pcDNA3-hCluFL generated by Dr. Paola Martinelli. CLUH with p3x FLAG (Sigma-Aldrich, E7980) at its C-terminus was created by inserting full length human CLUH into the multiple cloning site of p3xFLAG-CMV-14 via HindIII and EcoRI. Addition of restriction sites HindIII and EcoRI to CLUH and the removal of stop codon were conducted by PCR (forward primer contains HindIII restriction site: 5'- GCAAAGCTTATGGTTATCAAGACG-3' reverse primer contains EcoRI site: 5'- CTCCGAGCGTGCAGGGACGGAATTCCG-3'). PCR was performed with *Pfu* DNA polymerase (Life Technologies EP0571), 1 μ M final concentration of primers, 200 μ M final concentration of dNTPs and 1 x *Pfu* buffer. PCR thermocycler was set as below:

Temperature	Time	
95°C	3 min	} 35 Cycles
95°C	30 s	
55°C	30 s	
72°C	9 min	
72°C	15 min	
16°C	Hold	

PCR products were then resolved in terms of agarose gel electrophoresis. The gels were prepared in TAE buffer (40 mM Tris-Cl pH8, 40 mM acetic acid and 1 mM EDTA). Ethidium bromide was used to the gel for DNA visualisation. The samples were mixed with loading dye (0.1 % SDS, 15 % glycerol, 10 mM Tris-Cl pH8, xylene cyanol FF, bromophenolblue). GeneRuler 1 kb (Fermentas SM0313) was used as a marker.

3.2.2 Gel extraction, DNA extraction, DNA digestion and ligation

After excising the PCR product from the agarose gel, DNA was extracted with Gel Extraction Kit (Qiagen, 28706) following the manufacturer's manual. PCR products and p3xFLAG-CMV-14 vector were restricted by HindIII (NEB, R0104) and EcoRI (NEB, R0101) at 37°C for 2 hours. The restricted vectors were separated and purified by agarose gel electrophoresis and gel extraction, respectively, whereas the PCR products were precipitated with ethanol. DNA precipitation was achieved by mixing the PCR product with 1 µl of glycogen, 300 mM final concentration of sodium acetate and equal volume (to PCR product) of absolute ethanol. The mixture was incubated at -20°C for 10 min and centrifuged at 20,000 g for 30 min at 4°C. After removing the supernatant, DNA pellet was air dried and dissolved in 50 µl of H₂O. The ligation reaction between restricted PCR products and vectors were performed with the T4 DNA ligase (NEB, M0202) according to the manual at 16°C for overnight.

3.2.3 Bacterial transformation and colony selection

Competent *E. coli* (strain DH5α) were transformed by heat shock with the ligated plasmids. Bacteria and DNA were incubated on ice for 30 min and heat shocked for 2 min at 42°C followed by incubation on ice for 2 min. Then 900 µl of SOC medium (20 g Tryptone (NZCym), 0.5 % (wt/v) of yeast extract, 8.6 mM NaCl, 25 mM KCl, 10 mM MgCl₂, 2 mM glucose) was added to the bacterial mixture and incubated for 30 min at 37°C. After centrifugation of bacteria at 4,000 g for 1 min, the transformed bacterial pellet was plated on a LB-agar plate containing 100 µg/ml of ampicillin and incubated for overnight at 37°C.

Colonies were picked on the next day and inoculated into LB-medium containing 100 µg/ml of ampicillin and grown for overnight. DNAs were extracted by using Miniprep Kit (Qiagen, 27106).

3.2.4 Generation of CLUH-FLAG and CLUH deletion HEK 293T cell lines

Recombination sites attB1 and attB2 were inserted to all CLUH constructs by PCR (see Table 7 and 8 for primer information) with *Pfu* DNA polymerase.

Table 7 PCR primers used to add adapters to CLUH constructs for BP recombination

Primer Sequence
CluC_st_F 5'-GGGGACAAGTTTGTACAAAAAAGCAGGCTATGGTTATCAAGACGGAC-3'
CluC_st_R 5'-GGGGACCACTTTGTACAAGAAAGCTGGGTCCTTGTCATCGTCATCCTT-3'
ΔGSKIP_st_F 5'-GGGGACAAGTTTGTACAAAAAAGCAGGCTATGCCCGTGCCTGGCGAG-3'
ΔGSKIP_st_F 5'-GGGGACAAGTTTGTACAAAAAAGCAGGCTATGACCCCATTCAGGTGTAC-3'

Table 8 Combinations of primers used for different constructs

Construct	Forward primer	Reverse primer
Δ1021-1347	CluC_st_F	CluC_st_R
Δ801-1347	CluC_st_F	CluC_st_R
Δ1-352	ΔGSKIP_st_F	CluC_st_R
Δ1-615	ΔGSKIP_Δclu_st_F	CluC_st_R

After agarose gel electrophoresis and gel extraction, the PCR products were then inserted into Gateway® pDONR™ 221 (Life Technologies, 12536-017) using Gateway® BP Clonase® (Life Technologies, 11789-021) according to instruction. The BP recombination reaction was performed for overnight at RT. On the next day, the recombined vector was transformed into One Shot® OmniMAX™ 2 T1^R cells (Life Technologies, C8540-03) with heat shock. The transformed bacteria were then allowed to grow on LB-plate containing 50 µg/ml kanamycin. After picking the positive clones and sequencing, the correct constructs were subjected to LR recombination reaction to facilitate the transfer of CLUH constructs to Gateway® pT-REx™-DEST30 vector (Life Technologies, 12301-016) using Gateway® LR Clonase® (Life Technologies, 11791-019) for overnight at RT according to instruction. The reaction mix was then transformed into One Shot® STBL3 cells by heat shock (Life Technologies, C7373-03). After overnight growth on LB plate containing 50 µg/ml of

ampicillin, positive clones were picked and inoculated for culturing. The final constructs were obtained by Miniprep Kit.

HEK 293T cells were cultured without any antibiotics and passaged for five times before transfection. 0.5 µg of DNA constructs and 2.5 µg of pOG44 Flp-Recombinase expression vector (Life Technologies, V6005-20) were transfected with Lipofetamine[®] 2000 per 6 well plate. Selection started 24 hours after transfection by replacing culturing media to that containing hygromycin and blasticidin. Clones were picked by pipetting.

3.2.5 Crosslinking immunoprecipitation (CLIP) and RNA immunoprecipitation

Cells were splitted one night before UV crosslinking and harvested at about 70-80 % of confluence. HeLa and HEK 293T cells were rinsed with DPBS (Life Technologies, 14190169) and crosslinked with 300 mJ and 400 mJ, respectively (UVP UV crosslinker, CX2000). Afterwards, cells were collected and centrifuged at 21,000 g for 15 s. Cell pellets were then either stored at -80°C or used immediately for CLIP experiment. Cell pellet was lysed in cold lysis buffer (50 mM Tris-Cl pH 7.4, 100 mM NaCl, 1 mM MgCl₂, 0.1 mM CaCl₂, 1 % IGEPAL[®] CA-630, 0.1 % SDS and 0.5 % sodium deoxycholate) supplemented with different concentrations of RNase I (Life Technologies, AM2294) (50 U/500 µl lysate or 1 U/500 µl lysate) and 4 U Turbo[™] DNase (Life Technologies, AM2238) per 500 µl of lysate. DNase/RNase treatment was conducted at 37°C for 5 min with shaking (1100 rpm) and then cooled on ice for 2 min. Cell lysate was cleared by centrifugation at 21,000 g for 25 min. 450 µl of cleared lysate was then incubated with 0.5 µg of anti-CLUH 06, 0.5 µg anti-Afg311(Koppen, Metodiev et al. 2007), no antibody, or 3 µg of anti-FLAG for 1 h at 4°C with head-to-toe rotation. The complex was immunoprecipitated by adding 20 µl protein G Dynabeads (Life Technologies, 10003D) for 1 h at 4°C. The beads were then washed extensively with 1 ml lysis buffer (3 times and each time with 5 min head-to-toe rotation) followed by 1 ml of high salt buffer (50 mM Tris-Cl pH 7.4, 1 M NaCl, 1 % IGEPAL[®] CA-630, 0.1 % SDS, 0.5 % sodium deoxycholate and 1 mM EDTA) (2 times and each time with 5 min head-to-toe rotation). Immunoprecipitated complexes were then washed with 1 ml T4 PNK buffer (20 mM Tris-HCl pH 7.4, 10 mM MgCl₂ and 0.2 % Tween-20). RNA end-labeling was carried out by

incubating the beads with 1 μ l PNK buffer, 2 μ l T4 PNK (20 unit, NEB), 1 μ l of ATP γ -P³² (10 mCi/ml, Perkin-Elmer) and 33 μ l of H₂O at 37°C for 5 min with agitation. The beads were then washed with 1 ml PNK buffer plus 20 mM EGTA (for 3 times and each time for 5 min), and then with 1 ml high salt buffer (for 2 times and each time for 5 min). The RNP complex was then released by incubating the beads with 1x Bolt™ LDS sample buffer (Life Technologies, B0007) and 1x of Bolt™ reducing agent (Life Technologies, B0004) at 70°C for 10 min with agitation. The samples were resolved onto 4-12 % Bolt® Bis-Tris Plus (Life Technologies, NW04120BOX), the gel was dried and exposed to obtain autoradiograph. For RNA immunoprecipitation, the procedure was the same, except that no RNase I was added to the lysis buffer and without RNA end labelling.

3.2.6 RNA extraction

The immunoprecipitated RNA was extracted by incubating the beads with 10 % SDS and 100 μ g of proteinase K (Promega, V3021) at 37°C for 30 min, followed by phenol/chloroform/isoamyl and acid/chloroform extraction (ToTALLY RNA™ kit, Life Technologies AM1910,). Precipitation of RNA was achieved by addition of isopropanol and GlycoBlue (Life Technologies, AM9515) and incubation at -20°C for overnight. After centrifugation at 12,000 g for 15 min, the RNA pellet was washed with 70 % ethanol and dried in the air.

RNA extractions of HeLa cells after galactose treatment and MEF cells were performed with TRIzol® and RNA was extracted according to the manufacturer's manual (Life Technologies, 15596-026,).

3.2.7 Reverse transcription and quantitative real-time PCR

The immunoprecipitated RNA from CLIP experiments or 5 μ g of total RNA from total RNA extracts were reverse transcribed with SuperScript® First-Strand Synthesis System (Life Technologies, 11904-018) with oligodT as primers according to manufacturer's manual.

Real-time PCR was performed with SYBR[®] green Master Mix (Life Technologies, 4309155,) and 500 nM of each primer (Table 9). cDNA from whole cell extracts were diluted 1:10 and 1 µl was used per 12.5 µl of reaction per well. cDNA synthesized from RNA immunoprecipitation was used without any dilution. Each reaction was performed in triplicate, and at least three biological repeats were conducted. The fold enrichment was calculated with formula: $2^{(-DDCt)}$.

Table 9: Primers used for Q-PCR

Gene	Primer name	Sequence 5'-3'
Human <i>OGDH</i> NM_001003941	hOGDH_Q_F	AAGACCAAAGCCGAACAGTTTTA
	hOGDH_Q_R	CGCCTCTCTCTGGGCCTTA
Human <i>ATP5a1</i> NM_001001937.1	hATP5a1_Q_F	GATCCGCTGCCCAAACC
	hATP5a1_Q_R	GCCAATTCCAGCTTCATGGT
Human <i>Got2</i> NM_002080	hGOT2_Q_F	CACATCACCGACCAAATTGG
	hGOT2_Q_R	AGCCGCTCCACCTGTTC
Human <i>OPA1</i> NM_015560.2	hOPA1_Q_F	CCCTTCATAGCCAGCGAAGA
	hOPA1_Q_R	AGAGTGAGAAAACAGCAACTGAATCA
Human <i>SPG7</i> NM_003119.2	hSPG7_Q_F	TCCAGTTTTCTACAAGCGAA
	hSPG7_Q_R	CCGTCATCCCCACAGAGTACA
Human <i>Cox10</i> NM_001303	hCOX10_Q_F	TCCAATCACTGTTTGCCTTATCTG
	hCOX10_Q_R	TGCAATGTTCTCCACAGTAAATACC
Human <i>AFG3L2</i> NM_006796.2	hAfg3L2_Q_F	AACACTTTGAACAGGCAATTGAAC
	hAfg3L2_Q_R	GCTGCAGAACCTGCGTTTTTC
Human <i>GAPDH</i>	hGAPDH_Q_F2	AATCCCATCACCATCTTCCA
	hGAPDH_Q_R2	TGGACTCCACGACGTACTION
Human <i>β-actin</i>	hbActin_Q_F	TCCCTGGAGAAGAGCTACGA
	hbActin_Q_R	AGCACTGTGTTGGCGTACAG
Human <i>TBP</i> NM_001172085.1	hTBP_Q_F2	GCCCGAAACGCCGAATAT
	hTBP_Q_R2	CGTGGCTCTTATCCTCATGA
Human <i>CLUH</i>	hCLUH_Q_F	ACCGGCAAGTCAGCATCAC
	hCLUH_Q_R1	AAGGTCGGGCTGATCTGGTT
Mouse <i>Cluh</i>	forward	GGTAGCGGGCACGGTACA
	reverse	GCATTGAGCACCCCAACAC
Mouse <i>Afg3l2</i>	forward	AGGACGACTTGAGGAAGGTTACC
	reverse	GCCCCACTTTCTCGTTCATG
Mouse <i>Atp5a1</i>	forward	TGGGCCGTGTGGTTGAC
	reverse	CGTCTGCGGGTCTTGGA
Mouse <i>Ogdh</i>	forward	TGGTGTCGGCGCTTCACT
	reverse	TGTCCTGAAGCCTCCACAAG
Mouse <i>Sdha</i>	forward	GGCAGGCTCATCGGTGTT
	reverse	CATATCGCAGAGATCTTCCATAC
Mouse <i>Tom20</i>	forward	AGCTGGGCTTTCCAAGTTACC
	reverse	ACCAAGCTGTATCTCTTCAAGGA

3.2.8 RNA sequencing and analysis

For RIP, the procedure was the same as described above, except that no RNase I was added to the lysis buffer. The following steps were conducted by Cologne Center for Genomics (CCG). Libraries were prepared using the Illumina® TruSeq® RNA Sample Preparation Kit v2. Starting material was 1µg total RNA from the input samples, and complete material of the RIP experiments (240-550ng RIP RNA). After poly-A selection (using poly-T oligo-attached magnetic beads), mRNA was purified and fragmented using divalent cations under elevated temperature. The RNA fragments underwent reverse transcription using random primers. This was followed by second strand cDNA synthesis with DNA Polymerase I and RNase H. After end repair and A-tailing indexing adapters were ligated. The products were then purified and amplified (15 PCR cycles) to create the final cDNA libraries. After validation (Agilent 2200 TapeStation) and quantification (Life Technologies Qubit System) the pool was quantified by using the Peqlab KAPA Library Quantification Kit and the Applied Biosystems 7900HT Sequence Detection System. The pool was loaded on an Illumina HiSeq sequencer and TruSeq PE Cluster FlowCell and sequenced by using one 2x100bp lane on an Illumina HiSeq 2000 Sequencer.

The following steps were performed by Dr. Peter Frommolt, Bioinformatics Facility, CECAD. Data were analyzed using a high-throughput Next-Generation Sequencing analysis pipeline: Basic read quality check was carried out using FastQC and read statistics were obtained with SAMtools. Reads were mapped to the human reference assembly, version GRCh37, using TopHat2 (Kim, Pertea et al. 2013), and gene quantification was carried out using a combination of Cufflinks (Trapnell, Williams et al. 2010) and the DESeq2 package (Anders and Huber 2010) with genomic annotation from the Ensembl database, version 77. The results were uploaded into an in-house MySQL database and merged with annotations obtained with BiomaRt from Ensembl, version 77. The gene lists were filtered according to FC and P-value in comparison of the library-size normalized read counts between samples and controls. The sample and control means as well as FC and P- were calculated with the DESeq2 package from the Bioconductor project. Wald's test was used for significance testing. In contrast, gene expression for the individual samples was calculated by the Cufflinks package and returned as FPKM (Fragments Per Kilobase of transcript per Million mapped reads) values, which means that they have been

normalized also by the molecule size. Analysis of enriched pathways and gene annotations were performed using Ingenuity Pathway Analysis. To exclude false positives among the enriched genes which are due to empty input, we only considered transcripts for which sufficient reads were detected in the input samples.

3.3 Biochemistry

3.3.1 Protein extraction for western blot analysis

Cells were washed with PBS, scraped off and centrifuged at 21,000 g for 15 s. After removing the PBS, cells were either frozen at -80°C or lysed directly in Radioimmunoprecipitation assay (RIPA) buffer containing 50 mM Tris-Cl pH 7.4, 150 mM NaCl, 1 mM EDTA, 1 % IGEPAL[®] CA-630, 0.25 % sodium deoxycholate and freshly added protease inhibitor (Sigma-Aldrich, P2714). The lysate was then incubated on ice for 30 min followed by centrifugation at 20,000 g for 30 min to remove the debris and insoluble proteins.

The procedure to extract proteins from animal tissues was similarly conducted with minor modification: RIPA buffer also contained 0.1 % SDS. Tissues were homogenised in Dounce tissue grinder before incubation on ice.

3.3.2 Protein quantification and preparation

Protein concentration was determined using Bradford assay (Protein Assay Dye reagent concentrate, Bio-Rad 500-0006) according to manufacturer's manual. Proteins were then diluted to either 1 µg/µl or 2 µg/µl with sample loading dye containing a final concentration of 0.03 M Tris-Cl pH6.8, 1 % SDS, 10 % glycerol, 0.1 % bromophenol blue and 5 % of β-mercaptoethanol. Proteins were then boiled for 5 min.

3.3.3 SDS-PAGE, western blot analysis and quantification

Proteins were resolved by SDS-Polyacrylamide gels together with protein marker (PageRuler™ Plus Prestained Protein ladder, Life Technologies, 26620). Gels ranging from 7.5 % to 12% (1.5 mm, 10 or 15 well combs) were casted with 30 % acrylamide (37.5:1 = acrylamide:bisacrylamide), 1 % ammoniumpersulfate (final concentrations), 0.1 % TEMED (N,N,N',N'-Tetramethylethylenediamine), 0.1 % SDS, separation buffer final concentration 0.375 M Tris-Cl pH 8.8 and stacking buffer final 0.125 M Tris-Cl pH 6.8. Proteins were separated in the gel soaked in running buffer (25 mM Tris, 0.192 mM glycine, 0.1 % SDS) at 30 mA per gel and blotted with wet transfer system either at 300 mA for 90 min or 30 V overnight at 4°C in blotting buffer (25 mM Tris, 0.192 mM glycine, 20 % methanol). Absolute methanol was used to reactivate the membranes. Residual methanol was rinsed off with TBST (20 mM Tris-Cl pH7.4, 150 mM NaCl). The membranes were then blocked in either 5 % non-fat milk in TBST (20 mM Tris-Cl pH 7.4, 150 mM NaCl, 0.1 % Tween 20) or in 1 % western blot reagent (Western Blocking Reagent, Roche 11 921 673 001) in TBST according to the antibodies used. Primary antibodies (Table 10) were incubated on the membrane for 1 hour at room temperature (RT) or overnight at 4°C. The membranes were washed for three times and each time for 5 min with TBST. Secondary antibody was incubated for 1 hour at RT, the membrane was washed as that for primary antibodies. The membranes were developed using ECL or ECL prime and X-ray films (GEHealthcare RPN2106, RPN2232, SuperRX films, Fuji Films 4741019236).

Table 10: Primary antibodies for western blot used in this study

Antibody	Company and catalogue	Dilution
Afg3l2	Kind gift from Prof. Langer	1:12,500
Astrin, SPAG5	Proteintech, 14726-1-AP,	1:1000
ATP5A1	Abcam, ab14748	1:1000
calnexin	Biotrend/ Assay Designs, SPA-860	1:2000
CLUH (N-ter)	Abcam, Ab178342	1:1000
CLUH 05	Novus Biologicals, NB100-93305	1:500
CLUH 06	Novus Biologicals, NB100-93306	1:1000
COX1	Life Tecnologies, A6403	
EIF3G	Novus Biologicals, NB100-93298	1:1000
FLAG	Sigma-Aldrich, F3165	1:10,000
GAPDH	Chemicon/Millipore, MAB374	1:1000
HADHA	Abcam, ab54477	1:1000
LC3	Novus Biologicals, NB100-2220	1:1000
OGDH	Proteintech, 15212-1-AP	1:1000
OPA1	Abcam, ab42364	1:1000
P62	PROGEN, GP62-C	1:1000
pan-actin	MAB1501R, Millipore	1:1000
PCB	Abcam, ab128952	1:1000
POR	Stressgen, OSA-300	1:1000
RPL7	Novus Biologicals, NB100-2269	1:1000
RPS6	Novus Biologicals, NB100-1595	1:1000
S6K1 ^{Thr389}	Cell Signaling, 9234	1:1000
SDHA	Molecular Probes, Life Technologies, A-11142	1:2000
SKAP	Sigma-Aldrich, SAB1103031	1:1000
TOM20	Santa Cruz, sc-11415	1:2000
UQCRC2	Molecular Probes, Life Technologies, A-11143	1:2000
B-tubulin	Sigma-Aldrich, T4026	1:10,000

3.3.4 Cell fractionation

Mouse tissues and MEFs were homogenized using automatic Potter S homogenizer (Sartorius, 8533024) in buffer containing 220 mM mannitol, 70 mM sucrose, 20 mM HEPES-NaOH pH7.4, 1 mM EDTA and 0.1 % BSA. Large debris was eliminated by centrifugation at 500 g at 4°C for 10 min. The supernatant was then centrifuged at 1,000 g to remove the nuclear fraction. Mitochondria were obtained by centrifugation at 8,000 g for 10 min. The resulting supernatant was then centrifuged at 20,000 g for 10 min. The supernatant was further separated by ultracentrifugation at 170,000 g for 45 min. Light membranes were harvested by dissolving the pellet in buffer containing 50 mM Tris-Cl pH

7.4, 150 mM NaCl, 1 mM EDTA pH 8, 1 % IGEPAL® CA-630, 0.25 % sodium deoxycholate and protease inhibitor cocktail. The protein concentration was measured with Bio-Rad Protein Assay (Bio-Rad) and same concentration of protein was loaded from each fraction.

3.3.5 Sucrose gradient and polysome profiling

All procedures were carried out in strictly RNase free environment. Samples were kept cool at all time unless stated otherwise. HeLa or NSC34 cells were plated one night before and harvested at 70-80 % of confluence. Polysomes were stalled by treating the cells with 100 µg/ml of cycloheximide (Sigma-Aldrich, C4859) for 15 min in the cell incubator. Cells were washed twice and scraped in DPBS containing cycloheximide at 4°C. After pelleting cells at 21,000 g for 15 s, the pellet was lysed in buffer containing 20 mM Tris-Cl pH 7.4, 30 mM KCl, 0.5 % Triton X-100, 2 mM DTT, 1 mg/ml heparin, 100 µg/ml cycloheximide and 0.16 unit/ml RNasin® Plus RNase Inhibitor (Promega, N2615). The lysates were then loaded onto a 7–47 % (mol wt/vol) continuous sucrose gradient and centrifuged at 97,658 g for 3 h at 4°C in a Beckman SW41 rotor.

Sucrose gradient was prepared with Gradient Master (BioComp Instruments) at RT according to manufacture's instruction. Level of 47 % of sucrose was labelled by inserting the tube into the aluminium gig and marking the top edge (for short cap) of the gig. 47 % sucrose was pipetted into the tube first and 7 % sucrose was then carefully added on top of the 47 % sucrose without disturbing the interface. After placing the short cap on the tube, extra sucrose was pipetted off from the cap. The level of the gradient master was adjusted and the gradients were prepared by selecting short cap and 7-47% on the menu. After gradient master stop rotating and returned to the starting position, cap was removed and 500 µl of sucrose was taken from the top of the gradient. Keep the sucrose gradient at 4°C until use.

For polysome profiling, fractions were monitored at 254 nm and collected using ISCO fractionation system (ISCO, Lincoln, NE). For western blot analysis, the same volume of samples from each fraction was loaded on the SDS-PAGE.

3.3.6 Metabolic labeling and biotinylation of the newly synthesised proteins

MEFs were cultured one night before the experiment. MEFs were washed twice with 5 ml methionine free media containing DMEM (L-methionine, L-Cystine free, Life Technologies, 21013-024), supplemented with 10 % dialysed serum, 2 % penicillin-streptomycin, 1 mM pyruvate, 1x non-essential amino acid and 2 mM L-glutamine. Cells were then incubated with methionine free media for 30 min in the cell incubator. Afterwards, the media was replaced with metabolic labeling media containing methionine free media supplemented with L-azidohomoalaine (AHA, Click-iT™, Life Technologies, C10102) and incubated for 1 hour. Treated cells were then washed with cold PBS for three times, scraped off and centrifuged down at 21,000 g for 15 s. Cell pellets were lysed with buffer containing 50 mM Tris-Cl, pH 8.0 and 1 % SDS and lysed for 30 min in a head-to-toe shaker at 4°C. Cell lysates were then sonicated and centrifuged for 10 min at 15,000 g at 4°C. Protein concentrations were estimated using BCA protein assay reagent (Life Technologies, 23255).

Biotinylation of AHA labeled proteins was performed using Click-iT™ protein reaction buffer kit (Life Technologies, C10276). Up to 200 µg cell lysates in 50 µl were subjected to Click-iT™ azide/alkyne reaction according to manufacturer's instruction. The resulting protein pellets were dissolved in 200 µl of IP150 buffer including 150 mM NaCl, 20 mM Tris-Cl, pH7.5, 0.3 % IGEPAL® CA-630, 1 mM EDTA, and fresh 1 mM DTT supplemented with protease inhibitor cocktails. Dissolved proteins were incubated with 50 µl of Dynabeads® M-280 Streptavidin (Life Technologies, 11205D) for overnight at 4°C. Dynabeads were washed for 5 times with 1 ml of IP350 (350 mM NaCl, 20 mM Tris-Cl, pH7.5, 1 mM EDTA, 0.3 % NP-40, and fresh 1 mM DTT). The beads were then resuspended in SDS sample buffer, mixed thoroughly with vortex for 1 min. Proteins were denature by boiling for 10 min and the supernatants were then subjected to western blotting.

3.4 Obtaining mouse tissues

Mice at different ages were prepared by crossing full body Afg3l2 flox/flox lines. The organs were harvested according to standard animal procedures. E18.5 mice were obtained

by C-section. Organs were frozen on dry ice and stored at -80°C after harvesting till use.

3.5 Statistical analysis

Statistical analyses were performed using unpaired Student's t-test. Error bars show standard deviations.

4 Results

4.1 CLUH is coregulated with genes encoding mitochondrial proteins and involved in translation

In order to understand the function of CLUH in mammalian system, we examined genes that coregulate with *Cluh/CLUH* in mouse and human. This was achieved by analysing the publicly available microarray data from different samples under different conditions (Sardiello, Palmieri et al. 2009). Interestingly, both mouse/human *Cluh/CLUH* are significantly coexpressed with two clusters of genes. One includes genes involved in RNP complex biogenesis, ribosome biogenesis and the other is mitochondrial genes involved in electron transport chain, oxidative phosphorylation, TCA cycle, and generation of small metabolites and energy (Figure 10A and B). The analysis was performed by Dr. Marco Sardiello from Jan and Dan Duncan Neurological Research Institute in Houston, USA.

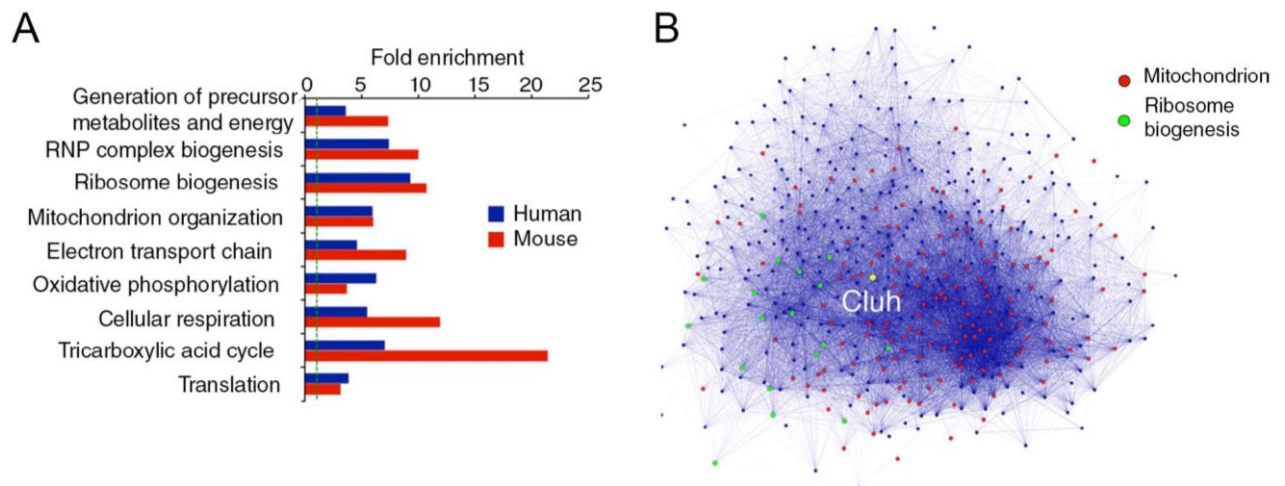


Figure 10: Coregulation analysis of *CLUH/Cluh*. (A) Analysis of Gene Ontology of the group of genes coexpressed with *CLUH/Cluh*. The fold enrichment for the biological process Gene Ontology terms is shown ($P < 10^{-4}$). The green dotted line corresponds to fold enrichment of 1. (B) Cytoscape-generated *Cluh* gene regulatory network. Genes encoding mitochondrial- and ribosomal biogenesis- related proteins are highlighted and are connected by blue lines whose color intensity is proportional to the extent of their coregulation.

4.2 CLUH is an RNA binding protein

Based on the coexpression analysis of the *CLUH* gene regulatory network and the finding that yeast Clu was identified as a component of eIF3 (Vornlocher, Hanachi et al. 1999), we hypothesised that CLUH could be an important mediator connecting cytosolic translation to mitochondrial biogenesis. One possibility is that, CLUH could act as an mRNA binding protein that binds to NEMP mRNAs. This hypothesis could also explain the reduction of steady state protein levels of CV α (α subunit of complex V) and PDH (pyruvate dehydrogenase) in *Drosophila* Clu mutant (Cox and Spradling 2009).

To assess if CLUH is an RNA binding protein, UV crosslinking immunoprecipitation (CLIP) was employed: briefly, HeLa cells were exposed to 300 mJ of UV at 254 nm in order to generate a covalent bond between proteins and mRNAs only when they are at close proximity (i.e. interacting) (Darnell 2012). This was followed by DNase/RNaseI digestions of the cell lysate. Different concentrations of RNase I can generate different RNA-protein complexes determined by the length of the RNAs. The endogenous RNP complexes were subsequently immunoprecipitated and washed extensively to eliminate the unspecifically bound proteins and RNAs. Antibodies against Afg311, the subunit of mAAA-protease in the mouse were used as a control IgG for RNA binding specificity. The nucleic acids were then radio-labeled at their 5'-hydroxyl group in a reaction catalysed by T4 polynucleotide kinase from [γ - 32 P] ATP. The RNP complex was then separated from the other proteins and RNAs by means of SDS-PAGE.

CLUH could be successfully precipitated with antibodies against the endogenous CLUH (Figure 11). Moreover, at its corresponding position in the autoradiogram, a discrete RNA band appeared with high concentration of RNase I (Figure 11, shown with arrow), and this band became an upward smear with low concentration of RNase I (Figure 11, shown with bracket). Without UV crosslinking, no RNAs could be pulled down with CLUH. The smearing effect is essential to demonstrate that the nucleic acids bound to CLUH are RNA, not DNA since this phenomenon is RNase I dependent.

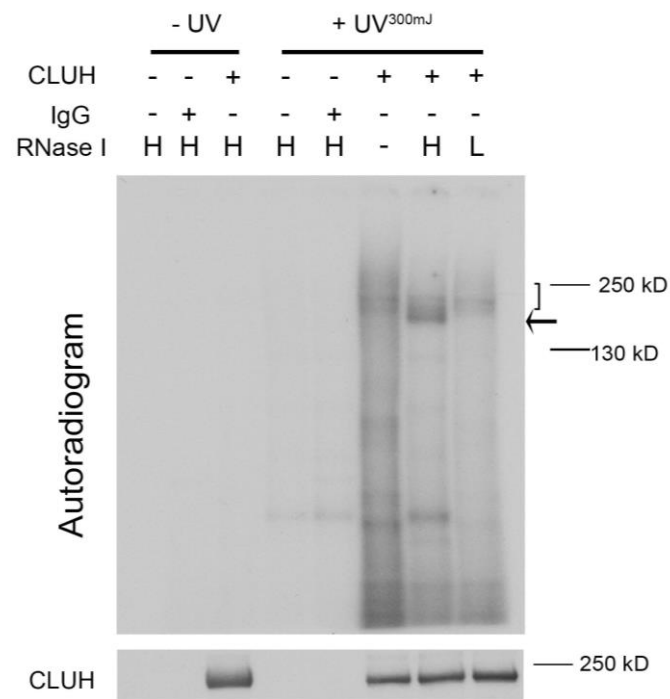


Figure 11: CLUH is an RNA binding protein. (A) CLIP with anti-CLUH antibodies in HeLa lysate after crosslinking with 300mJ UV. Two different concentrations of RNase I were used to distinguish the difference between RNA and DNA species. Lower panel shows the western blot of the corresponding experiment showing the efficiency of immunoprecipitation. Arrow indicates the CLUH-nucleic acid complexes whereas the bracket shows the smear formed by RNase I digestion.

In order to confirm the above finding and reduce the chance of obtaining false positive result, different system was adopted for CLIP analysis. HEK 293T cell lines were generated either stably expressing CLUH tagged with FLAG at its C-terminus or empty FLAG (see more about this cell line below). Expression of these proteins was induced with tetracycline. In contrast to CLIP in HeLa cells, this system allows the utilisation of same antibodies for control and overexpressed proteins.

CLIP experiment was performed with minor modification: 400 mJ of UV at 254 nm was applied to crosslink the protein-RNA complex instead of 300 mJ based on the optimisation experiments conducted previously. Overexpressed CLUH could be immunoprecipitated with anti-FLAG antibodies (Figure 12, lower panel). After UV crosslinking, the amount of immunoprecipitated CLUH was considerably less than that without UV. However, no nucleic acid signals could be seen for the non-crosslinked

sample. Overexpressed CLUH could be crosslinked to RNA. The RNA signal appeared at the expected size of CLUH (Figure 12, shown with arrow) and smears with RNase I treatment (Figure 12, shown with bracket).

Taken together, these experiments provide strong evidences that the mammalian CLUH is undoubtedly an RNA binding protein.

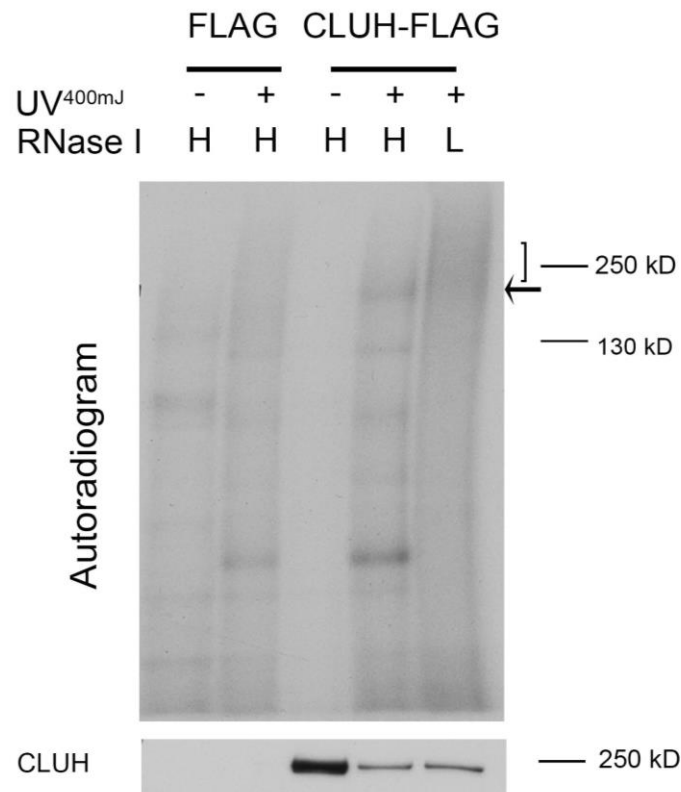


Figure 12: CLIP with anti-FLAG in HEK 293T cells overexpressing CLUH-FLAG or empty FLAG. Cells were induced for 24 hours with tetracycline. Lower panel is the western blot of the corresponding experiment showing the efficiency of immunoprecipitation. Arrow indicates the CLUH-nucleic acid complexes whereas the bracket shows the smear formed by RNase I digestion.

4.3 CLUH preferentially binds to mRNAs encoded in the nucleus for mitochondrial proteins

Next, we ought to find out what are the RNAs that are bound by CLUH. We hypothesised that NEMPs mRNAs that were highly coexpressed with CLUH could be the potential targets. Consequently, CLIP experiments with HeLa cells were conducted

to immunoprecipitate (RNA immunoprecipitation, or RIP) the endogenous CLUH but without RNase I treatment. After immunoprecipitation, RNAs were purified and extracted with proteinase K and phenol-chloroform. The final RNA products were reverse transcribed into cDNAs and analysed with quantitative reverse transcription PCR (qRT-PCR). Several genes were tested based on their coexpression relationship with *CLUH*: *OGDH*, *ATP5A1*, *GOT2*, *OPA1*, *SPG7*, *COX10* and *AFG3L2*. Three housekeeping genes were selected as controls: *ACTIN*, *GAPDH* and *TBP*.

Intriguingly, these mRNAs were all enriched by CLUH immunoprecipitation when compare to control IgG (anti-Afg311) with *OGDH* being the most enriched and *AFG3L2* the least (Figure 13A and B). There might be a subtle enrichment of actin by CLUH but not with the other two housekeeping controls. It is worth mentioning that the enrichments of these genes measured by qRT-PCR for different genes varies from one experiment to another, this is due to the fact that this experiment includes many steps that could affect the final RNA/cDNA quality, namely: quality of antibodies, immunoprecipitation, integrity of the mRNAs and loss of materials in any of the procedures.

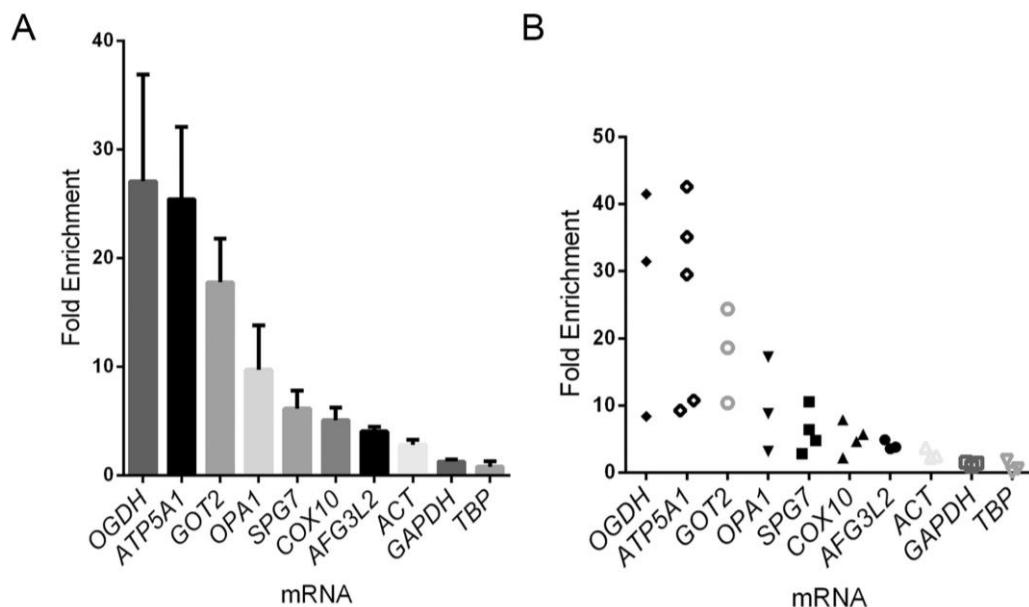


Figure 13: mRNAs bound by CLUH with qRT-PCR. (A) The average enrichment for each mRNA. (B) The plot of fold enrichment from individual experiment for each gene. Fold enrichment is compared with the immunoprecipitation with anti-Afg311 antibody. $n \geq 3$

4.4 Global analysis of the mRNAs bounds by CLUH

To gain a comprehensive view of the mRNA targets of CLUH, and confirm that CLUH binds to NEMP mRNAs specifically, next generation RNA sequencing were performed on mRNAs pulled down with CLUH. As before, after UV irradiation, endogenous CLUH was captured together with the RNA crosslinked to CLUH. For this experiment, RNase I treatment was also omitted preceding immunoprecipitation. The RNA was extracted and purified as well as the input RNA (total transcriptome). Three biological replicates were conducted and the RNA was submitted to Cologne Center for Genomics (CCG) to carry out next generation sequencing. The analysis and the quality control of the sequencing data were performed by the Bioinformatics facility in CECAD, Cologne (See appendix, Table 16).

RNAs that were enriched for more than five times with a P value of less than 0.01 in CLUH-RIP against Afg311-RIP were chosen for further bioinformatics analysis. There were 288 genes in total in this list, 272 encode for proteins, 16 fall in the class of miRNA (one miRNA is enriched 41.01 times), pseudogene and long non-coding RNA. 87.9 % of protein coding mRNAs belong to the NEMPs (239 mRNAs) (Figure 14) (Full list of NEMPS mRNA can be found in the appendix Table 17). Among the top 40 genes enriched by CLUH (Table 11), only one encodes for a cytosolic protein: *SPAG5* (encoding for astrin). The 33 non-mitochondrial mRNAs bound by CLUH encode for proteins localise throughout the cell without any apparent relationship with each other (Table 12).

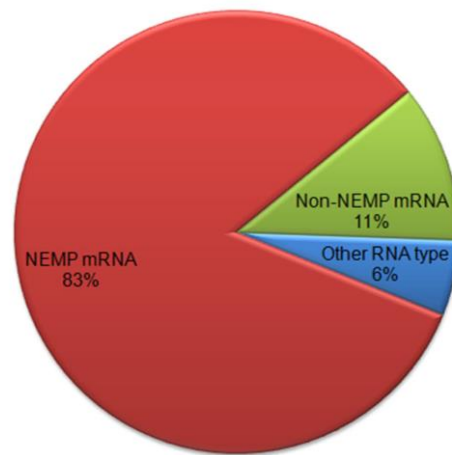


Figure 14: Category of the RNAs bound by CLUH. Only RNAs enriched more than five times with a P value of less than 0.01 in CLUH-RIP against IgG-RIP were chosen for analysis. NEMP, nuclear encoded mitochondrial protein.

The protein products of CLUH target mRNAs were found to participate in diverse mitochondrial pathways identified by Ingenuity Pathway Analysis (IPA) (Table 13 and 14), ranging from branched-chain amino acid degradation, oxidative phosphorylation, tRNA charging to mitochondrial quality control. Interestingly, the ten most significant canonical pathways are closely related to mitochondrial energy production from different sources: degradation of branched-chain amino acids: valine (glucogenic, to succinyl-CoA), leucine (ketogenic, to acetyl-CoA) and isoleucine (glucogenic and ketogenic, to both succinyl-CoA and acetyl-CoA). Acetyl-CoA enters the TCA cycle whereas succinyl-CoA is an important intermediate of the TCA cycle.

In fact, almost half enzymes involved in branched-chain amino acids (leucine, isoleucine and valine) degradation are encoded by mRNAs bound by CLUH (20 from IPA compare to a total of 46 genes involved in these pathways listed in KEGG, Figure 15). More strikingly, beside branched-chain amino acids, other amino acid degradation pathways could also be found on this list: tryptophan, methionine, alanine, arginine, aspartate, glutamine, phenylalanine, proline, lysine, and glycine. Genes involved in degradation pathway for these amino acids are not present (with our setting criteria, genes enriched for more than five times with a P value less than 0.01): cysteine, serine, threonine and tyrosine. Interestingly, the mRNAs of eight out of 19 aminoacyl tRNA synthases were also found to be bound by CLUH: *PARS2* (prolyl-), *TARS2* (threonyl-),

IARS2 (isoleucyl-), *FARS2* (phenylalanyl-), *CARS2* (cysteinyl-), *LARS2* (leucyl-), *EARS2* (glutamyl-) and *DARS2* (aspartyl-).

The mRNAs of all enzymes involved in pyruvate conversion to acetyl-CoA were targets of CLUH. More than half of the components of TCA cycle were CLUH targets, apart from the immediate enzymes involved in the conversion to succinate, α -ketoglutarate and citrate (Figure 16).

Among the CLUH targets, there are also components belonging to oxidative phosphorylation (Figure 17). CLUH binds to the mRNAs of seven subunits of complex I (three from NADH dehydrogenase (ubiquinone) 1 alpha subcomplex: *NDUFA10*, *NDUFA9* and *NDUFAB1*, three from NADH dehydrogenase (ubiquinone) Fe-S protein: *NDUFS1*, *NDUFS2*, *NDUFS7* and one from NADH dehydrogenase (ubiquinone) flavoprotein: *NDUFV1* and one assembly factor *NDUFAF5*). The mRNAs of all four subunits of complex II or succinate dehydrogenase (*SDHA*, *SDHB*, *SDHC* and *SDHD*, *SDHA* being the most enriched among the four) were found to be bound by CLUH. For complex III, the targets were the core protein ISP (*UQCRFSL1*) or Rieske iron-sulfur protein and *QCR2*. Only assembly factor *COX15* from complex IV was found. Whereas in complex V, *ATP5A1* and the assembly factors *ATPAF1*, *TMEM70* and *ATPAF2* were found to bind to CLUH (Figure 17).

There are also genes involved in mitochondrial quality control and dynamics: *PINK1*, *SPG7*, *CLPP*, *HSP70*, *HSP60*, *HSCB*, *LONP1*, *PITRM1*, *PMPCA*, *OPA1* and *OMA1*.

Table 11: Top 40 genes bound by CLUH. FC, fold Change. * indicates non-mitochondrial.

FC	Symbol	Description
57,35	<i>GFMI</i>	G elongation factor, mitochondrial 1
57,35	<i>PCCA</i>	propionyl CoA carboxylase, alpha polypeptide
43,97	<i>HIBADH</i>	3-hydroxyisobutyrate dehydrogenase
42,97	<i>ALDH6A1</i>	aldehyde dehydrogenase 6 family, member A1
41,85	<i>PCB</i>	pyruvate carboxylase
41,1	<i>LACTB</i>	lactamase, beta
41,06	<i>OGDH</i>	oxoglutarate (alpha-ketoglutarate) dehydrogenase (lipoamide)
39,82	<i>PINK1</i>	PTEN induced putative kinase 1
39,4	<i>SPAG5*</i>	sperm associated antigen 5
39,12	<i>LARS2</i>	leucyl-tRNA synthetase 2, mitochondrial
38,73	<i>PMPCA</i>	peptidase (mitochondrial processing) alpha
38,23	<i>DARS2</i>	aspartyl-tRNA synthetase 2, mitochondrial
37,78	<i>GHITM</i>	growth hormone inducible transmembrane protein
37,77	<i>HSPA9</i>	heat shock 70kDa protein 9 (mortalin)
37,6	<i>ATPAF2</i>	ATP synthase mitochondrial F1 complex assembly factor 2
37,26	<i>CHDH</i>	choline dehydrogenase
37,06	<i>PPA2</i>	pyrophosphatase (inorganic) 2
36,76	<i>DLAT</i>	dihydrolipoamide S-acetyltransferase
35,27	<i>CPT2</i>	carnitine palmitoyltransferase 2
35,22	<i>ACADM</i>	acyl-CoA dehydrogenase, C-4 to C-12 straight chain
34,22	<i>ALDH18A</i>	aldehyde dehydrogenase 18 family, member A1
33,05	<i>MRPL16</i>	mitochondrial ribosomal protein L16
32,86	<i>ACSF2</i>	acyl-CoA synthetase family member 2
31,17	<i>IARS2</i>	isoleucyl-tRNA synthetase 2, mitochondrial
31,02	<i>SDHA</i>	succinate dehydrogenase complex, subunit A, flavoprotein (Fp)
30,99	<i>ALAS1</i>	aminolevulinic acid, delta-, synthase 1
30,93	<i>NNT</i>	nicotinamide nucleotide transhydrogenase
30,3	<i>ETFDH</i>	electron-transferring-flavoprotein dehydrogenase
29,64	<i>MUT</i>	methylmalonyl CoA mutase
28,76	<i>AIFM1</i>	apoptosis-inducing factor, mitochondrion-associated, 1
26,94	<i>PITRM1</i>	Pitriysin metalloproteinase 1
26,16	<i>IMMT</i>	inner membrane protein, mitochondrial
26,04	<i>LRPPRC</i>	leucine-rich pentatricopeptide repeat containing
25,98	<i>ALDH7A1</i>	aldehyde dehydrogenase 7 family, member A1
25,24	<i>ABCB7</i>	ATP-binding cassette, sub-family B (MDR/TAP), member 7
25,24	<i>GBAS</i>	glioblastoma amplified sequence
24,81	<i>CKMT1B;</i>	creatine kinase, mitochondrial 1A
24,28	<i>DLD</i>	dihydrolipoamide dehydrogenase
24,04	<i>ABCB8</i>	ATP-binding cassette, sub-family B (MDR/TAP), member 8
23,94	<i>BDHI</i>	3-hydroxybutyrate dehydrogenase, type 1

Table 12: Nuclear-encoded mRNAs for non-mitochondrial proteins.

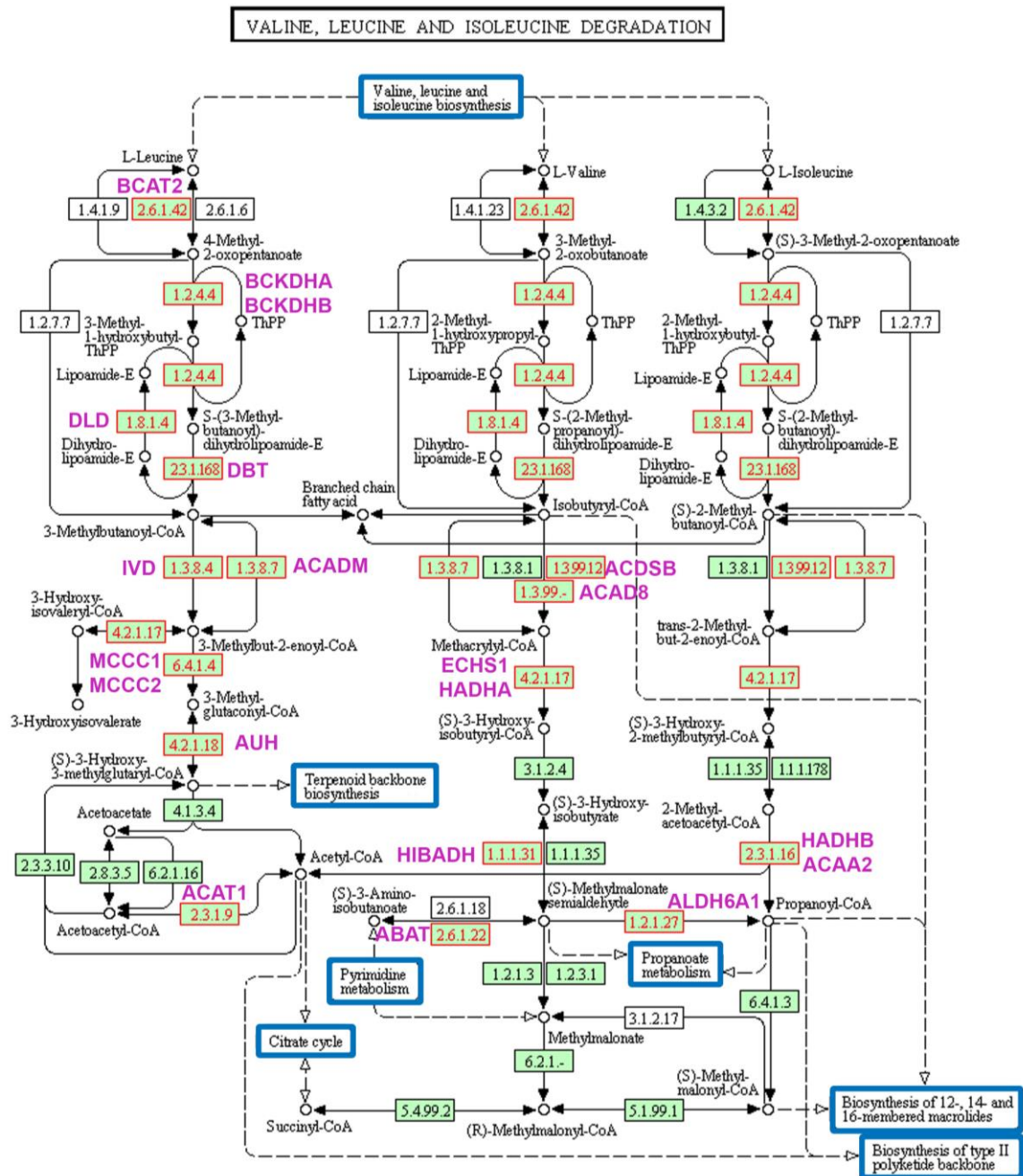
FC	Symbol	Cellular Location	Description
39,44	SPAG5	Cytosol	sperm associated antigen 5
23,48	NEK11	Nucleus	NIMA-related kinase 11
16,39	GALK2;LOC102723	Cytosol	galactokinase 2
16,03	HLTF	Nucleus	helicase-like transcription factor
12,95	JSRP1	Nucleus , Cytosol	junctional sarcoplasmic reticulum protein 1
12,68	TMEM69	Plasma Membrane	transmembrane protein 69
11,96	CCRN4L	Nucleus, Cytosol	CCR4 carbon catabolite repression 4-like (<i>S. cerevisiae</i>)
10,87	NIPSNAP3A	Nucleus, Cytosol	nipsnap homolog 3A (<i>C. elegans</i>)
9,16	GTPBP6	Nucleus ?	GTP binding protein 6 (putative)
8,2	DHRS4;DHRS4L2	Extracellular, Mitochondrion	dehydrogenase/reductase (SDR family) member 4 like 2
7,76	MLF2	Cytosol	myeloid leukemia factor 2
7,49	GAS5-AS1	non-protein coding	GAS5 antisense RNA 1
7,34	ANGEL2	Cytosol ?	angel homolog 2 (<i>Drosophila</i>)
7,31	C1orf53	?	chromosome 1 open reading frame
7,07	RNLS	Extracellular	renalase, FAD-dependent amine oxidase
6,42	SLC30A9	Nucleus, Cytoskeleton	solute carrier family 30 (zinc transporter), member 9
6,28	VPS37D	Endosome	vacuolar protein sorting 37 homolog
6,21	PRSS57	Extracellular	protease, serine, 57
6,2	HNRNPA2B1	Nucleus	heterogeneous nuclear ribonucleoprotein A2/B1
6,19	RPUSD2	Cytosol	RNA pseudouridylylase synthase domain containing 2
6,07	AKR1B1	Extracellular, Cytosol, Nucleus	aldo-ketoreductase family 1, member B1 (aldose reductase)
6,01	RPP40	Nucleus	ribonuclease P/MRP 40kDa subunit
5,88	WDR13	Nucleus, Cytosol	WD repeat domain 13
5,87	ABHD16A	?	abhydrolase domain containing 16A
5,87	PCDH12	Plasma Membrane	protocadherin
5,78	PCED1B	?	PC-esterase domain containing 1B
5,74	MTM1	Endosome, Plasm Membrane	myotubularin 1
5,74	PEX3	ER, Peroxisome	peroxisomal biogenesis factor 3
5,69	MBLAC2	Cytosol	metallo-beta-lactamase domain containing 2
5,6	PRMT6	Nucleus	protein arginine methyltransferase 6
5,58	AIMP2	Cytosol	aminoacyl tRNA synthetase complex-interacting multifunctional protein 2
5,48	INHBE	Extracellular	inhibin, beta E
5,04	PAX9	Nucleus	paired box 9

Table 13: Top 20 canonical pathways identified by Ingenuity Pathway Analysis.

Canonical Pathways	$-\log(p\text{-value})$	Molecules
Valine Degradation I	2.32E01	<i>ECHS1, ABAT, ACADSB, BCKDHB, HADHB, BCAT2, BCKDHA, HIBADH, AUH, ACAD8, DLD, DBT, HADHA, ALDH6A1</i>
Mitochondrial Dysfunction	1.99E01	<i>SDHB, NDUFA9, ACO2, DHODH, PDHA1, NDUFS1, NDUFAB1, NDUFA10, UQCRC1, ATPAF1, NDUFS2, OGDH, AIFM1, SDHA, NDUFV1, NDUFS7, ATP5A1, GLRX2, SDHC, PRDX3, UQCRC2, SDHD, ATPAF2, TXNRD2, PINK1, COX15</i>
TCA Cycle II (Eukaryotic)	1.68E01	<i>SDHA, SDHB, OGDHL, DHTKD1, ACO2, DLST, DLD, SDHD, SDHC, FH, MDH2, OGDH</i>
Isoleucine Degradation I	1.38E01	<i>HADHB, ECHS1, BCAT2, AUH, ACAD8, ACAT1, DLD, ACADSB, HADHA</i>
Oxidative Phosphorylation	1.33E01	<i>SDHA, NDUFV1, SDHB, NDUFA9, NDUFS7, ATP5A1, SDHC, NDUFS1, NDUFAB1, UQCRC2, UQCRC1, NDUFS2, SDHD, NDUFA10, ATPAF1, ATPAF2, COX15</i>
Leucine Degradation I	9.48E00	<i>BCAT2, AUH, MCCC1, IVD, ACADM, MCCC2</i>
Fatty Acid α -oxidation	9.28E00	<i>TMLHE, ALDH4A1, ALDH1B1, ALDH2, BCO2, ALDH9A1, ALDH7A1</i>
Acetyl-CoA Biosynthesis I (Pyruvate Dehydrogenase 2-ketoglutarate Dehydrogenase Complex)	8.18E00	<i>PDHA1, DLAT, DLD, DBT, PDHB</i>
Branched-chain α -keto acid Dehydrogenase	7.59E00	<i>DHTKD1, DLST, DLD, OGDH</i>
tRNA Charging	7.56E00	<i>PARS2, TARS2, IARS2, FARS2, CARS2, LARS2, EARS2, DARS2</i>
Ketolysis	7.41E00	<i>HADHB, BDH1, ACAT1, OXCT1, HADHA</i>
Fatty Acid β -oxidation I	7.1E00	<i>HADHB, ECHS1, AUH, IVD, ACADM, ACAA2, HADHA</i>
2-oxobutanoate Degradation I	6.89E00	<i>PCCA, DLD, PCCB, MUT</i>
Histamine Degradation	6.42E00	<i>ALDH4A1, ALDH1B1, ALDH2, ALDH9A1, ALDH7A1</i>
Oxidative Ethanol Degradation III	5.9E00	<i>ALDH4A1, ALDH1B1, ALDH2, ALDH9A1, ALDH7A1</i>
Putrescine Degradation III	5.75E00	<i>ALDH4A1, ALDH1B1, ALDH2, ALDH9A1, ALDH7A1</i>
Superpathway of Methionine Degradation	5.64E00	<i>PCCA, DLD, PCCB, MUT, FTSJ2, SUOX</i>
Tryptophan Degradation X (Mammalian, via	5.62E00	<i>ALDH4A1, ALDH1B1, ALDH2, ALDH9A1, ALDH7A1</i>

Table 14: The top 17 function and diseases pathways identified with Ingenuity Pathway Analysis

Diseases or Functions	p-Value	Molecules
Mitochondrial disorder	1.25E-34	<i>AGK,AIFM1,ATP5A1,ATPAF2,C10orf2,COX15,EARS2,ELAC2,FARS2,FOXRED1,FXN,GFM1,IBA57,LRPPRC,MRPL44,NDUFA10,NDUFA9,NDUFAF5,NDUFS1,NDUFS2,NDUFS7,NDUFV1,NUBPL,OPA1,PC,PCK2,PDHA1,PNPT1,PUS1,SCO1,SDHA,TMEM70,TSFM</i>
Inborn error of amino acid metabolism	5.17E-25	<i>ABAT,ACAT1,ACSF3,ALDH4A1,ALDH5A1,ALDH6A1,BCKDHA,BCKDHB,DBT,DLD,ETFA,ETFDH,GATM,GLDC,GLUD1,IVD,MCCC1,MCCC2,MMAA,MUT,OGDH,PCCA,PCCB,SUGCT,SUOX</i>
Organic aciduria	1.56E-24	<i>ACSF3,BCKDHA,BCKDHB,D2HGDH,DBT,DLD,ETFA,ETFDH,IDH2,IVD,L2HGDH,MCCC1,MCCC2,MMAA,MUT,OGDH,PCCA,PCCB,SUGCT</i>
Aciduria	1.79E-24	<i>ACADL,ACSF3,BCKDHA,BCKDHB,D2HGDH,DBT,DHTKD1,DLD,ETFA,ETFDH,IDH2,IVD,L2HGDH,MCCC1,MCCC2,MMAA,MUT,OGDH,PCCA,PCCB,SUGCT</i>
Fatty acid oxidation disorder	1.55E-18	<i>ACAD8,ACADM,ACADS,ACADVL,ACSF3,CPT2,ETFA,ETFDH,HADHA,HADHB,OGDH,OXCT1,SUGCT</i>
Mitochondrial respiratory chain deficiency	2.57E-16	<i>ATP5A1,ATPAF2,FOXRED1,LRPPRC,NDUFA10,NDUFA9,NDUFAF5,NDUFS1,NDUFS2,NDUFS7,NDUFV1,NUBPL,SCO1,SDHA,TMEM70</i>
Metabolism of amino acids	5.78E-16	<i>ABAT,ALDH18A1,ALDH5A1,ALDH6A1,BCAT2,BCKDHA,BCKDHB,BCKDK,BPHL,CKMT1A/CKMT1B,GATM,GLDC,GLS,GLUD1,HIBADH,IVD,MCCC2,ME2,NFS1,OAT,PCCA,PCCB</i>
Catabolism of branched-chain amino acids	5.56E-15	<i>ALDH6A1,BCAT2,BCKDHA,BCKDHB,BCKDK,HIBADH,IVD,MCCC2</i>
Degradation of amino acids	8.97E-14	<i>ABAT,ALDH5A1,ALDH6A1,BCAT2,BCKDHA,BCKDHB,BCKDK,GLS,GLUD1,HIBADH,IVD,MCCC2,PCCA,PCCB</i>
Catabolism of amino acids	4.15E-13	<i>ALDH5A1,ALDH6A1,BCAT2,BCKDHA,BCKDHB,BCKDK,GLS,GLUD1,HIBADH,IVD,MCCC2,PCCA,PCCB</i>
Beta-oxidation of fatty acid	3.54E-12	<i>ACAA2,ACADL,ACADM,ACADS,ACADSB,ACADVL,CPT2,DECRI,ECHS1,HADHA,HADHB,LRPPRC,TK2</i>
Oxidative phosphorylation deficiency	4.18E-11	<i>AIFM1,EARS2,ELAC2,FARS2,GFM1,MRPL44,PNPT1,TSFM</i>
Urination disorder	1.48E-10	<i>ACADL,ACSF3,AKR1B1,BCAT2,BCKDHA,BCKDHB,D2HGDH,DBT,DHTKD1,DLD,ETFA,ETFDH,IDH2,IVD,L2HGDH,MCCC1,MCCC2,MMAA,MUT,OGDH,PCCA,PCCB,SUGCT</i>
Mitochondrial complex I deficiency	2.28E-10	<i>FOXRED1,NDUFA10,NDUFA9,NDUFAF5,NDUFS1,NDUFS2,NDUFS7,NDUFV1,NUBPL</i>
Mitochondrial myopathy	2.30E-10	<i>AIFM1,COX15,FOXRED1,LRPPRC,NDUFA10,NDUFA9,NDUFS7,PDHA1,PUS1,SDHA,TMEM70</i>
Mitochondrial encephalomyopathy	6.23E-10	<i>AIFM1,COX15,FOXRED1,LRPPRC,NDUFA10,NDUFA9,NDUFS7,PDHA1,SDHA,TMEM70</i>
Leigh syndrome	1.56E-09	<i>COX15,FOXRED1,LRPPRC,NDUFA10,NDUFA9,NDUFS7,PDHA1,SDHA</i>



00280 10/22/14
(c) Kanehisa Laboratories

- Gene product, most protein but include RNA
- Organism specific pathway, human in this case
- Other molecules, mostly chemical compound
- Protein product of mRNA bound by CLUH
- Molecular interaction or relation
- Protein product of mRNA not bound by CLUH
- Link to another map
- Metabolic pathways
- ABC Name of protein product bound by CLUH

Figure 15: Highlight of protein products of mRNAs bound by CLUH involved in branched-chain amino acids metabolism pathway. Created by KEGG pathway.

4.5 The mRNA of the cytosolic protein astrin is bound by CLUH

Among many of the highly enriched mRNAs bound by CLUH (Table 11), one mRNA of a cytosolic protein caught our attention: *SPAG5*. Work carried out in our lab has identified the protein product of this mRNA to be an interactor of CLUH (Désirée Schatton, personal communication). Astrin is involved in mitosis and the mTOR pathway (Mack and Compton 2001; Thedieck, Holzwarth et al. 2013). *SPAG5* mRNA binding by CLUH was also validated with qRT-PCR performed on RNA immunoprecipitated by anti-CLUH antibodies (Figure 18 A and B).

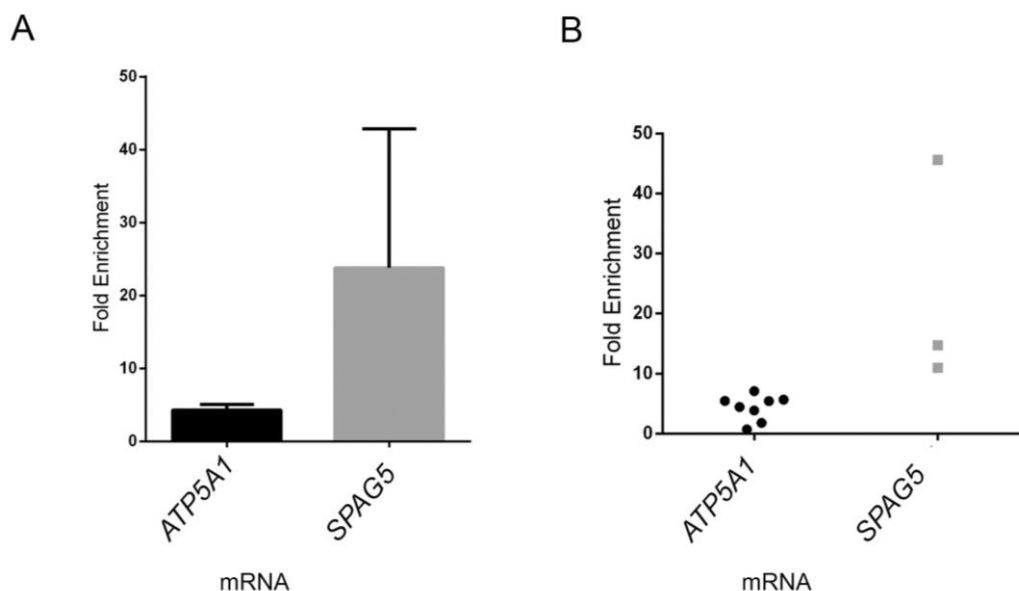


Figure 18: Validation of *SPAG5* bound by CLUH. (A) The average enrichment for each mRNA. (B) The plot of fold enrichment from individual experiment for each gene. Fold enrichment is compared with the immunoprecipitation with anti-Afg311 antibody. $n \geq 3$

4.6 CLUH affects the protein level of its mRNA targets

mRNA binding proteins can facilitate the transport of mRNAs to their destinations or regulate the half-life and translation of mRNAs in response to cellular cues or anchoring mRNAs to their destination. Therefore, we started with investigating the possible role of

CLUH in regulating translation of its target mRNAs. First, we evaluated if CLUH affects the steady state protein level of its targets. Dr. Henriette Hansen in our lab had previously generated the immortalized MEFs from wildtype and *Cluh* knockout embryos at E14.5 of age by C-section.

The protein level of some targets were examined from two pairs of wildtype and *Cluh* knockout MEFs: OGDH, ATP5A1, AFG3L2, OPA1, SDHA and UQCRC2 (Figure 19 A). Pan-actin and GAPDH was used here as a loading control, TOM20 was used as a control for mitochondrial mass. The protein levels of the tested targets were reduced with the exception of SDHA and UQCRC2. However, the levels of SDHA and UQCRC2 were significantly decreased in the liver of CLUH knockout (personal communication with Désirée Schatton). Mitochondrial mass, did not seem to be altered as indicated by TOM20.

Since the decrease of transcript levels can also lead to reduction of the respective protein level, initial investigation was conducted on the transcript level of *Atp5a1* and *Afg3l2* in these MEFs using qRT-PCR. The mRNA levels of tested CLUH targets remain unchanged with the notable exception of *Atp5a1* (Figure 19 B, more qRT-PCR data can be found from Gao et al. 2014, conducted by Désirée Schatton), hinting to a possible role of CLUH in regulating the translation of its targets at different levels.

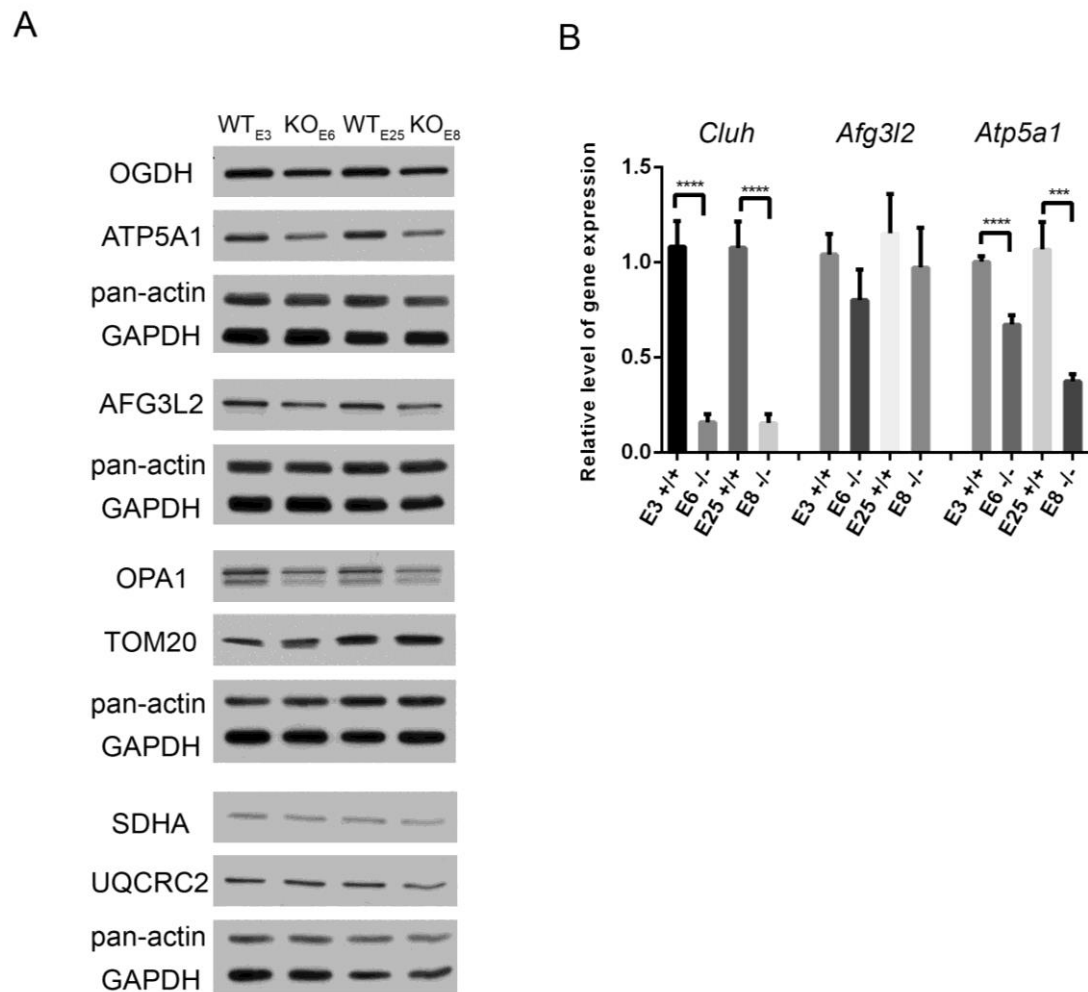


Figure 19: CLUH affects the protein levels of its target mRNAs. (A) Four immortalised MEF lines were generated by Dr. Hansen, E3 and E25 are the wildtypes whereas E6 and E8 are the *Cluh* knockout. The protein levels of CLUH targets were tested by western blots, pan-actin and GAPDH were used as loading controls. (B) The mRNA levels of *Atp5a1*, and *Afg3l2* were measured with q RT-PCR with *Gapdh* as an endogenous control.

4.7 CLUH overexpression upregulates the protein level of some of its targets

Does CLUH overexpression lead to the opposite effect in contrast to *Cluh* knockout? To address this, CLUH with a C-terminal FLAG tag was overexpressed by induction of HEK 293T with 1 $\mu\text{g/ml}$ of tetracycline for different time. Four target proteins were selected here to examine their response to CLUH overexpression: ATP5A1, HADHA, astrin and OPA1. However they display three different responses to the increase of CLUH: ATP5A1 remains mostly unchanged while OPA1 is increased, and to our

surprise, HADHA is decreased (Figure 20). When comparing the expression level of these proteins at different time points, a non-linear relationship between CLUH expression level and the level of its targets was observed (see OPA1 from time 0 to 16 h to 48 h). On the other hand, CLUH cytosolic target astrin (the upper band) is in a linear relationship with CLUH.

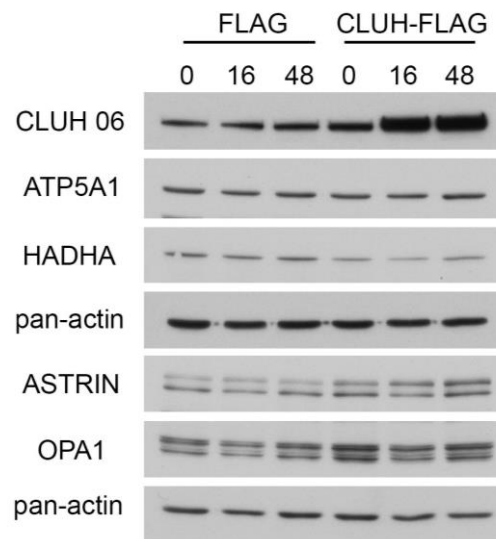


Figure 20: CLUH overexpression induces different target responses. (A) CLUH-FLAG and empty FLAG were expressed with induction of 1 $\mu\text{g/ml}$ of tetracycline for different times points. Same volume of EtOH was added to HEK 293T as a control (final concentration 0.18 %). $n=3$, see appendix Figure 34 for the other two repeats.

4.8 Global cytosolic translation is unaffected in the absence of CLUH

Since yeast Clu1 has been identified to be associated with the translation initiation factor 3 (Vornlocher, Hanachi et al. 1999), it is crucial to examine if the reduction in steady state protein levels in CLUH deficient cells is due to a general defect in translation. Two approaches were undertaken here: first, radioactive ^{35}S methionine /cysteine was fed to cells in order to incorporate it into newly synthesised proteins. The total protein lysate was then resolved by SDS-PAGE and revealed with autoradiogram (Figure 21 A and C). Secondly, cells were treated with cycloheximide, a translation elongation inhibitor in order to stabilise the 80S and the polysome, followed by mild

cell lysis to minimise the damage to the integrity of the ribosomes. The lysate was then subjected to sucrose gradient ultracentrifugation for the separation of 40S, 60S, 80S and polysome (Figure 21 B and D). The first method provides a general impression as to whether the translation is impaired, whereas polysome profiling provides higher resolution at which step that translation might be affected.

The two methods were used in parallel in cells either transiently (knockdown for 72 hours with different siRNA combinations in murine NSC34 cells, Figure 21A and B) or permanently (MEFs, Figure 21C and D) depleted of CLUH to exclude compensatory cellular responses from the loss of CLUH. There were no major changes of newly synthesised proteins or in the translation machinery: equal amount of proteins were synthesised at different time points and the traits of 40S, 60S, 80S and polysomes appeared to be almost identical between control and CLUH depleted cells. These results are consistent with the studies in yeast (Vornlocher, Hanachi et al. 1999) and the observation of normal growth rate and viability in *S. cerevisiae* (Fields, Conrad et al. 1998). In conclusion, CLUH depletion/deletion does not affect the cytosolic translation in general, therefore hinted that CLUH may act as a specific translation regulator for its targets.

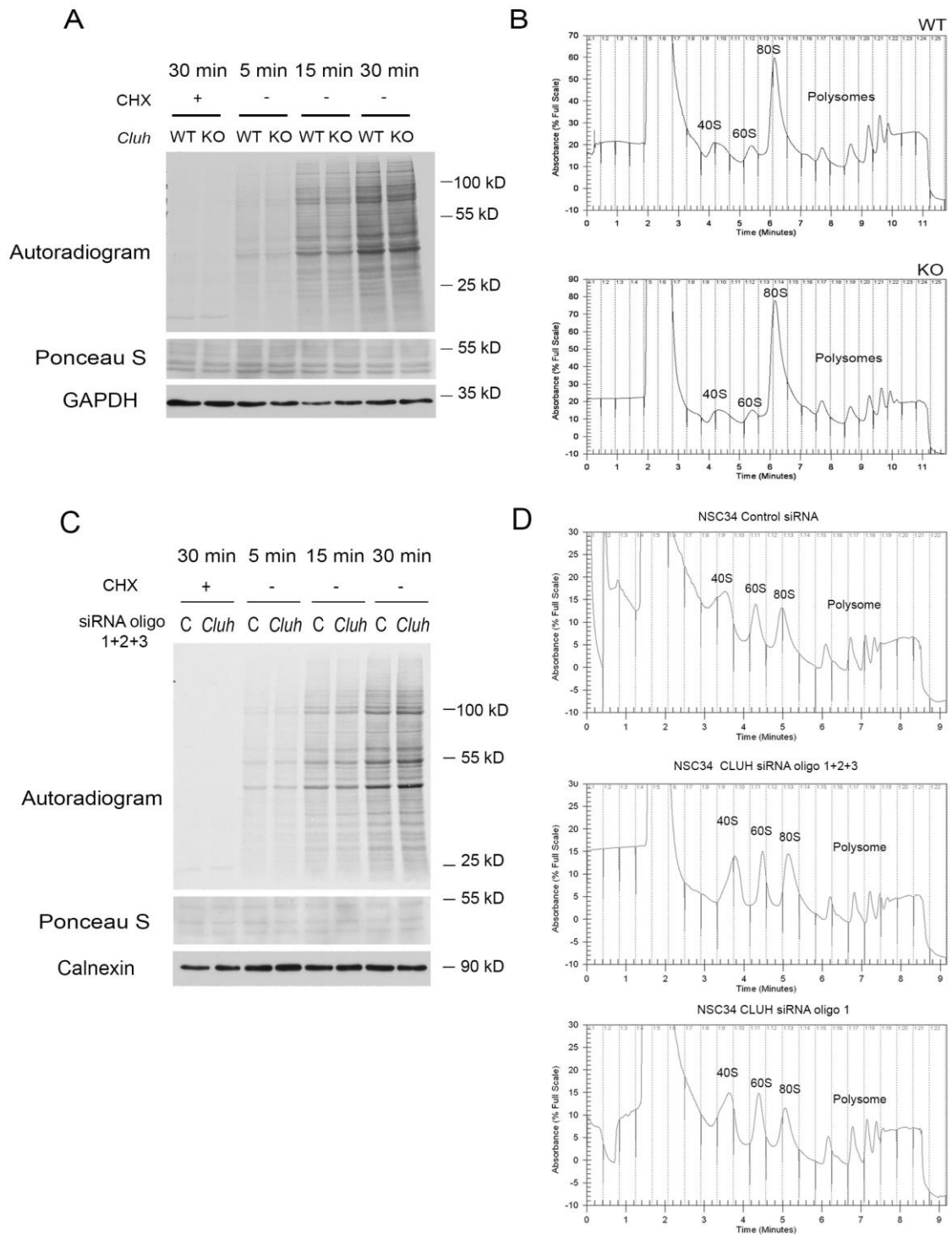


Figure 21: Global cellular translation is unaffected in the absence of CLUH. (A and C) Autoradiogram of *in vitro* translation assay in MEFs and NSC34 cells, showed no major change in the *Cluh* knockout and knockdown, respectively. (B and D) Polysome profilings consistently showed no obvious alterations in general translation machinery.

4.9 Translation of CLUH targets is affected

Since the steady state levels of CLUH targets were significantly reduced. We propose that CLUH is a positive translational regulator of its target mRNAs. That is in the absence of CLUH, translation of its targets is affected. To assess this question, methionine analogues L-azidohomoalanine (AHA) was used to incorporate into the nascent proteins similar to *in vitro* translation assay mentioned above. This was followed by copper catalysed click reaction that adds biotin to AHA modified proteins (Figure 22A). The nascent biotinylated proteins were then captured with magnetic beads coupled with streptavidin. To determine the translation of a particular protein, two parameters must be taken into account: the amount of protein being translated and its respective mRNA levels. The transcript levels of the tested targets *Sdha* (0.66), *Atp5a1* (0.48) and *Ogdh* (0.49) were reduced in *Cluh* knockout MEFs compared to the control. So were the target protein levels. However, the reduction of transcription could not be responsible for the reduction of their proteins levels for SDHA, ATP5A1 and OGDH. Moreover, the non-target mitochondrial control of TOM20 and housekeeping GAPDH were not affected. Therefore, CLUH is likely to affect the translation of SDHA, ATP5A1 and OGDH specifically. However, the exact mechanism needs to be elucidated further. The next step would be to conduct a systematic analysis to understand if the translation of all targets is affected, this can be achieved by using either ribosome profiling or polysome profiling coupled with RNA-sequencing.

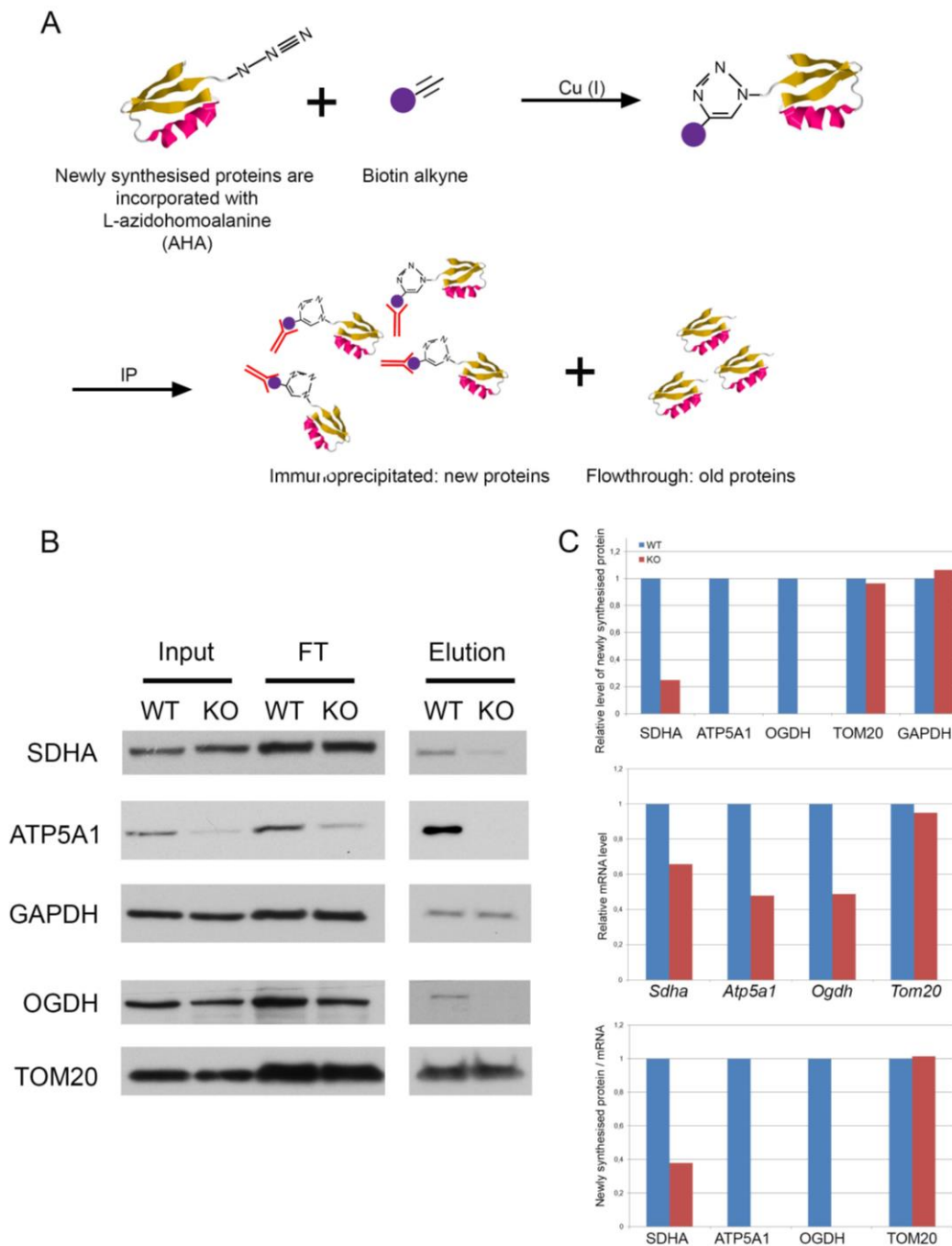


Figure 22: The translation of CLUH targets is affected in the absence of CLUH. (A) Brief illustration of the experimental procedure. (B) Western blot of input, flowthrough and elution decorated with antibodies against the protein products of different CLUH targets, GAPDH is a cytosolic non-target control and TOM20 is a mitochondrial non-target control. (C) Quantification of the newly synthesised proteins (elution) of knockout against wildtype. Quantification of transcript levels measured by qRT-PCR. The transcripts were normalized to GAPDH. The normalised transcripts level in knockout was compared to wildtype. Translational arrest was estimated by normalizing the protein level to the mRNA level. n=1

4.10 Localisation of CLUH

CLUH does not contain any mitochondrial targeting signal (MTS) when analysed with Predotar, TargetP and MitoProt (Table 15). Moreover, it is a cytosolic protein from various immunocytochemistry studies performed in different organisms. Intriguingly, Clu particles are found to be at the close proximity to mitochondria in flies (Cox and Spradling 2009). Since CLUH binds to the mRNAs of NEMP and might regulate their translation specifically, this suggests that it is possible that a small portion of CLUH can be located outside or close to mitochondria in order to deliver the mRNAs/proteins close to mitochondria. Therefore, we investigated if a population of CLUH proteins is located close to mitochondria.

Table 15 : Mitochondrial proteins prediction with different online tools for CLUH.

Predotar	Mitochondrial	ER	Elsewhere	Prediction	
	0,00	0,01	0,99	none	
TargetP 1.1	mTP	SP	other	Loc	RC
	0,063	0,062	0,937	-	1
MitoProt II	Probability of export to mitochondria				
	0,023				

mTp, mitochondrial targeting peptide; SP, signal peptide; Loc, prediction of localization; RC, reliability class, from 1 to 5, with 1 being the most reliable.

To examine the subcellular localisation of CLUH, we employed immunocytochemistry with specific antibody against human CLUH in HeLa Cells. CLUH (red) in HeLa cells formed puncta/granular structure in the cytoplasm with no obvious colocalisation to mitochondria (anti-COX1, green) in culturing conditions containing either high glucose or galactose (condition to enhance OXPHOS) (Figure 23). Sometimes, orange colors were observed in the merged images that indicating a colocalisation of CLUH with mitochondria. However, it is not clear if this is a genuine colocalisation, because CLUH

is an abundant cytosolic protein, it may be present in a similar space with mitochondria without colocalising with mitochondria.

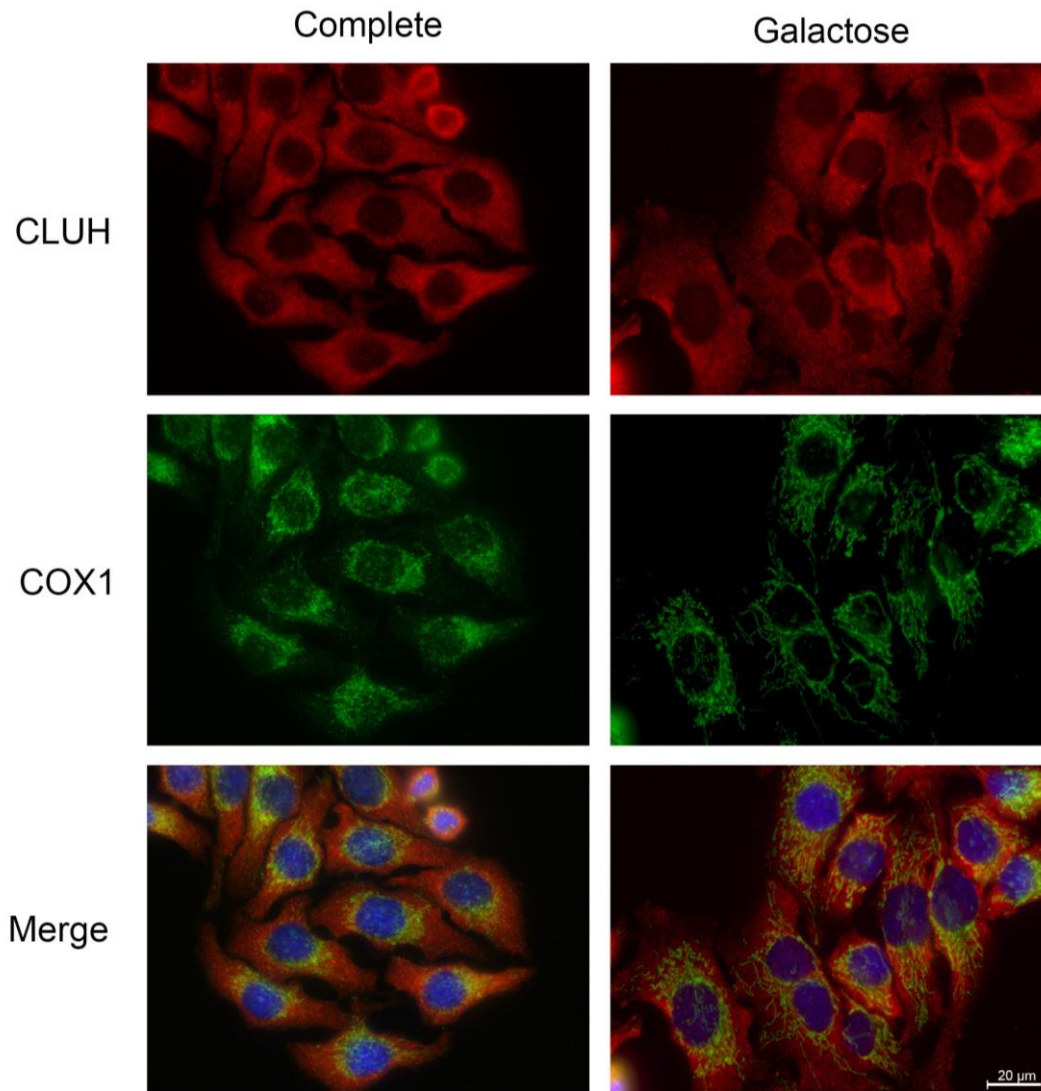


Figure 23 : CLUH does not show obvious colocalisation with mitochondria in immunocytochemistry. HeLa cells were cultured either with complete or galactose media for 72 hours. CLUH was decorated with anti-CLUH 06 (c-ter) antibody, red. Mitochondria were stained with anti-COX1, green, and nuclei with DAPI, blue. Bar: 20 μM.

To validate these data, crude cell fractionation was performed to enrich mitochondria and separate cytosol from the light membrane fraction (Figure 24). Mitochondria were enriched, as indicated by SDHA. However, this fraction was contaminated with ER, as indicated by the presence of POR. The majority of CLUH was present in the light membrane fraction, which also contained ribosomes (RPL7) and ER membranes (POR).

However, a small portion of CLUH was observed in the mitochondrial fraction in mouse liver, brain (Figure 24A), and cultured primary MEFs (Figure 24B). The ribosomal large subunit RPL7 shared a similar localisation pattern to CLUH in both brain and liver. In the crude fractionation of *Cluh* knockout primary MEFs, CLUH was absent at the expected size (Figure 24B).

At this point, it is impossible to distinguish if CLUH is a genuine protein that resides outside of mitochondria or if it is a contamination rooted from the failure of obtaining an absolute mitochondrial fraction completely devoid of ER components.

Considering that CLUH might associate with the translation initiation factor (Vornlocher, Hanachi et al. 1999), polysome profiling was performed to evaluate whether CLUH peaks with any of the translational components such as EIF3G, RPS6 and RPL7 (Figure 24C). RPS6, a component of small ribosome was located in the expected fractions: the 40S, 80S and the polysomes. RPL7, the component of the large ribosome was located in the 80S and polysomes. The subunit of translation initiation factor EIF3G cofractionated with 40S and 60S but was depleted from the polysome fractions. Despite the fact that the majority of CLUH was present in the light membrane fraction in the crude fractionation, CLUH peaked at the non-ribosomal fractions. Some CLUH might form heavier complexes, which could be seen in the later fractions. In conclusion, this hinted that CLUH is not a main component of the translation machinery, which is in line with the evidence that yeast *Clu* and mammalian CLUH are not essential components of eIF3 complex and is not essential for general translation (Browning, Gallie et al. ; Vornlocher, Hanachi et al. 1999; Fields, Arana et al. 2002).

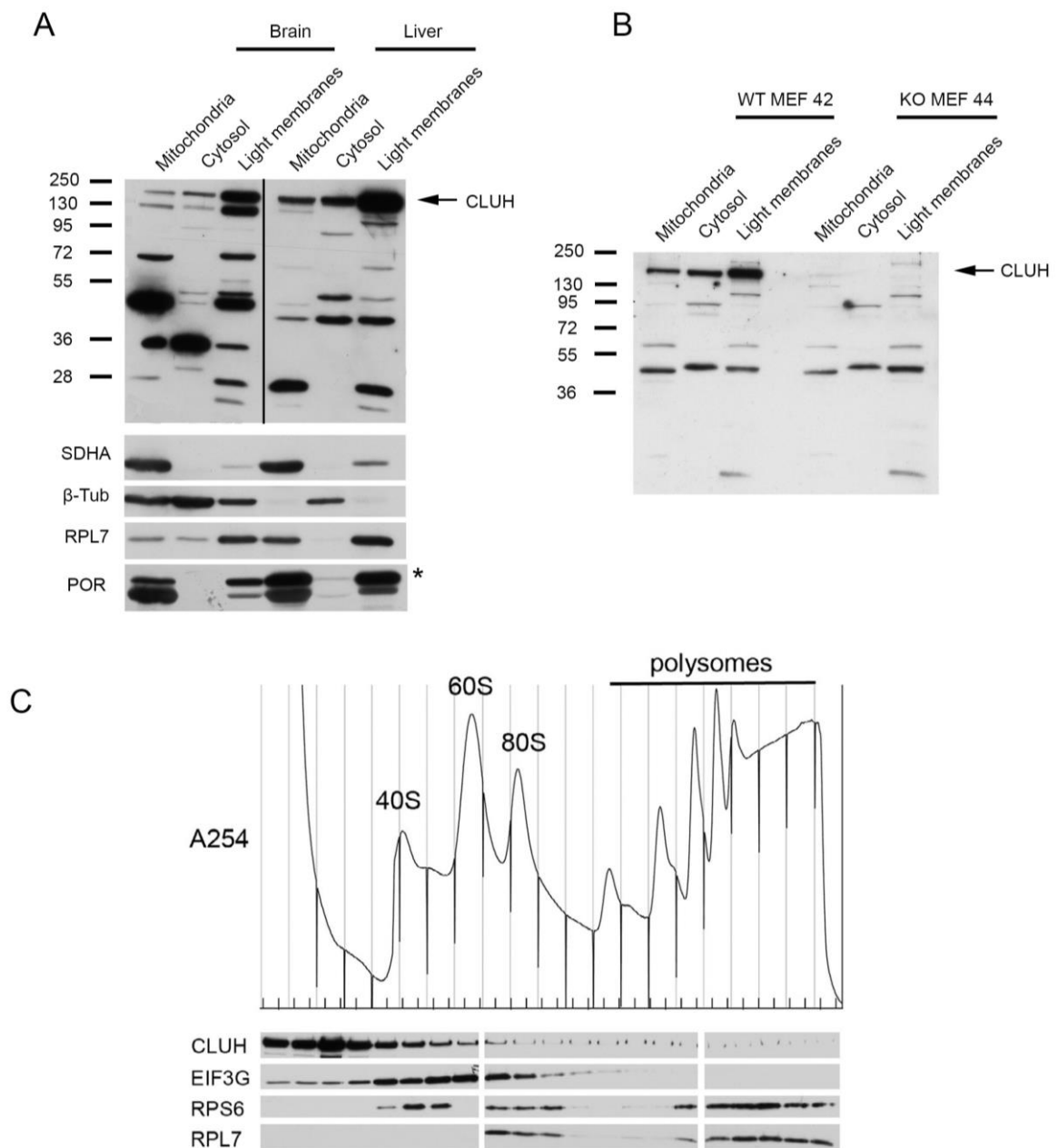


Figure 24: A small portion of CLUH is found to co-fractionate with mitochondria. (A) Crude cellular fractionation of murine brain and liver. Anti-CLUH (N-ter, CLUH 05) was used to decorate the whole membrane. SDHA, β -tub and RPL7 were used as a cocktail. POR was probed afterwards. * indicates that POR at its expected size (B) Crude cellular fractionation of primary MEFs. Arrow indicates CLUH at the expected size. Asterisk indicates the POR at expected size, the other band is the leftover signal from SDHA. (C) Polysome profiling of cell lysate from HeLa. The upper part shows the UV absorbance whereas the lower part, the western blot of corresponding fractions probed with translation related markers.

4.11 CLUH level in response to galactose and acetoacetate treatment

CLUH binds to the mRNAs of NEMPs and regulates their translation by an unknown mechanism, but is CLUH an essential component for mitochondrial biogenesis? ATP can be produced from different sources, for example: amino acids, fatty acids or glucose. As mentioned above, CLUH binds to many mRNAs involved in energy production from different carbon sources. Routine culturing media contain high concentrations of glucose (4.5g/L), which renders the cells to rely on glycolysis for energy supply. Different metabolite media were used here to shift the ATP production from glycolysis to OXPHOS. Galactose medium, containing galactose (the C-4 epimer of glucose) and glutamine was used to “push” OXPHOS provided by glutamine-driven oxidative phosphorylation (Reitzer, Wice et al. 1979).

When HeLa cells were forced to use OXPHOS when cultured in galactose (or under starvation of glucose), the cytosolic translation components EIF3G and RPL7 were not affected in large (Figure 25A). Mitochondrial biogenesis occurred after 24 hours as indicated by the increase of ATP5A1 and SDHA. Galactose treatment resulted in a starvation response and autophagy was triggered as indicated by LC3-II activation which is consistent with previous report (Melser, Chatelain et al. 2013). During prolonged starvation, LC3-II was persistently activated compared to that without galactose treatment. P62, also known as sequestosome 1, can bind to ubiquitinated proteins and LC3-II directly (Chang, Huang et al. 2001) and this interaction leads to degradation by autophagy. When autophagy is ablated, p62 accumulates and forms p62-positive inclusion bodies (Mack and Compton 2001). The steady state levels of p62 were relatively stable in comparison to LC3. Starvation induced autophagy is mediated via mTORC1 inhibition (Valente, Abou-Sleiman et al. 2004), as shown by the decrease of phosphorylation state of mTORC1 substrate S6K1, (S6K1^{Thr389}).

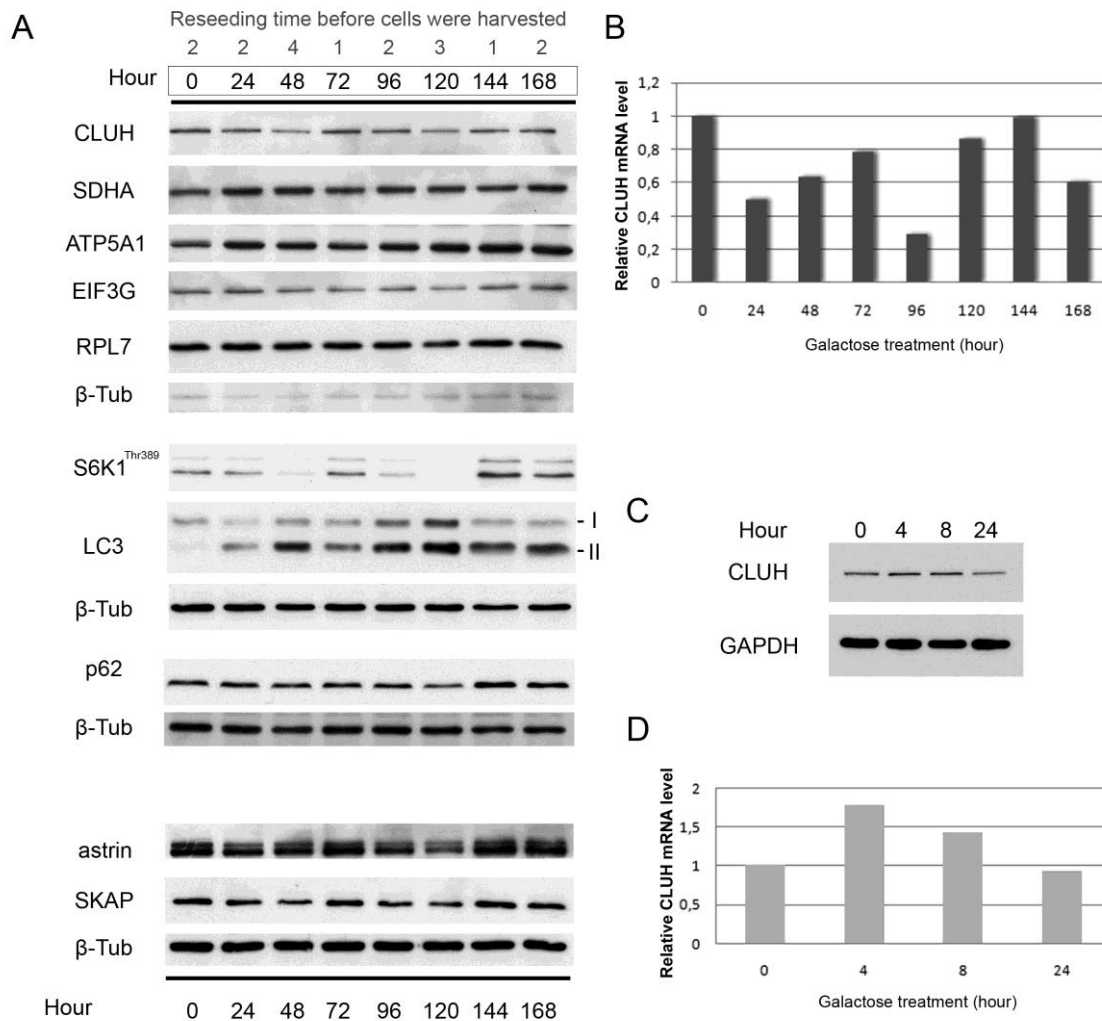


Figure 25: CLUH level fluctuates with galactose treatment at different time points. (A) Western blot of HeLa cell lysate treated with galactose media for different times. (B) CLUH mRNA levels measured with qRT-PCR relative to GAPDH. Samples for A and B were from the same treatment. n=1 (C) CLUH level in HeLa cells in short-term galactose treatment. n=1 (D) CLUH transcript level measured with qRT-PCR relative to GAPDH.

Intriguingly, CLUH responded to the time course treatment in an on-and-off manner, in both the protein and mRNA levels (Figure 25A and B). Increase of CLUH and mitochondrial proteins did not occur at the same time, moreover the increase of CLUH level seemed to precede the increase of mitochondrial proteins, ATP5A1 and SDHA (See CLUH level at 72 hours and 144 hours and SDHA at 96 hours and 168 hours.). With galactose treatment, astrin followed the same trend as CLUH, this was also true for SKAP, the interactor of astrin (Clark, Dodson et al. 2006) and CLUH (Désirée

Schatton, personal communication). Interestingly, CLUH changes overlap the changes seen in mTORC1 activity as indicated by S6K1^{Thr389}.

Briefly, in conclusion, under starvation or metabolic challenges, the mTORC1 pathway was inhibited in order to activate autophagy and provide cells with nutrients, the protein levels of CLUH and its interactors followed the same pattern as mTORC1 while CLUH targets were elevated after the increase of CLUH. Importantly, CLUH was not upregulated in routine galactose treatment time course (i.e. compare 48 hour to time 0, CLUH level is decreased, this is reproducible in MEF, COS7 and HeLa cells. Data is not shown). Moreover, this regulation is most likely to be transcriptional since the mRNA level of CLUH also changed with time. However, the rise of mRNA level did not completely correspond to the rise of its protein level (compare the mRNA and protein level in 48 hours and 120 hours). Interestingly, response of CLUH, astrin, SKAP, mitochondrial protein, mTORC1 and LC3-II also correlated with the reseeding time of the cells. This complicates the interpretation of whether the fluctuation responses were due to the availability of nutrients, cell densities or the cell cycle.

Nevertheless, the protein level of CLUH was reduced when treated with galactose. This outcome is very puzzling since CLUH binds specifically to mRNA of NEMPs and the steady state protein level of the targets was reduced in the absence of CLUH. These data support a role of CLUH in mitochondrial biogenesis. Therefore, an attempt was made to find the possible reasons: is RBP protein involved in translation expressed before its transcripts? Indeed, CLUH level increased as early as four hours with galactose treatment and lasted until eight hours, however at the same time point, its mRNA level already started to decline at 8 hours and remained even lower at 24 hours (Figure 25C and D). In conclusion, it is conceivable to propose that the protein level of CLUH increases soon after the switch from glucose to galactose. Instead of remaining at the increased level, CLUH level declined with prolonged galactose treatment. The reason for the decline remains hidden.

Therefore, to understand the relationship between CLUH and mitochondrial biogenesis, we explored the question from a different angle: regardless of the changes of the protein level of CLUH in response to galactose, do the protein levels of CLUH target increase in the absence of CLUH? ATP5A1 was used here as a marker of mitochondrial

biogenesis (Short time course galactose treatment in MEFs was conducted in collaboration with Dr. David Pla-Martin). As observed in HeLa cells (Figure 25C), CLUH in wildtype MEF increased gradually from 4-16 hours and then decreased at 24 hours (Figure 26A and B). However, this result was not statistically significant when comparing each time point to time 0. Furthermore, ATP5A1 level remained low in each time point in the knockout comparing to the wildtype (Figure 26A and C). This suggests that in the absence of CLUH, mitochondria might encounter difficulty with replenishing themselves with new proteins.

MEFs were also treated with acetoacetate, a ketone body in order to switch ATP production from glycolysis to OXPHOS. Acetoacetate enters the TCA cycle by converting to acetyl-CoA by a process called ketolysis. NADH and FADH₂ are then utilised to produce ATP. In addition to this, genes involved in ketolysis pathway were also found to be targets of CLUH (Table 13). These genes are *HADHA*, *HADHB*, *BDH1*, *ACAT1* and *OXCT1*.

In average, CLUH levels decreased after 4 and 8 hours of supply of acetoacetate followed by increase from 16-24 hours (Figure 26D and E). The protein levels of HADHA fluctuated in the wildtype MEFs: its level declined at 4 hours significantly and increased from 8-24 hours (Figure 26D and F). The trend of HADHA was similar to that of CLUH. In contrast, in *Cluh* knockout, HADHA level remained low at each time point compared to the wildtype counterpart, and was further reduced at 24 hours. This might be due to two possibilities: either HADHA was sensitized by CLUH, that is without CLUH, HADHA failed to respond. Alternatively, HADHA responded to the change of carbon source 20 hours later in the knockout.

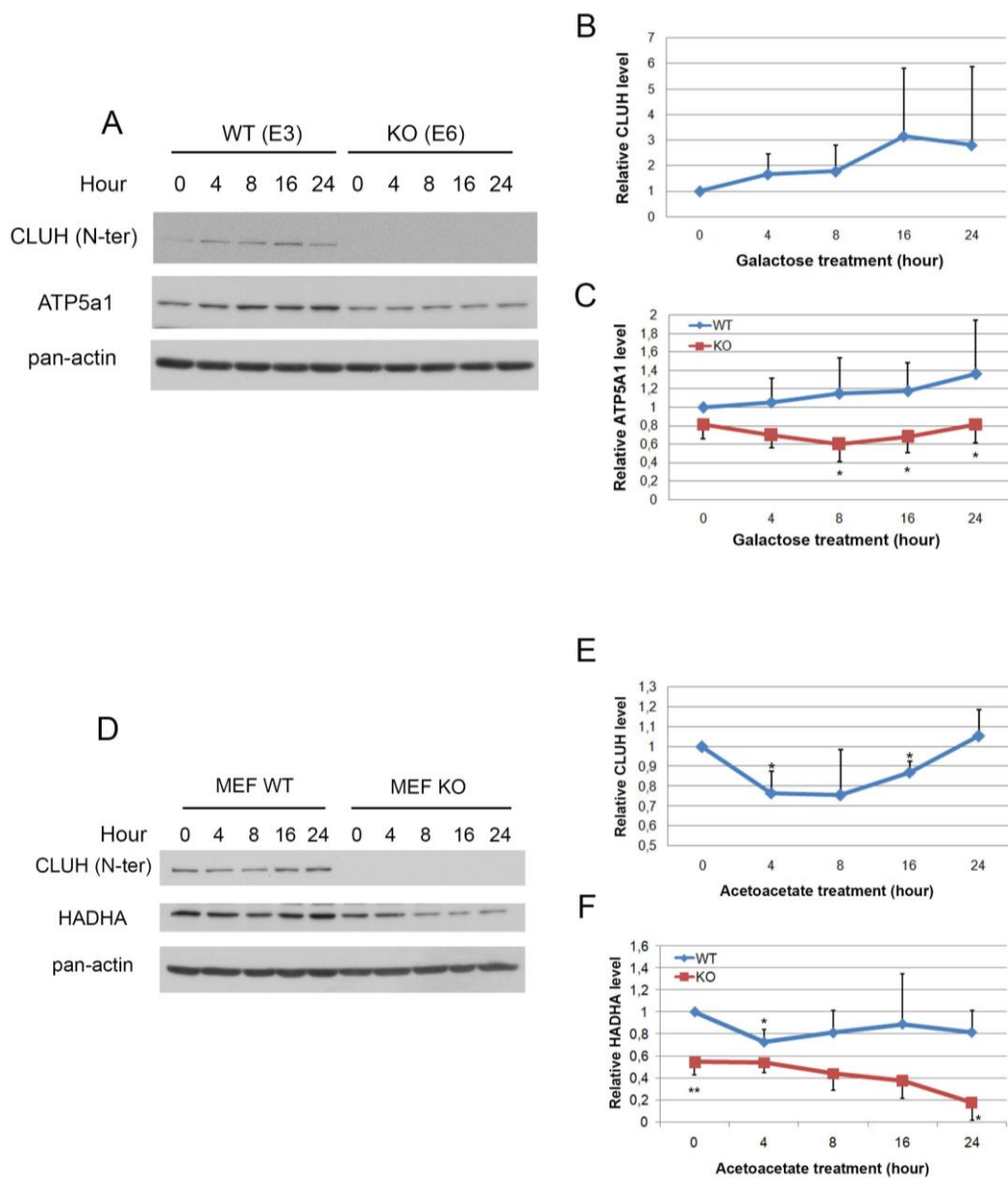


Figure 26: CLUH levels may increase as an early response. (A, B and C) Response of CLUH and its target ATP5A1 to galactose treatment in wildtype and *Cluh* knockout MEFs. (D E and F) Response of CLUH and its target HADHA to acetoacetate treatment treatment in wildtype and *Cluh* knockout MEFs. Quantifications were performed using ImageJ and then standardised to pan-actin and time 0 of wildtype, the protein level of each point of knockout was compared to the corresponding point in the wildtype. Error bar represents standard deviation * $p \leq 0.05$, ** $p \leq 0.01$.

4.12 CLUH protein level is reduced in PGC-1 α deficient MEFs

CLUH binds to a subset of NEMP mRNAs, the steady state protein level of these targets decreases upon CLUH deletion. It is then plausible to assume that CLUH and its targets could be regulated like many other mitochondrial genes under the control of major transcription coactivator PGC-1 α in the nucleus. To testify this, protein and mRNA levels of CLUH/*Cluh* in PGC-1 α knockout MEFs (kindly provided by Dr. Tina Wenz) were examined: in the absence of PGC-1 α , both the mRNA and the protein level of CLUH were reduced to 0.46 and 0.51, respectively (Figure 27A and B). The extent of reduction of mRNA approximates the one of the protein. In line with this, CLUH could be upregulated when cells were treated with bezafibrate (Figure 27D). Bezafibrate is a pan-PPAR agonist that was shown to increase the expression of PGC-1 α and is commonly used as a treatment for hyperlipidaemia (Tenenbaum, Motro et al. 2005; Bastin, Aubey et al. 2008; Srivastava, Diaz et al. 2009).

It is worth mentioning that, when MEFs were treated with DMSO, levels of CLUH and its targets (ATP5A1 and OPA1) were elevated. Treatment with 550 μ M of bezafibrate failed to induce the level of ATP5A1 or OPA1. In conclusion, bezafibrate was able to upregulate protein levels of CLUH additionally to that of DMSO. However, the upregulation of the two mitochondrial markers seemed to be mainly due to DMSO and bezafibrate did not give a cumulative result.

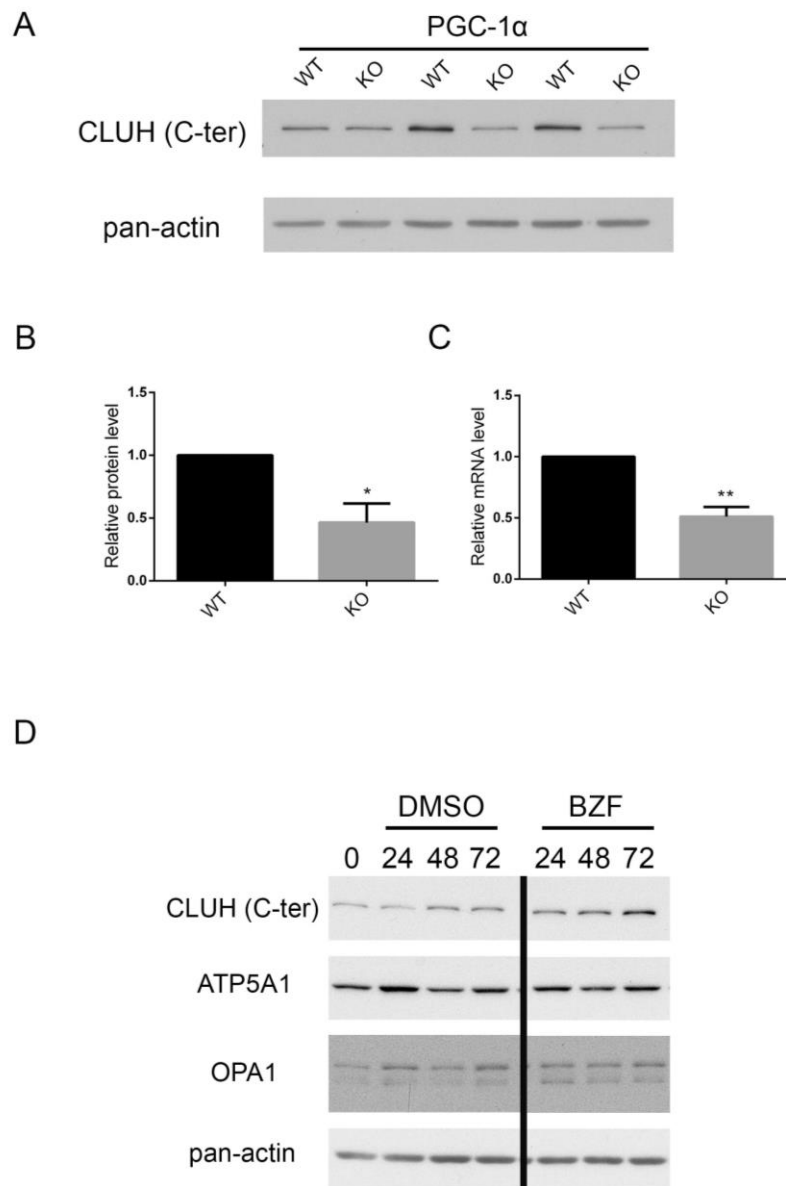


Figure 27: CLUH level is under the regulation of PGC-1 α . (A) CLUH protein level (with CLUH (c-ter), also known as CLUH 05) in PGC-1 α MEFs. WT and KO MEFs were collected at three different days and analysed by western blot. (B) Quantification of (A) relative to pan-actin. (C) Relative mRNA level of CLUH to β -actin. Error bar is standard deviation. * $p \leq 0.05$, ** $p \leq 0.01$. (D) Protein level of CLUH and targets of wildtype MEFs treated with either bezafibrate or its carrier DMSO (final concentration, 0.2 %) for different time points. The line indicates that the proteins were loaded on the same gel but some lanes were cutout in between.

4.13 CLUH levels in mouse liver during development and aging

Since CLUH level is sensitive to metabolic changes, and CLUH binds to many mRNAs involved in different metabolic pathways such as the TCA cycle, amino acid catabolism, it is plausible to postulate that either the protein or the mRNA, or both are subjected to regulation depending on the metabolic state of an organism. In *Dictyostelium*, the *cluA* mRNA increases in developing cells (Zhu, Hulen et al. 1997). The mRNA level of PGC-1 is elevated in mouse heart immediately after birth or 24 hours of fasting and this is coupled with the induction of mitochondrial genes (Lehman, Barger et al. 2000). The mRNA of HADHA is also induced in murine liver one day after birth (Ibdah, Paul et al. 2001). Therefore, the level of CLUH was examined in mouse liver at embryonic stage 18.5, two days after birth, 20 days and 20 weeks (Figure 28A and B). During development, there were extensive changes in the liver proteome as shown by the ponceau staining (Figure 28A). CLUH levels remained relatively constant until 20 weeks of age, however the protein levels of HADHA, PCB and ATP5A1 were upregulated two days after birth (Figure 28B) and then decreased at 20 weeks. This result raised the question of whether CLUH protein level fluctuates during early development and hence regulating the level of its target protein, however to address this, one needs to examine CLUH level at different hours or one day after birth or after starvation. It is worth noticing that at 20 weeks, the level of CLUH as well as its targets declined, whether CLUH is directly involved in this regulation is unknown. This observation has motivated me to examine the protein levels of the targets in the liver from *Cluh* knockout mice (Figure 28C and D). Since *Cluh* knockout mice died soon after birth, we could only obtain the organ at E18.5 by C-section. However, the protein levels of PCB (about 23 % remaining) and HADHA (about 21 % remaining) were both significantly decreased before birth.

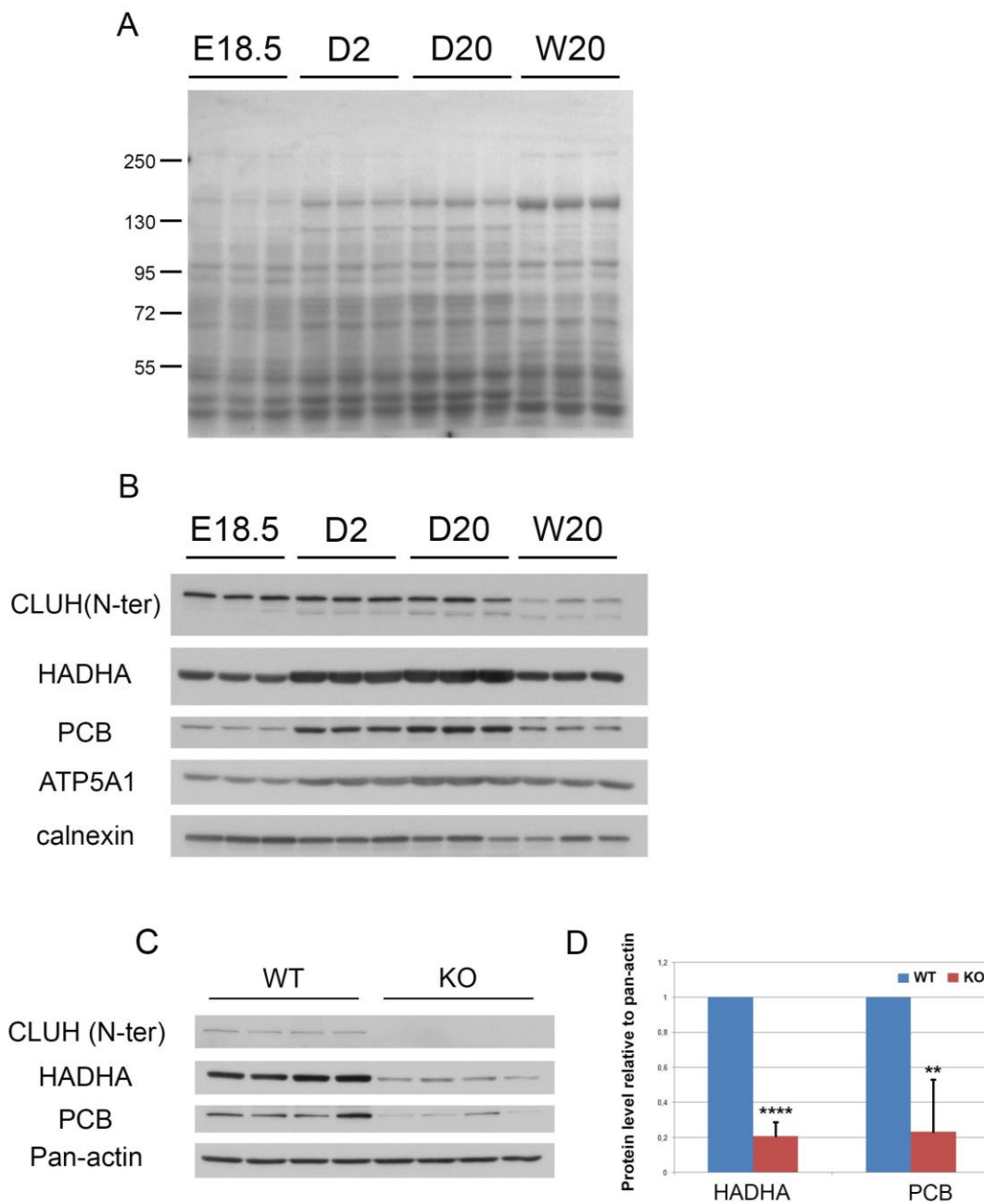


Figure 28: CLUH targets are subjected to developmental changes. (A) Ponceau staining of membrane in (B) showing the differences of total proteomes at different developmental stage of murine liver. (B) Western blot with CLUH targets decorated. (C and D) In the absence of CLUH in liver, CLUH targets level were decreased significantly. **** $p \leq 0.0001$, ** $p \leq 0.001$.

4.14 Identification of the function of CLUH protein domains

Despite the conservation of CLUH across evolution (introduction Figure 7), little is known regarding the function of its domains. As mentioned earlier, human CLUH is comprised of 1347 amino acids. Five protein domains can be identified by EMBL-EBI combined with NCBI Conserved Domains. CLU_N domain is also known as TIF31-like, eIF_ p135 domain is also known as CLU-central. In order to study the molecular function of CLUH, we established inducible HEK 293T cell lines that overexpress different CLUH deletion constructs lacking one or more identified domains (Figure 29A). All of the constructs were tagged with FLAG at their C-termini. The preliminary data showed that, after 16 hours of induction, the proteins can be overexpressed and this did not lead to obvious cell death (based on observation) in all clones for each construct. The respective proteins could be extracted with RIPA buffer (Figure 29B-E) however, the amount of the protein remaining in cell pellet after lysis was unknown, therefore it is not sure if all proteins could be solubilised by RIPA. All non-induced constructs were leaky; this could be seen in the non-induced lanes. The tagged proteins migrated according to their expected size: Δ 1021-1347 at 114 kDa and Δ 1-352 at 111 kDa, however Δ 801-1347 (expected: 89 kDa) and Δ 1-615 (expected: 81kDa), somehow shows a bigger than expected size. One clone of each constructs was chosen for further analysis and annotated later as “c1” or “c2”.

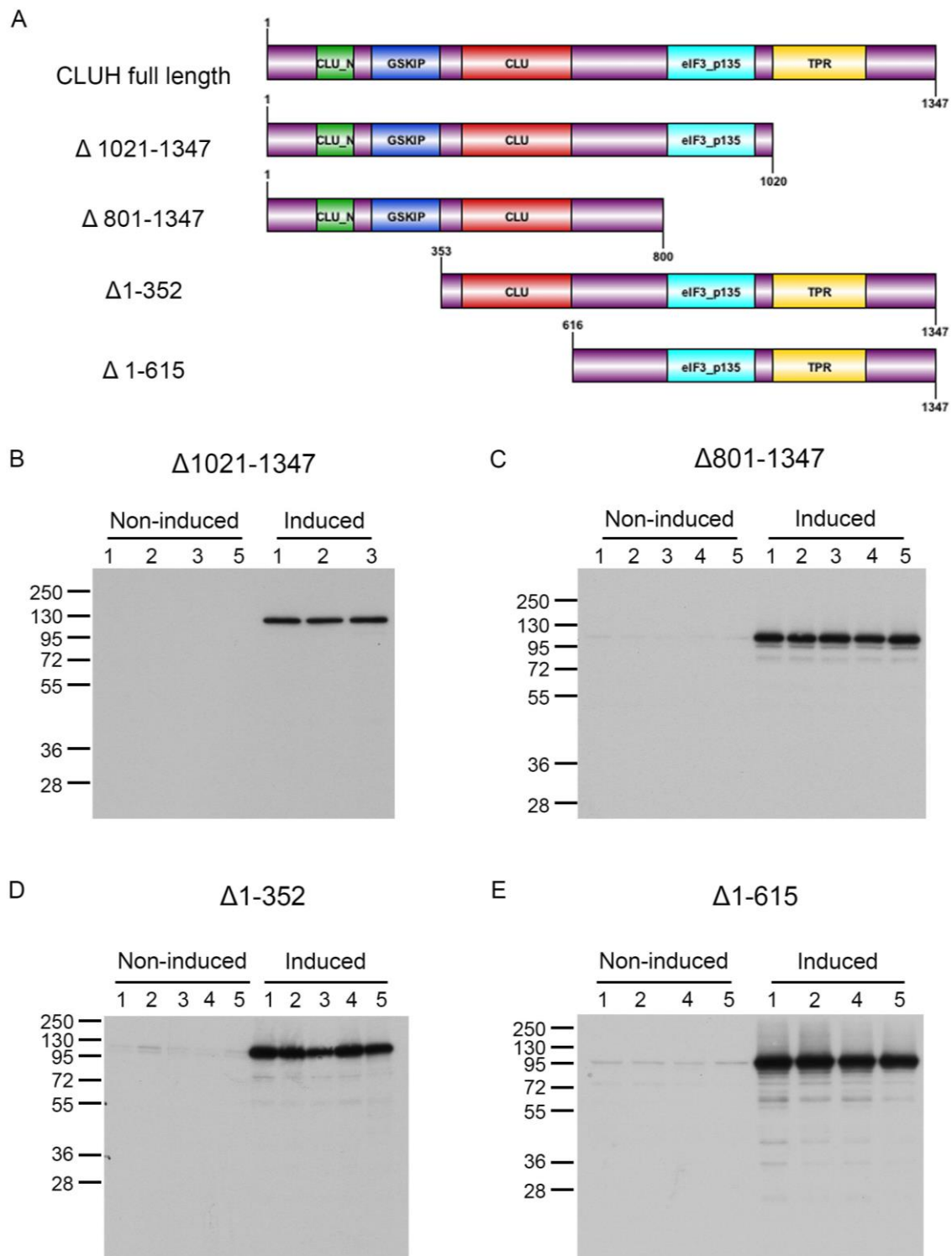


Figure 29: Generation of inducible HEK 293T cell lines with deletion of different domains of CLUH. (A) Illustration of the constructs. (B-E) Western blot with anti-FLAG antibody to test the expression level of the corresponding proteins. Δ 1021-1347, expected size: 114 kDa; Δ 801-1347, expected size: 89 kDa Δ 1-352, expected size: 111 kDa; and Δ 1-615 expected size: 81kDa.

To identify the RNA binding domains of CLUH, CLIP experiments using different deletion constructs were conducted. After overexpression, the HEK 293T cells were exposed to 400 mJ (same as for CLUH-FALG and FLAG) of UV irradiation at 254 nm and CLIP was conducted similarly as before. One tenth of the elution before end-labeling was reserved for western blot analysis. The autoradiogram did not reveal if any of the constructs were able to bind to RNA, Δ 1-352 might be able to bind but this need to be validated with less RNase I treatment to see if the band smears up. However considering its presence in Δ 801-1347, the identity of this band is questionable. The positive control CLUH-FLAG worked (as indicated by the arrowhead in long exposure), though with considerable amount of background RNA signals (Figure 30B). All constructs could be immunoprecipitated (Figure 30C) but in different quantities. Since the starting amount of proteins were not known here, it was not possible to conclude whether the immunoprecipitation efficiency was low for the other constructs or if these constructs were expressed at a lower level.

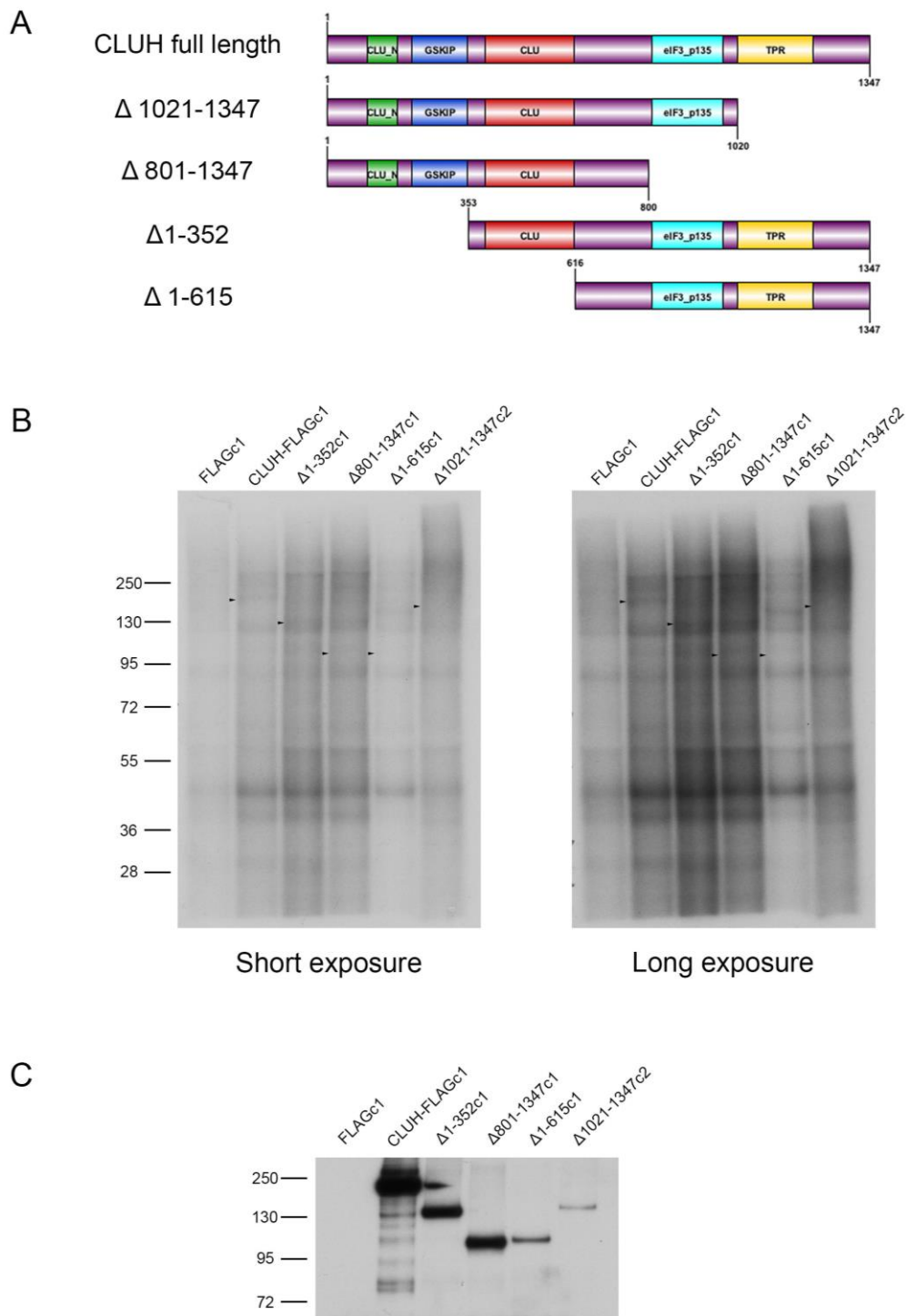


Figure 30 : Preliminary CLIP experiment to test the RNA binding activity of the constructs of CLUH. (A) Illustration of the CLUH constructs. (B) CLIP with anti-FLAG antibody of each constructs. The dried gel was exposed for short (2 hours) and long (5 hours) time. Arrowheads indicate the approximate locations of the expected RNA-Protein complexes. (C) Western blot of (B) indicating the efficiency of immunoprecipitation.

To examine the cell morphology after overexpression of different CLUH constructs and to ensure that CLUH overexpression is not lethal or harmful to the cells, immunocytochemistry was applied to examine the subcellular localisation of CLUH, and the general morphology of mitochondria and cells (Figure 31). First of all, the morphology of the full length CLUH was assessed. A small portion of CLUH-FLAG cells was able to express the protein without induction (Figure 31G). When overexpressed, CLUH was present in the cytosol as puncta/granular structures without forming any observable aggregates (Figure 31G and J). However, some cells displayed many vacuole structures devoid of CLUH, the identity of this structure is unknown (Figure 31J, white box). Clustered mitochondria were observed in both empty FLAG and CLUH-FLAG overexpressed cells indicating that mitochondrial clustering was independent of CLUH overexpression (see white arrows in Figure 31C, F, I and L). However, mitochondria in FLAG cell line without induction revealed more elongated morphology than the other three conditions (compare B to E, H and K)

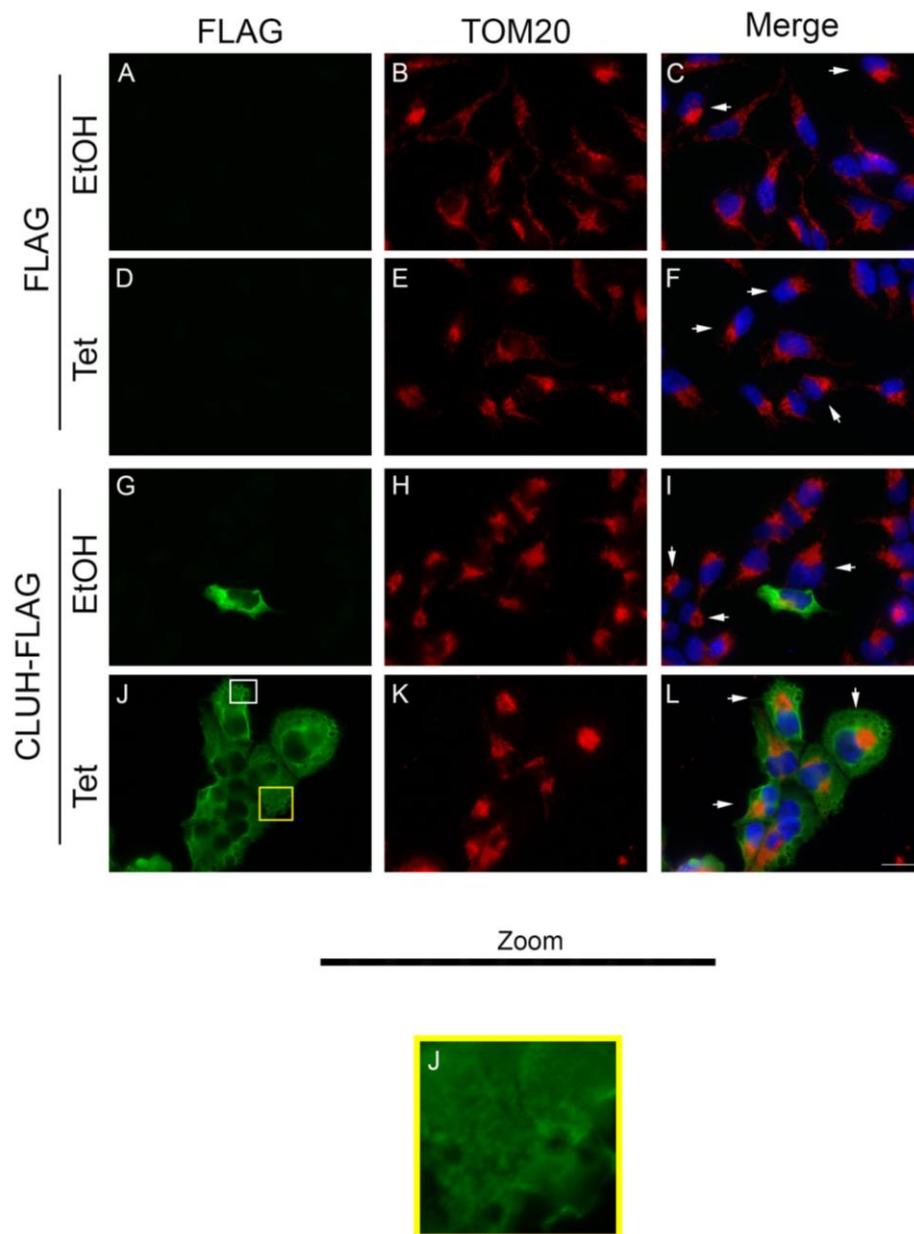


Figure 31: Morphology of CLUH, mitochondria and HEK 293T upon CLUH overexpr (A-L) After 16 hours of induction, cells were fixed and stained to visualise CLUH (green) and mitochondria (red). Blue staining is DAPI for nuclei. White box area highlights the cytosolic space that is devoid of CLUH. Yellow box shows the enlarged image. Arrows indicate cells with clustered mitochondria. Bar: 20 μ M for A-L, 141 μ M for the enlarged image J.

In comparison, no overt abnormality of mitochondria could be observed in the CLUH deletion constructs compared to their non-induced controls, such as mitochondrial clustering, fission and fusion problems. Different CLUH constructs displayed cytosolic staining of CLUH with punctate structures (Figure 32A, D, G and J). $\Delta 801-1347c1$ puncta appeared to be more granular compared to full-length CLUH construct. The vacuole structures were present in the cytosol of $\Delta 1-352c1$ and $\Delta 1-615c1$, but were not evident in $\Delta 1021-1347c2$ and $\Delta 801-1347c1$.

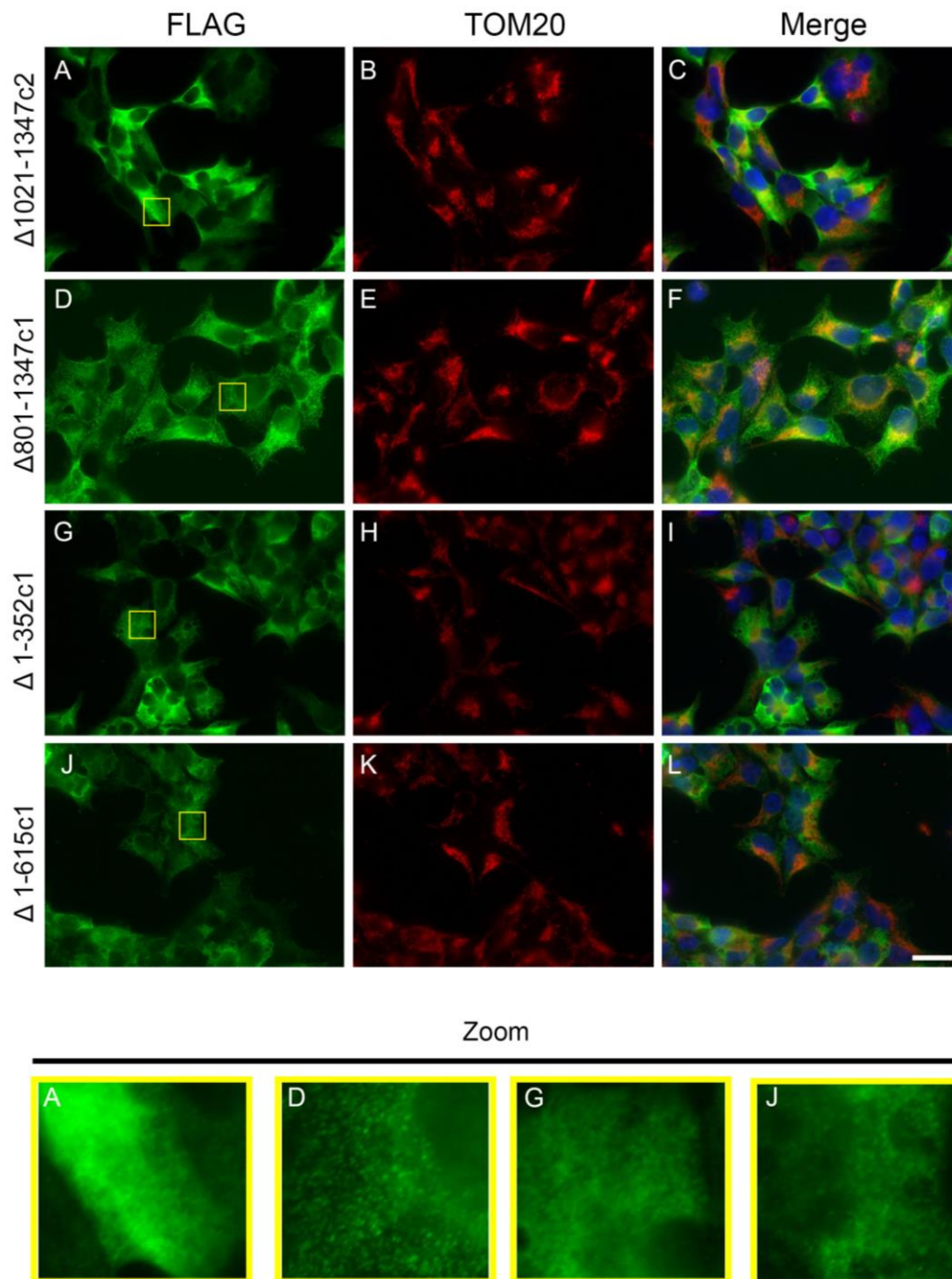


Figure 32: Overexpression CLUH deletion constructs. Cells were induced with 1 μ g/ml of tetracycline for 16 hours. (A, D, G and J) are the overexpressed proteins stained with anti-FLAG antibody. (B, E, H and K) are mitochondria stained with TOM20. (C, F, I and L) are the merged images between Anti-FLAG, TOM20 and DAPI (for nuclei staining). Bar: 20 μ M for A-L, 120 μ M for the zoomed images. Images were taken with Apotome with one Z- stack.

5 Discussion

5.1 Elucidation of the molecular function of CLUH unravels the cause of Clu mutant phenotypes.

Clu is well conserved throughout evolution and yet not much is known about its molecular function. In this study, we discovered that CLUH is coregulated with two gene clusters: one included genes involved in RNP complex biogenesis, ribosome biogenesis, and the other included mitochondrial genes involved in electron transport chain, oxidative phosphorylation, TCA cycle, and generation of small metabolite and energy (Figure 10). Next, we identified that CLUH is a genuine RNA binding protein (Gao, Schatton et al. 2014). This finding is in agreement with a systematic study in HeLa cells to identify mammalian mRNA binding proteins, which proposed CLUH (KIAA0664) as a candidate mRNA binding protein (Castello, Fischer et al. 2012). Among the RNAs bound by CLUH, we found a significant enrichment of mRNAs encoding for mitochondrial proteins. Canonical pathways analysis of these genes indicated clusters of genes involved in various metabolic pathways: branched-chain amino acid degradation, TCA cycle and oxidative phosphorylation (Table 13). However, our analysis has been so far restricted to mRNAs enriched for more than five times with a P value of less than 0.01. The steady state protein levels of CLUH targets were reduced (Figure 19A, see discussion below) and this was likely to be caused by specific regulation of translation of these transcripts (Figure 19B, 21 and 22) in the absence of CLUH.

Our findings help to explain some of the phenotypes observed in Clu mutants. Reduction of mitochondrial protein levels, aconitase activity and ATP in *Drosophila* mutant (Cox and Spradling 2009; Sen, Damm et al. 2013) could be direct results from failure in translation of these targets. This is strongly supported by our data wherein many enzymes participating directly in TCA cycle are targets of CLUH, including aconitase 2 (*ACO2*). In fact, only three enzymatic steps in TCA cycle are devoid of CLUH targets: conversions to succinate, α -ketoglutarate and citrate. Therefore, it is reasonable to speculate that NADH and FADH₂ levels also decline as a result of an insufficient TCA cycle. Subsequently, ATP production by OXPHOS could also be affected. Furthermore, our data hinted that CLUH is engaged in coordinating mitochondrial adaptation to the change of metabolism in the cells, because of the

involvement of CLUH targets in pathways interconverting different metabolites (especially amino acids) within TCA cycle.

The molecular function of Clu was long speculated to be involved in the transport of mitochondria. The reason for this was mainly due to the well-known mitochondrial clustering phenotype in the absence of Clu in all organisms investigated by the other research groups. The hypothesis was also supported by other observations: (1) Disruption of microtubules or actin did not lead to clustering of already positioned mitochondria in *Dictyostelium*. (2) Microtubule network was intact in Clu mutant. (3) Some Clu particles were found to be close to mitochondria. (4) Some Clu particles were also found to be close to microtubules. (5) Mitochondria accumulated at the microtubule plus end in fly mutant.

However, there is no direct evidence to support this hypothesis. A thorough study of the *Arabidopsis* mitochondrial cluster shed light on whether Clu was the linker between mitochondria and the cytoskeleton. Transport of mitochondria and mitochondrial clusters were intact along the actin filaments. The formation of clusters is likely due to prolonged association between the mitochondria (El Zawily, Schwarzlander et al. 2014). The authors proposed that mitochondrial clustering might be a secondary response to cell stress.

Our finding of the molecular function of Clu partially agree with El Zawily *et al.* that mitochondrial clustering phenotype may be secondary in Clu mutants. Moreover, Clu that associates with microtubules could be transporting mRNP (Figure 33). There are three possible causes for the mitochondrial clustering phenotype. First of all, lack of ATP due to reduced production of mitochondrial proteins leads to mitochondrial clustering. This is because the limited amount of energy is being used for primary cellular functions such as nuclear replication, protein synthesis and cell proliferation. Therefore, less ATP is available to transport mitochondria. Secondly, if CLUH is important for the transport of the mRNP to mitochondria, mitochondria might cluster to the region where mRNAs are present in the absence of CLUH. In fly Clu mutant, mitochondria are still transported to Balbiani body (Cox and Spradling 2009). However, translation inhibition with 30 min treatment of cycloheximide did not cause mitochondria to cluster in HeLa cells (data not shown), which argues against this

hypothesis. Nevertheless, it is likely that the treatment time was not long enough for mitochondria to accumulate. Lastly, the clustering phenotype could be due to longer association of mitochondria in order to facilitate content exchange to overcome limited protein supply as proposed by El Zawily and colleagues.

Other two very interesting CLUH targets are *SPAG5* and *PINK1* (Table 11). *SPAG5* encodes for astrin, a cytosolic protein. This protein is a mitotic spindle associated protein and regulates mitotic progression (Chang, Huang et al. 2001; Mack and Compton 2001). Recently Thedieck and colleagues discovered that astrin is a negative regulator of mTORC1 in cellular stress response (Thedieck, Holzwarth et al. 2013). Our proteomics study in HeLa cells show interaction of CLUH with astrin (Désirée Schatton, personal communication), moreover the steady state level of CLUH and astrin are tightly coupled. Therefore CLUH associates with both the mRNA and the protein of astrin and regulates it through a yet to be determined function. The reason behind such level of regulation remains unsolved. However, it is reasonable to speculate that by modulating astrin, CLUH participates in the regulation of mTORC1 pathway and hence connecting mTORC1 to mitochondria in the respect of metabolic alterations.

PINK1 (Pten-induced kinase 1) is a mitochondrial Ser/Thr kinase (Valente, Abou-Sleiman et al. 2004) that genetically interacts with Parkin (E3 ubiquitin ligase) in *Drosophila* for maintenance of mitochondrial function upon stress via mitophagy (Clark, Dodson et al. 2006; Narendra, Jin et al. 2010). PINK1 accumulates on the mitochondrial OM when mitochondria are dysfunctional and recruits Parkin to evoke mitophagy. Mutations in both genes can cause Parkinson's disease (Kitada, Asakawa et al. 1998; Valente, Bentivoglio et al. 2001). Interestingly, *Drosophila Clueless* and *park* mutants share many similar features and these two genes also interact genetically and may function in a similar pathway (Cox and Spradling 2009). More strikingly, however, Gehrke and colleagues recently discovered that PINK1 is an RNA binding protein. It associates with OXPHOS related mRNAs and translation initiation factors. PINK1/Parkin is involved in the translation of the localised mRNAs by replacing the translation repressors (Gehrke, Wu et al. 2015). Our finding of *PINK1* being a target of CLUH provides a possible explanation for the genetic interaction between *Clu* and *Park*: *Clu* could regulate the protein level of PINK1, without *Clu*, PINK1 is reduced and gives rise to defective mitophagy as well as reduced translation initiation of some of the

OXPHOS mRNAs bound by PINK1. Whether CLUH is directly involved in PINK1/Parkin mediated RNA translation pathway awaits to be solved. However PINK1 under normal physiological conditions is constantly degraded by mitochondrial proteases as well as the proteasome (Jin, Lazarou et al. 2010; Greene, Grenier et al. 2012; Yamano and Youle 2013) whereas the translation of mitochondrial proteins needs to be maintained under physiological conditions. Therefore, it is difficult to comprehend how PINK1 might play a role to constantly facilitate localised translation of these mRNAs.

Identification of CLUH as an mRNA binding protein also explains the association of Clu1 with translation initiation eIF3 complex (Vornlocher, Hanachi et al. 1999). First of all, in line with the observation from Vornlocher *et al.*, we did not observe any alteration of global translation in the absence of CLUH (Figure 21) and the main portion of CLUH did not peak with any of the translation machineries (Figure 24C). However, it is possible that CLUH interacts with the translation machineries only when translating the target mRNAs. It is also possible that this interaction is transient and difficult to catch, for example, CLUH might play a role in transferring translationally repressed mRNP complex to translationally activated mRNPs.

There are still several questions that need to be addressed in understanding the molecular function of CLUH. Primarily, since the function of each CLUH domain is unknown, evaluation of each protein domain and their post-translational modification will provide important information on the activity of CLUH and its regulation. Furthermore, study of CLUH domains can expand our knowledge on mRNA binding proteins and help to identify similar proteins. In addition, identifying the RNA signature recognised by CLUH also serve the same purpose.

Next, because CLUH disperses in the cytosol (Figure 23), it is not known at which stage during an mRNA's life does CLUH bind to the target mRNAs. Since CLUH is not found in the nucleus, it is likely that it binds to its mRNAs after the nuclear export of the mRNP. Because some CLUH associates with microtubules (Cox and Spradling 2009; Gao, Schatton et al. 2014), this points to a possible role of CLUH in mRNP transport/localisation. Based on the observations that the protein levels of CLUH targets are reduced in Clu mutant possibly due to specific translational regulation (Figure 19 21

and 22), it is conceivable that CLUH is a positive and specific regulator of translation. However, whether CLUH regulates mRNA stability or translation directly or acts in both processes are so far not very clear.

The last question with respect to the molecular function of CLUH would be the elucidation of the function of CLUH that associates with mitochondria (Figure 24) (Cox and Spradling 2009; Gao, Schatton et al. 2014). Two possibilities could be postulated here: either CLUH anchors mRNPs on the surface of mitochondria or CLUH transiently associates with mitochondria and transfer the mRNP to a receptor or a protein present on mitochondria. To address these questions, it is important to understand if all CLUH molecules bind to RNA or only the ones associated with microtubules and mitochondria contain RNA. This can be achieved by double staining of CLUH and RNA. In this study, mRNAs bound by CLUH were analysed regardless of their subcellular location, however it is conceivable that the mRNP components containing CLUH vary considerably depending on its subcellular localisation. Therefore, to facilitate the understanding of CLUH function, it is pivotal to study its interacting partners in different subcellular location. This can be achieved by immunoprecipitating CLUH and its interactors after crude cell fractionation.

In a genome wide analysis of mRNAs that are targeted to yeast mitochondria, the NEMP mRNAs can be divided into two pools: proteins with eukaryotic origin are translated in the cytosolic polysomes whereas proteins with bacterial origin are translated on the mitochondrial bound polysomes (Marc, Margeot et al. 2002). The mitochondrial bound mRNAs can be further divided to class I mRNAs, which contain 3'-UTR Puf3p binding motif, and class II mRNA that does not contain Puf3p binding site (Saint-Georges, Garcia et al. 2008). Similarly, it would be interesting to compare the mRNAs bound to mitochondria in *Cluh* knockout MEFs to conclude if CLUH is important for mRNA targeting/anchorage to mitochondria and identify the mislocalised mRNAs if there is any.

Considering the conservation of Clu proteins, it would be extremely informative to investigate if Clu binds to similar mRNAs in the other organisms. It is possible that Clu is an RNA binding protein in the other organisms due to its high conservation. However, whether Clu binds to a similar set of mRNA is doubtful. A good example is the PUF

proteins: apart from yeast Puf3p, none of PUF proteins in the other organisms are found to associate with the NEMP mRNAs of mitochondrial proteins in spite of conservation of their RNA binding domain and the RNA motif recognised by PUFs (Quenault, Lithgow et al. 2011). However, since the absence of Clu leads to mitochondrial clustering in all organisms tested, if the clustering phenotype is a secondary response to reduction of certain mitochondrial proteins, it is possible that Clu associates with a similar set of mRNAs encoding NEMPs.

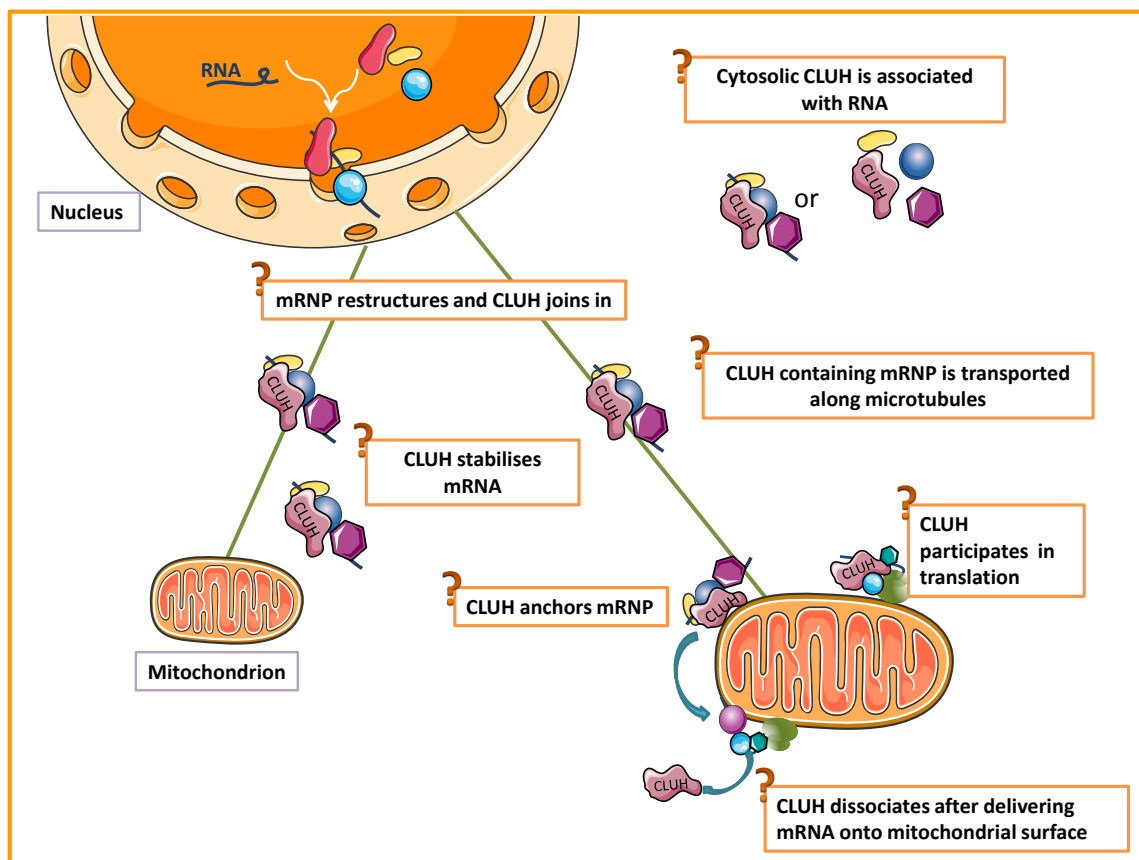


Figure 33: Schematics of possible molecular function of CLUH in respect to its RNA binding activity.

5.2 Identification of the molecular function of CLUH could be a support for co-translational import

Identification of the molecular function of CLUH inevitably raises the discussion over co-translational versus post-translational import. The main dispute is focused on whether mRNAs or proteins are being targeted to mitochondria (see introduction).

However if post-translational import were the only model for protein targeting to mitochondria, then the existence of mRNA sorting and targeting to mitochondria would be redundant. CLUH, on the other hand is a member of mRNA targeting machinery due to its RNA binding activity and possible localisation to mitochondria (see discussion about the localisation below). Nevertheless, CLUH might not be the only protein conducting this role; other RBPs might have a similar function and binds to another subset of mRNAs.

So far, there is no strong evidence that CLUH is localised to mitochondrial outer membrane. Immunocytochemistry under high glucose and galactose condition does not reveal any observable difference in CLUH/mitochondria colocalisation (Figure 23). Presence of CLUH in mitochondrial fraction could be a result of contamination from the ER (Figure 24A). The colocalisation between CLUH and mitochondria was observed upon extraction of the the soluble cytosolic CLUH with detergent (Gao, Schatton et al. 2014). However, it is not known if the observation was caused due to the the extraction (Gao, Schatton et al. 2014). On the other hand, researchers from other labs observed that *Drosophila clu* is in close proximity to mitochondria (Cox and Spradling 2009). To better understand the localisation of Clu to mitochondria, EM coupled with immunogold labeling of CLUH can be used. It is also possible that like PINK1 and Puf3p, CLUH interacts with one of the TOM receptors such as TOM20 and TOM70 or the translocase TOM40. Undoubtedly, if CLUH resides on mitochondria together with mRNAs, then mRNA targeting to mitochondria exists in mammals as previously shown (Matsumoto, Uchiumi et al. 2012; Gehrke, Wu et al. 2015) and this would provide a strong support for co-translational import of mitochondrial proteins.

5.3 CLUH affects the levels of protein encoded by target mRNAs

As mentioned before, the steady state protein levels of CLUH targets were reduced in *Clu* mutants. The steady state transcripts level of CLUH targets remains unchanged at large when CLUH is deleted or depleted (Figure 19B) and (Gao, Schatton et al. 2014). However, *Atp5a1* transcript level is consistently reduced. Nevertheless, the reduction of steady state protein level is more than the steady state level of its transcripts (Figure 19

and 21). In line with this observation, preliminary data in *cluh* knockout MEFs indicated a failure of translation for target SDHA, ATP5A1 and OGDH but not cytosolic protein GAPDH and the mitochondrial OM protein TOM20 (Figure 21 and 22). However, we have several limitations to conclude that CLUH controls the translation of its target mRNA directly. First of all, there is no data so far showing the stability of the target mRNAs in the absence of CLUH. The steady state mRNA level is an outcome of transcription and degradation. Increased mRNA degradation can also lead to translation reduction of the respective proteins. Furthermore, mRNA degradation could induce the compensatory increase in nuclear transcriptions which masks the unstability of the mRNA and displays an unchanged level in the transcripts. The second drawback lies within the system due to compensatory mechanisms: it is difficult to distinguish direct and indirect responses in mRNA stability and translation.

For some target mRNAs, we did not observe a decrease in their protein products. For example, the steady state protein level of SDHA was unchanged in *Cluh* knockout MEFs. It is conceivable that the immortalised MEFs adapted to the culturing conditions, for example some of the target proteins could have adapted to a slower protein turnover rate or the transcription or translation machineries compensated for the loss of CLUH. The steady state level of proteins is also the result of the existing and the newly synthesised proteins. Therefore, proteins with a slow turnover rate and a reduced translation might not be readily detected without looking into the two subspecies separately. In fact, reduction of newly synthesized SDHA was observed while the steady state level of SDHA remains unchanged (Figure 22).

The effect of CLUH over its targets cannot be simply explored by modulating CLUH protein levels. This is based on two observations: (1) as aforementioned, in the absence of CLUH, steady state level of SDHA is not affected in MEFs. (2) CLUH overexpression in HEK 293T cells results in increased, decreased or unchanged protein levels of its targets (Figure 20). The above observations raise the possibility that CLUH does not regulate its targets mRNA in the same manner. Furthermore, overexpressed CLUH could overstabilise its targets and inhibit the subsequent translation. Global analysis of translation of CLUH targets should be conducted in *Cluh* knockout as well as overexpression to identify targets whose translation is directly influenced by the level

of CLUH. Caution should be taken for possible compensatory effects in translation in the absence of CLUH.

If CLUH is indeed involved in the translation of its targets, initiation of translation of the targets mRNAs might require special signals and thus without it, translation cannot be initiated and results in unchanged protein levels. Signals can be in the forms of change of interactors or post-translational modification of CLUH. Moreover, this upstream modification can be a result of cellular alteration of, for example, a metabolic shift upon stress, development growth and aging. In other word, under physiological conditions, it is the “activation” of CLUH function rather quantitative elevation that drives the translation of some of its target mRNAs.

Another interesting observation is that up or down regulation of CLUH can both lead to reduction of HADHA. This indicates that CLUH levels are closely affecting the steady state protein level of HADHA which implies the importance of maintaining the homeostatic state of CLUH for regulating its targets. In conclusion, CLUH is a positive translation regulator, because its deletion never led to increase in the steady state target protein levels. CLUH could stabilise mRNAs and promote translation upon receiving signals or bring mRNA to the right place for translation. On the other hand, CLUH overexpression data implicates complex interactions with other factors to regulate expression of target mRNA.

5.4 Regulation of CLUH

5.4.1 Effect of galactose treatment on CLUH

CLUH affects the expression of its target mRNAs and RNA binding proteins have been shown to be coregulated with their target genes (Jiang, Xu et al. 2014). Therefore I anticipated that CLUH expression increases when mitochondrial biogenesis occur. Consequently, I used galactose treatment to induce mitochondrial biogenesis in order to examine the response of CLUH. In galactose media, glutamine is the main carbon source for ATP production. After entering mitochondria, glutamine is converted to

glutamate and α -ketoglutarate, which joins the TCA cycle. Intriguingly, CLUH decreases after 24 hours and longer galactose treatment (Figure 25A and C). This conflicts with the hypothesis that CLUH is involved in mitochondrial biogenesis. However, by chance when I treated MEFs for 16 hours with galactose as a positive control, I observed that CLUH level was increased. Inspired by this, I cultured HeLa cells in galactose for a shorter time and observed that CLUH levels increased after 4-8 hours of treatment. Similar observation was made also in MEFs (Figure 26A and B). Therefore, I propose that CLUH is important very early on when metabolic switch occurs. This hypothesis is supported by examining the CLUH target ATP5A1. ATP5A1 failed to be expressed to the wildtype level in the absence of CLUH after short galactose treatment (Figure 26A and C).

I then attempted to investigate if CLUH expression is under the control of the master transcriptional coactivator PGC-1 α , an important indicator for mitochondrial biogenesis. In favor of the hypothesis, about 50% of *Cluh* was not expressed in the absence of PGC-1 α (Figure 27A, B and C). Moreover, CLUH level could be induced by the pan-PPAR agonist bezafibrate (Figure 27D). In line with the above observations, Nsiah-Sefaa *et al.* demonstrated that *Cluh* mRNA level increased with PGC-1 α overexpression in mouse myotubes as well as treatment with AICAR (activator of AMPK). Furthermore they postulated through bioinformatics studies that PGC-1 α co-activates ERR α , and binds to the promoter of *Cluh* (Nsiah-Sefaa, Brown *et al.* 2014). Together, the above observations provide strong indications that CLUH is involved in mitochondrial biogenesis. This is consistent with our observation that CLUH is a positive regulator of translation of its target mRNA and coregulated with some of its target genes (Figure 10). The coregulation might be under the control of PGC-1 α .

However, it is still enigmatic why levels of CLUH are reduced after long galactose treatment. It is plausible that CLUH needs to be translated first and then facilitate the translation of its targets. However, prolonged expression of CLUH might inhibit expression of its targets or the other proteins. The evidence to support this is the reduction of HADHA after CLUH overexpression (Figure 20). Another possibility is that CLUH is involved in another pathway and needs to be regulated accordingly. CLUH might be involved in the mTORC1 pathway for nutrient related response. CLUH level changed through different time points and correlated with the level of

phosphorylation of S6K1 at Thr389 (this site is directly phosphorylated by mTORC1/raptor) and activation of LC3-II (indicator of autophagy activation, downstream of mTORC1). Another possibility is that CLUH could be affected by cell cycle. This is supported by the observation that CLUH level fluctuated and correlated with the reseeded time and the mitotic marker astrin and SKAP.

The protein levels of astrin and SKAP are known to be mitotically upregulated to facilitate chromosome alignment (Fang, Seki et al. 2009; Dunsch, Linnane et al. 2011; Thedieck, Holzwarth et al. 2013). However, astrin can interact with SKAP in interphase and in asynchronised cells. Both proteins interact with CLUH in asynchronised cells (Désirée Schatton, personal communication). S6K1 phosphorylation can be affected by multiple cells signaling pathways: Ser-411 phosphorylation is mediated by Cdk5 not mTOR/raptor. It is a prerequisite for subsequent phosphorylation of Thr389. Therefore, phosphorylation of S6K1 is also subjected to cell cycle control through G1 to S phase (Hou, He et al. 2007). In mitotic cells, Cdk1 phosphorylates multiple sites of S6K1, but correlates with reduced level of Thr389 phosphorylation (Shah, Ghosh et al. 2003). Therefore, in long-term galactose experiments, if the cyclic response of CLUH is due to cell cycle, then there is a conflict between cell cycle makers. Mitotic marker SKAP and astrin activations cannot occur at the same time as Thr389 phosphorylation of S6K1. Fluctuation of CLUH in regard to the cell cycles seems to be unlikely.

On the other hand, nutrient availability in combination with cell density might be a plausible cause for the change of CLUH. The level of S6K1 activation is in agreement with the availability of nutrients. As mentioned before, astrin and SKAP form complexes in interphase with a yet unknown function. Therefore, it is difficult to interpret its fluctuation upon galactose treatment. However, in our lab we observed that the protein levels of CLUH, astrin and SKAP are closely coupled. Astrin and SKAP are always influenced by the level of CLUH. Therefore, I propose that astrin and SKAP fluctuated because of the change of CLUH in galactose treatment. However, whether CLUH fluctuated with nutrients availability/cell density regardless of galactose needs to be investigated further. Nevertheless, it is difficult to look into nutrients availability/cell density and cell cycle independently since they are interconnected: the nutrient sensing mTORC1 controls cell growth and proliferation while mTORC1 inhibition by rapamycin arrests cell cycle at G1(Heitman, Movva et al. 1991).

5.4.2 CLUH level during acetoacetate

Acetoacetate is another media routinely used to induce mitochondrial biogenesis. In contrast to glutamine, acetoacetate converge to the TCA cycle by conversion to acetyl-CoA via acetoacetyl-CoA. Since both galactose and acetoacetate media enhance OXPHOS by providing excessive substrate to the TCA cycle, the response of CLUH was assumed to be very similar between these two treatments. Even though galactose and acetoacetate both induce mitochondrial biogenesis by feeding the TCA cycle, CLUH responded very differently to each of them. Four hours after the treatment with acetoacetate, CLUH was reduced, however its level increased from 16-24 hours. This is in contrast to an increase of CLUH from 4-16 hours in galactose and a reduction after 24 hours. Its target HADHA followed the same trend as CLUH upon treatment with acetoacetate. HADHA is an enzyme involved in the last three steps of branched-chain fatty acid beta-oxidation and participates in branched-chain amino acid catabolism as well as ketolysis. CLUH should be very similar between galactose treatment and acetoacetate treatment. CLUH target ACAT1 is directly involved in ketolysis to convert acetoacetate-CoA to two molecules of acetyl-CoA. Therefore, I suspect the difference in CLUH could be a result of different nutrient response mediated by other cellular signaling pathways. One report observed decrease mTOR1 activity in rat liver and hippocampus when fed with ketogenic diet (McDaniel, Rensing et al. 2011). As seen in galactose treatment, CLUH level correlated well with activation of mTOR1. However, it might be possible that mTORC1 modulates CLUH level in the early hour of acetoacetate treatment.

Change in the steady state level of HADHA could be a consequence of metabolic shifts. When acetoacetate was first added to cells, the source of acetyl-CoA is shifted from pyruvate to ketone bodies. After persistent supply, excess acetyl-CoA is converted to fatty acids. Until this step HADHA is not required and resulted in a reduction in protein level. From 8 to 24 hours, levels of HADHA increased and this might due be to the upregulated pathways in fatty acids or branched-chain amino acids catabolism.

5.4.3 CLUHs level during different life stages in mouse liver

Metabolic switch appears to influence at least the steady state protein level of CLUH (Figure 25 and 26). Moreover, many multicellular organisms experience metabolic switch during their development. Fly *Clu* larval mutant that mainly utilise glycolysis for energy supply do not show any defect in ATP production, aconitase activity and growth defect compared to the wildtype. However the mutant adult displayed all defects of the aforementioned phenotypes. Moreover the newly formed adult mutants have problems in utilising the larval fat body. Therefore, I hypothesised that CLUH plays a role in metabolic switch *in vivo*.

During mammalian embryogenesis and fetal development, glycolysis is the main source for energy supply (Cuezva, Ostronoff et al. 1997). As soon as one hour after birth, rat neonatal liver mitochondrial biogenesis occurs as a result of cytosolic translation (Valcarce, Navarrete et al. 1988). Concurrently, mRNAs of nuclear encoded mitochondrial proteins accumulate compared to adults as a result of stabilization of the transcripts (Izquierdo, Ricart et al. 1995). One of the transcripts *ATP5B* is even localised close to mitochondria (Egea, Izquierdo et al. 1997) and preferentially translated one hour after birth (Luis, Izquierdo et al. 1993).

To test if CLUH protein level is subjected to metabolic switch, I collected murine livers from different ages and examined the steady state level of CLUH and its targets. HADHA, PCB and ATP5A1 increased at D2, which are indications of mitochondrial biogenesis due to metabolic switch. However, CLUH protein level remains unchanged during this process. This paradoxical observation might be due to three possibilities. If CLUH participates in the translation of its target within one hour after birth, then (1) CLUH might be translated rapidly within this time before the translation of its targets (similar to the situation proposed for galactose treatment). Therefore, in order to see the difference of CLUH, one needs to examine its level in one hour or less after delivery. (2) CLUH protein is translated in the cytosol before birth and simply waiting for signals to be functional. This could be the availability of oxygen in the animal's system after birth or interruption of the umbilical supply of certain nutrients. (3) CLUH function is upregulated by regulating its activity not its quantity. The first two possibilities involve elevation of CLUH whereas the third requires participation of post-translational

modification or co-activator. In reality, all three hypotheses are plausible however considering the fluctuation of CLUH observed with galactose treatment, the first two hypotheses are favored.

CLUH is already important for the expression of its target at the basal level (E18.5, Figure 28 C and D). Therefore, when translation of CLUH targets fail after birth, severe defects can occur from multifaceted pathways. In fact, from function and diseases pathways analysis (Table 14), the top five pathways are involved in mitochondrial disorders, inborn error of amino acids metabolism, organic aciduria, aciduria and fatty acid oxidation disorder. Hence, short life expectancy in *Drosophila* could mainly be due to defect in metabolic imbalance. In fact, fat bodies were found to accumulate in adult fly mutants. The metabolic failure of the mutants could be tested by examining the metabolites of adult flies and the mutant might be rescued by feeding with special food supplement.

5.5 Conclusions

In conclusion, in the course of this study, I demonstrated the unexpected role of CLUH as an mRNA binding protein. It binds to a subset of mRNAs encoding NEMPs. A majority of CLUH does not associate with the 40S, 60S, 80S or polysomes even though a small portion of CLUH forms higher molecular complexes. Deletion or depletion of CLUH does not lead to obvious alteration of the general translation machinery. In the absence of CLUH, the protein levels of majority of its targets decrease and this is very likely due to failure in translating these targets specifically. CLUH levels are affected by different nutrients and the regulation of CLUH with respect to the nutrients can be important when metabolic switch is required *in vivo*.

Zusammenfassung

Das mitochondriale Proteom besteht sowohl aus mitochondrial- als auch aus nuklear-kodierten Proteinen. Bei Schwankungen in der Nährstoffverfügbarkeit und unter Stresszuständen ist die Restrukturierung des mitochondrialen Proteoms nötig. Um diesen Prozess zu ermöglichen, muss die Proteinexpression des nuklearen und des mitochondrialen Genomes genauestens koordiniert werden. Es sind zusätzliche Faktoren vorhanden, die diese Koordination bestimmen. Diese Faktoren haben verschiedene Funktionen von Energieregulation bis hin zu Translation von spezifischen nuklear-kodierten mitochondrialen Proteinen.

Clu ist ein hoch-konserviertes cytosolisches Protein, jedoch ist seine molekulare Funktion bis bisher unerforscht. In *Drosophila* wurde eine kleine Menge Clu an der Außenseite von Mitochondrien beobachtet. Clu-Mutanten in multi-zellulären Organismen zeigen einen Wachstumsdefekt, den Mangel sich an Stress anzupassen und frühzeitigen Tod. In einzelligen Organismen können diese Phänotypen jedoch nicht beobachtet werden. Nichtsdestotrotz, alle Clu-Mutanten besitzen akkumulierte Mitochondrien, dies eröffnet Raum zu spekulieren, dass die Funktion von CLUH eng mit Mitochondrien verwoben ist.

In dieser Studie haben wir Gene analysiert, die sowohl mit dem humanen als auch mit dem murinen *CLUH/Cluh*-Gen coreguliert sind. Dabei konnten wir zwei Haupt-Gencluster identifizieren: nuklear-kodierte mitochondriale Proteine und Gene, die in der cytosolischen Translation involviert sind. Danach haben wir mit Hilfe von Crosslinking Immunoprecipitations-Experimenten (CLIP) herausgefunden, dass das humane CLUH ein mRNA-Bindeprotein ist. Bei dem Vergleich der mRNAs, die mit CLUH angereichert wurden mit denen, die mit dem Kontroll-IgG angereichert wurden, konnten wir feststellen, dass CLUH spezifisch an die mRNA von nuklear-kodierten mitochondrialen Proteinen (NEMPs) bindet.

Unter den mRNAs, die von CLUH gebunden werden, haben wir eine Anreicherung von Genen festgestellt, die in dem Abbau von verzweigtkettigen Aminosäuren, mitochondrialer Dysfunktion, dem TCA-Zyklus, oxidativer Phosphorylierung und der α -Oxidation von Fettsäuren involviert sind. Des Weiteren konnten wir zeigen, dass

CLUH ein positiver Translations-Regulator seiner Ziel-mRNAs ist, da in Abwesenheit von CLUH die Translation der Ziel-mRNAs vermindert zu sein scheint. Jedoch ist die allgemeine Translation der Zelle nicht betroffen. Des Weiteren haben wir herausgefunden, dass das CLUH-Level in PGC-1 α -Ko-MEFs reduziert ist. Dies deutet darauf hin, dass die Expression von CLUH eventuell transkriptional von PGC-1 α kontrolliert wird. Zusammenfassend können wir schließen, dass unter dem Einfluss des zellulären Metabolismus` CLUH wahrscheinlich für die Biogenese seiner Ziel-mRNAs wichtig ist.

Reference

- Abaza, I. and F. Gebauer (2008). "Trading translation with RNA-binding proteins." Rna **14**(3): 404-409.
- Adams, K. L. and J. D. Palmer (2003). "Evolution of mitochondrial gene content: gene loss and transfer to the nucleus." Mol Phylogenet Evol **29**(3): 380-395.
- Ainger, K., D. Avossa, et al. (1997). "Transport and Localization Elements in Myelin Basic Protein mRNA." The Journal of Cell Biology **138**(5): 1077-1087.
- Anders, S. and W. Huber (2010). "Differential expression analysis for sequence count data." Genome Biology **11**(10): R106-R106.
- Anderson, P. and N. Kedersha (2006). "RNA granules." J Cell Biol **172**(6): 803-808.
- Anderson, P. and N. Kedersha (2009). "RNA granules: post-transcriptional and epigenetic modulators of gene expression." Nat Rev Mol Cell Biol **10**(6): 430-436.
- Anderson, S., A. T. Bankier, et al. (1981). "Sequence and organization of the human mitochondrial genome." Nature **290**(5806): 457-465.
- Bassell, G. J., H. Zhang, et al. (1998). "Sorting of beta-actin mRNA and protein to neurites and growth cones in culture." J Neurosci **18**(1): 251-265.
- Bastin, J., F. Aubey, et al. (2008). "Activation of peroxisome proliferator-activated receptor pathway stimulates the mitochondrial respiratory chain and can correct deficiencies in patients' cells lacking its components." J Clin Endocrinol Metab **93**(4): 1433-1441.
- Besse, F. and A. Ephrussi (2008). "Translational control of localized mRNAs: restricting protein synthesis in space and time." Nat Rev Mol Cell Biol **9**(12): 971-980.
- Blokhin, A., T. Vyshkina, et al. (2008). "Variations in mitochondrial DNA copy numbers in MS brains." J Mol Neurosci **35**(3): 283-287.
- Boesch, P., N. Ibrahim, et al. (2010). "Membrane association of mitochondrial DNA facilitates base excision repair in mammalian mitochondria." Nucleic Acids Res **38**(5): 1478-1488.
- Boesch, P., N. Ibrahim, et al. (2009). "Plant mitochondria possess a short-patch base excision DNA repair pathway." Nucleic Acids Res **37**(17): 5690-5700.
- Browning, K. S., D. R. Gallie, et al. Unified nomenclature for the subunits of eukaryotic initiation factor 3, Trends Biochem Sci. 2001 May;26(5):284.
- Calvo, S. E. and V. K. Mootha (2010). "The mitochondrial proteome and human disease." Annu Rev Genomics Hum Genet **11**: 25-44.
- Cashman, N. R., H. D. Durham, et al. (1992). "Neuroblastoma x spinal cord (NSC) hybrid cell lines resemble developing motor neurons." Dev Dyn **194**(3): 209-221.
- Castello, A., B. Fischer, et al. (2012). "Insights into RNA Biology from an Atlas of Mammalian mRNA-Binding Proteins." Cell **149**(6): 1393-1406.
- Chacinska, A., C. M. Koehler, et al. (2009). "Importing Mitochondrial Proteins: Machineries and Mechanisms." Cell **138**(4): 628-644.
- Chan, D. C. (2006). "Mitochondrial fusion and fission in mammals." Annu Rev Cell Dev Biol **22**: 79-99.
- Chan, K. W., D. J. Slotboom, et al. (2005). "A novel ADP/ATP transporter in the mitosome of the microaerophilic human parasite *Entamoeba histolytica*." Curr Biol **15**(8): 737-742.

- Chang, M. S., C. J. Huang, et al. (2001). "Cloning and characterization of hMAP126, a new member of mitotic spindle-associated proteins." Biochem Biophys Res Commun **287**(1): 116-121.
- Chartrand, P., X. H. Meng, et al. (1999). "Structural elements required for the localization of ASH1 mRNA and of a green fluorescent protein reporter particle in vivo." Curr Biol **9**(6): 333-336.
- Choi, Y. S., S. Kim, et al. (2001). "Mitochondrial transcription factor A (mtTFA) and diabetes." Diabetes Res Clin Pract **54**(2): S3-9.
- Clark, I. E., M. W. Dodson, et al. (2006). "Drosophila pink1 is required for mitochondrial function and interacts genetically with parkin." Nature **441**(7097): 1162-1166.
- Cox, R. T. and A. C. Spradling (2009). "Clueless, a conserved Drosophila gene required for mitochondrial subcellular localization, interacts genetically with parkin." Dis Model Mech **2**(9-10): 490-499.
- Cuezva, J. M., L. K. Ostronoff, et al. (1997). "Mitochondrial biogenesis in the liver during development and oncogenesis." J Bioenerg Biomembr **29**(4): 365-377.
- Darnell, J. C., S. J. Van Driesche, et al. (2011). "FMRP stalls ribosomal translocation on mRNAs linked to synaptic function and autism." Cell **146**(2): 247-261.
- Darnell, R. (2012). "CLIP (cross-linking and immunoprecipitation) identification of RNAs bound by a specific protein." Cold Spring Harb Protoc **1**(11): 1146-1160.
- Dianov, G. L., N. Souza-Pinto, et al. (2001). "Base excision repair in nuclear and mitochondrial DNA." Prog Nucleic Acid Res Mol Biol **68**: 285-297.
- Diaz, F., H. Kotarsky, et al. (2011). "Mitochondrial disorders caused by mutations in respiratory chain assembly factors." Semin Fetal Neonatal Med **16**(4): 197-204.
- Dudkina, N. V., S. Sunderhaus, et al. (2008). "The higher level of organization of the oxidative phosphorylation system: mitochondrial supercomplexes." Journal of Bioenergetics and Biomembranes **40**(5): 419-424.
- Dunsch, A. K., E. Linnane, et al. (2011). "The astrin-kinastrin/SKAP complex localizes to microtubule plus ends and facilitates chromosome alignment." J Cell Biol **192**(6): 959-968.
- Egea, G., J. M. Izquierdo, et al. (1997). "mRNA encoding the beta-subunit of the mitochondrial F1-ATPase complex is a localized mRNA in rat hepatocytes." Biochem J **322**(Pt 2): 557-565.
- El Zawily, A. M., M. Schwarzlander, et al. (2014). "FRIENDLY regulates mitochondrial distribution, fusion, and quality control in Arabidopsis." Plant Physiol **166**(2): 808-828.
- Eliyahu, E., L. Pnueli, et al. (2010). "Tom20 mediates localization of mRNAs to mitochondria in a translation-dependent manner." Mol Cell Biol **30**(1): 284-294.
- Fang, L., A. Seki, et al. (2009). "SKAP associates with kinetochores and promotes the metaphase-to-anaphase transition." Cell Cycle **8**(17): 2819-2827.
- Farrelly, F. and R. A. Butow (1983). "Rearranged mitochondrial genes in the yeast nuclear genome." Nature **301**(5898): 296-301.
- Ferrandon, D., I. Koch, et al. (1997). "RNA-RNA interaction is required for the formation of specific bicoid mRNA 3' UTR-STAUFIN ribonucleoprotein particles." The EMBO Journal **16**(7): 1751-1758.
- Fields, S. D., Q. Arana, et al. (2002). "Mitochondrial membrane dynamics are altered in cluA- mutants of Dictyostelium." J Muscle Res Cell Motil **23**(7-8): 829-838.

- Fields, S. D., M. N. Conrad, et al. (1998). "The *S. cerevisiae* CLU1 and *D. discoideum* cluA genes are functional homologues that influence mitochondrial morphology and distribution." *J Cell Sci* **111**(Pt 12): 1717-1727.
- Finkemeier, I., M. Laxa, et al. (2011). "Proteins of diverse function and subcellular location are lysine acetylated in Arabidopsis." *Plant Physiol* **155**(4): 1779-1790.
- Foat, B. C., S. S. Houshmandi, et al. (2005). "Profiling condition-specific, genome-wide regulation of mRNA stability in yeast." *Proc Natl Acad Sci U S A* **102**(49): 17675-17680.
- Frezza, C., S. Cipolat, et al. (2006). "OPA1 controls apoptotic cristae remodeling independently from mitochondrial fusion." *Cell* **126**(1): 177-189.
- Gadir, N., L. Haim-Vilmovsky, et al. (2011). "Localization of mRNAs coding for mitochondrial proteins in the yeast *Saccharomyces cerevisiae*." *Rna* **17**(8): 1551-1565.
- Gagnon, J. A. and K. L. Mowry (2011). "Molecular motors: directing traffic during RNA localization." *Crit Rev Biochem Mol Biol* **46**(3): 229-239.
- Galgano, A., M. Forrer, et al. (2008). "Comparative Analysis of mRNA Targets for Human PUF-Family Proteins Suggests Extensive Interaction with the miRNA Regulatory System." *PLoS One* **3**(9): e3164.
- Gao, J., D. Schatton, et al. (2014). "CLUH regulates mitochondrial biogenesis by binding mRNAs of nuclear-encoded mitochondrial proteins." *J Cell Biol* **207**(2): 213-223.
- Garcia-Rodriguez, L. J., A. C. Gay, et al. (2007). "Puf3p, a Pumilio family RNA binding protein, localizes to mitochondria and regulates mitochondrial biogenesis and motility in budding yeast." *J Cell Biol* **176**(2): 197-207.
- Gehrke, S., Z. Wu, et al. (2015). "PINK1 and Parkin Control Localized Translation of Respiratory Chain Component mRNAs on Mitochondria Outer Membrane." *Cell Metabolism* **21**(1): 95-108.
- Gerber, A. P., D. Herschlag, et al. (2004). "Extensive association of functionally and cytologically related mRNAs with Puf family RNA-binding proteins in yeast." *PLoS Biol* **2**(3): E79.
- Gerber, A. P., S. Luschig, et al. (2006). "Genome-wide identification of mRNAs associated with the translational regulator PUMILIO in *Drosophila melanogaster*." *Proc Natl Acad Sci U S A* **103**(12): 4487-4492.
- Goh, L. H., X. Zhou, et al. (2013). "Clueless regulates aPKC activity and promotes self-renewal cell fate in *Drosophila* lgl mutant larval brains." *Developmental Biology* **381**(2): 353-364.
- Greene, A. W., K. Grenier, et al. (2012). "Mitochondrial processing peptidase regulates PINK1 processing, import and Parkin recruitment." *EMBO Rep* **13**(4): 378-385.
- Hackenbrock, C. R. (1966). "Ultrastructural bases for metabolically linked mechanical activity in mitochondria. I. Reversible ultrastructural changes with change in metabolic steady state in isolated liver mitochondria." *J Cell Biol* **30**(2): 269-297.
- Harman, D. (1956). "Aging: a theory based on free radical and radiation chemistry." *J Gerontol* **11**(3): 298-300.
- Harmey, M. A., G. Hallermayer, et al. (1977). "Transport of cytoplasmically synthesized proteins into the mitochondria in a cell free system from *Neurospora crassa*." *Eur J Biochem* **81**(3): 533-544.
- Heitman, J., N. R. Movva, et al. (1991). "Targets for cell cycle arrest by the immunosuppressant rapamycin in yeast." *Science* **253**(5022): 905-909.

- Hervé, C., I. Mickleburgh, et al. (2004). "Zipcodes and postage stamps: mRNA localisation signals and their trans-acting binding proteins." Briefings in Functional Genomics & Proteomics **3**(3): 240-256.
- Holt, I. J., J. He, et al. (2007). "Mammalian mitochondrial nucleoids: organizing an independently minded genome." Mitochondrion **7**(5): 311-321.
- Hou, Z., L. He, et al. (2007). "Regulation of S6 Kinase 1 Activation by Phosphorylation at Ser-411." Journal of Biological Chemistry **282**(10): 6922-6928.
- Huh, W. K., J. V. Falvo, et al. (2003). "Global analysis of protein localization in budding yeast." Nature **425**(6959): 686-691.
- Huss, J. M., R. P. Kopp, et al. (2002). "Peroxisome proliferator-activated receptor coactivator-1alpha (PGC-1alpha) coactivates the cardiac-enriched nuclear receptors estrogen-related receptor-alpha and -gamma. Identification of novel leucine-rich interaction motif within PGC-1alpha." J Biol Chem **277**(43): 40265-40274.
- Ibdah, J. A., H. Paul, et al. (2001). "Lack of mitochondrial trifunctional protein in mice causes neonatal hypoglycemia and sudden death." J Clin Invest **107**(11): 1403-1409.
- Iborra, F., H. Kimura, et al. (2004). "The functional organization of mitochondrial genomes in human cells." BMC Biology **2**(1): 9.
- Izquierdo, J. M., J. Ricart, et al. (1995). "Changing patterns of transcriptional and post-transcriptional control of beta-F1-ATPase gene expression during mitochondrial biogenesis in liver." J Biol Chem **270**(17): 10342-10350.
- Jiang, H., L. Xu, et al. (2014). "Coordinating Expression of RNA Binding Proteins with Their mRNA Targets." Sci. Rep. **4**.
- Jin, S. M., M. Lazarou, et al. (2010). "Mitochondrial membrane potential regulates PINK1 import and proteolytic destabilization by PARL." J Cell Biol **191**(5): 933-942.
- Jonckheere, A. I., J. A. M. Smeitink, et al. (2012). "Mitochondrial ATP synthase: architecture, function and pathology." Journal of Inherited Metabolic Disease **35**(2): 211-225.
- Keene, J. D. (2007). "RNA regulons: coordination of post-transcriptional events." Nat Rev Genet **8**(7): 533-543.
- Kellems, R. E. and R. A. Butow (1972). "Cytoplasmic-type 80 S ribosomes associated with yeast mitochondria. I. Evidence for ribosome binding sites on yeast mitochondria." J Biol Chem **247**(24): 8043-8050.
- Keyhani, E. (1973). "RIBOSOMAL GRANULES ASSOCIATED WITH OUTER MITOCHONDRIAL MEMBRANE IN AEROBIC YEAST CELLS." The Journal of Cell Biology **58**(2): 480-484.
- Kilchert, C. and A. Spang (2011). "Cotranslational transport of ABP140 mRNA to the distal pole of *S. cerevisiae*." Embo j **30**(17): 3567-3580.
- Kim, D., G. Pertea, et al. (2013). "TopHat2: accurate alignment of transcriptomes in the presence of insertions, deletions and gene fusions." Genome Biol **14**(4): 2013-2014.
- Kitada, T., S. Asakawa, et al. (1998). "Mutations in the parkin gene cause autosomal recessive juvenile parkinsonism." Nature **392**(6676): 605-608.
- Kleiman, R., G. Banker, et al. (1990). "Differential subcellular localization of particular mRNAs in hippocampal neurons in culture." Neuron **5**(6): 821-830.
- Klionsky, D. J., F. C. Abdalla, et al. (2012). "Guidelines for the use and interpretation of assays for monitoring autophagy." Autophagy **8**(4): 445-544.

- Klitzman, R., M. Toynbee, et al. (2015). "Controversies concerning mitochondrial replacement therapy." Fertility and Sterility **103**(2): 344-346.
- Koppen, M., M. D. Metodiev, et al. (2007). "Variable and Tissue-Specific Subunit Composition of Mitochondrial m-AAA Protease Complexes Linked to Hereditary Spastic Paraplegia." Mol Cell Biol **27**(2): 758-767.
- Kukat, C. and N.-G. Larsson "mtDNA makes a U-turn for the mitochondrial nucleoid." Trends in Cell Biology **23**(9): 457-463.
- Kunji, E. R. S. (2004). "The role and structure of mitochondrial carriers." FEBS Letters **564**(3): 239-244.
- Lapuate-Brun, E., R. Moreno-Loshuertos, et al. (2013). "Supercomplex Assembly Determines Electron Flux in the Mitochondrial Electron Transport Chain." Science **340**(6140): 1567-1570.
- Lawrence, J. B. and R. H. Singer (1986). "Intracellular localization of messenger RNAs for cytoskeletal proteins." Cell **45**(3): 407-415.
- Lecuyer, E., H. Yoshida, et al. (2007). "Global analysis of mRNA localization reveals a prominent role in organizing cellular architecture and function." Cell **131**(1): 174-187.
- Lee, S. I., A. M. Dudley, et al. (2009). "Learning a prior on regulatory potential from eQTL data." PLoS Genet **5**(1): 30.
- Lehman, J. J., P. M. Barger, et al. (2000). "Peroxisome proliferator-activated receptor γ coactivator-1 promotes cardiac mitochondrial biogenesis." Journal of Clinical Investigation **106**(7): 847-856.
- Logan, D. C., I. Scott, et al. (2003). "The genetic control of plant mitochondrial morphology and dynamics." Plant J **36**(4): 500-509.
- Long, R. M., R. H. Singer, et al. (1997). "Mating type switching in yeast controlled by asymmetric localization of *ASH1* mRNA." Science **277**(5324): 383-387.
- Luis, A. M., J. M. Izquierdo, et al. (1993). "Translational regulation of mitochondrial differentiation in neonatal rat liver. Specific increase in the translational efficiency of the nuclear-encoded mitochondrial beta-F1-ATPase mRNA." J Biol Chem **268**(3): 1868-1875.
- Mack, G. J. and D. A. Compton (2001). "Analysis of mitotic microtubule-associated proteins using mass spectrometry identifies astrin, a spindle-associated protein." Proc Natl Acad Sci U S A **98**(25): 14434-14439.
- MacKenzie, J. A. and R. M. Payne (2007). "Mitochondrial protein import and human health and disease." Biochim Biophys Acta **5**: 509-523.
- Macklin, M. T. (1927). "Symbioticism and the Origin of Species." Canadian Medical Association Journal **17**(4): 498-498.
- Macmillan, C. J. and E. A. Shoubridge (1996). "Mitochondrial DNA depletion: prevalence in a pediatric population referred for neurologic evaluation." Pediatr Neurol **14**(3): 203-210.
- Maeda, I., Y. Kohara, et al. (2001). "Large-scale analysis of gene function in *Caenorhabditis elegans* by high-throughput RNAi." Curr Biol **11**(3): 171-176.
- Marc, P., A. Margeot, et al. (2002). "Genome-wide analysis of mRNAs targeted to yeast mitochondria." EMBO Rep **3**(2): 159-164.
- Matsumoto, S., T. Uchiumi, et al. (2012). "Localization of mRNAs encoding human mitochondrial oxidative phosphorylation proteins." Mitochondrion **12**(3): 391-398.
- McDaniel, S. S., N. R. Rensing, et al. (2011). "The ketogenic diet inhibits the mammalian target of rapamycin (mTOR) pathway." Epilepsia **52**(3): e7-e11.

- Melser, S., Etienne H. Chatelain, et al. (2013). "Rheb Regulates Mitophagy Induced by Mitochondrial Energetic Status." *Cell Metabolism* **17**(5): 719-730.
- Mihaylova, M. M. and R. J. Shaw (2011). "The AMP-activated protein kinase (AMPK) signaling pathway coordinates cell growth, autophagy, & metabolism." *Nature cell biology* **13**(9): 1016-1023.
- Model, K., C. Meisinger, et al. (2008). "Cryo-electron microscopy structure of a yeast mitochondrial preprotein translocase." *J Mol Biol* **383**(5): 1049-1057.
- Moreau, V., A. Madania, et al. (1996). "The *Saccharomyces cerevisiae* actin-related protein Arp2 is involved in the actin cytoskeleton." *J Cell Biol* **134**(1): 117-132.
- Morris, A. R., N. Mukherjee, et al. (2008). "Ribonomic Analysis of Human Pum1 Reveals cis-trans Conservation across Species despite Evolution of Diverse mRNA Target Sets." *Molecular and Cellular Biology* **28**(12): 4093-4103.
- Mukhopadhyay, A., L. Ni, et al. (2004). "A co-translational model to explain the in vivo import of proteins into HeLa cell mitochondria." *Biochem J* **382**(Pt 1): 385-392.
- Murata, Y. and R. P. Wharton (1995). "Binding of pumilio to maternal hunchback mRNA is required for posterior patterning in *Drosophila* embryos." *Cell* **80**(5): 747-756.
- Murphy, Michael P. (2009). "How mitochondria produce reactive oxygen species." *Biochemical Journal* **417**(Pt 1): 1-13.
- Narendra, D. P., S. M. Jin, et al. (2010). "PINK1 Is Selectively Stabilized on Impaired Mitochondria to Activate Parkin." *PLoS Biol* **8**(1): e1000298.
- Nass, M. M. and S. Nass (1963). "Intramitochondrial Fibers with DNA Characteristics. I. Fixation and Electron Staining Reactions." *J Cell Biol* **19**: 593-611.
- Neupert, W. and J. M. Herrmann (2007). "Translocation of proteins into mitochondria." *Annu Rev Biochem* **76**: 723-749.
- Nicchitta, C. V., R. S. Lerner, et al. (2005). "Pathways for compartmentalizing protein synthesis in eukaryotic cells: the template-partitioning model." *Biochem Cell Biol* **83**(6): 687-695.
- Nsiah-Sefaa, A., E. L. Brown, et al. (2014). "New gene targets of PGC-1alpha and ERRalpha co-regulation in C2C12 myotubes." *Mol Biol Rep* **6**: 6.
- Nunnari, J. and A. Suomalainen (2012). "Mitochondria: In Sickness and in Health." *Cell* **148**(6): 1145-1159.
- Olivas, W. and R. Parker (2000). "The Puf3 protein is a transcript - specific regulator of mRNA degradation in yeast." *The EMBO Journal* **19**(23): 6602-6611.
- Puigserver, P., Z. Wu, et al. (1998). "A Cold-Inducible Coactivator of Nuclear Receptors Linked to Adaptive Thermogenesis." *Cell* **92**(6): 829-839.
- Puigserver, P., Z. Wu, et al. (1998). "A cold-inducible coactivator of nuclear receptors linked to adaptive thermogenesis." *Cell* **92**(6): 829-839.
- Pyhtila, B., T. Zheng, et al. (2008). "Signal sequence- and translation-independent mRNA localization to the endoplasmic reticulum." *Rna* **14**(3): 445-453.
- Quenault, T., T. Lithgow, et al. (2011). "PUF proteins: repression, activation and mRNA localization." *Trends in Cell Biology* **21**(2): 104-112.
- Reitzer, L. J., B. M. Wice, et al. (1979). "Evidence that glutamine, not sugar, is the major energy source for cultured HeLa cells." *J Biol Chem* **254**(8): 2669-2676.
- Ren, J., L. Wen, et al. (2009). "DOG 1.0: illustrator of protein domain structures." *Cell Res* **19**(2): 271-273.
- Rodgers, J. T., C. Lerin, et al. (2005). "Nutrient control of glucose homeostasis through a complex of PGC-1[alpha] and SIRT1." *Nature* **434**(7029): 113-118.

- Saint-Georges, Y., M. Garcia, et al. (2008). "Yeast Mitochondrial Biogenesis: A Role for the PUF RNA-Binding Protein Puf3p in mRNA Localization." *PLoS One* **3**(6): e2293.
- Sardiello, M., M. Palmieri, et al. (2009). "A gene network regulating lysosomal biogenesis and function." *Science* **325**(5939): 473-477.
- Scarpulla, R. C. (2002). "Nuclear activators and coactivators in mammalian mitochondrial biogenesis." *Biochimica et Biophysica Acta (BBA) - Gene Structure and Expression* **1576**(1-2): 1-14.
- Scheffler, I. E. (2007). *Mitochondria*, Wiley-Liss.
- Schon, E. A., S. DiMauro, et al. (2012). "Human mitochondrial DNA: roles of inherited and somatic mutations." *Nat Rev Genet* **13**(12): 878-890.
- Schreiber, S. N., D. Knutti, et al. (2003). "The transcriptional coactivator PGC-1 regulates the expression and activity of the orphan nuclear receptor estrogen-related receptor alpha (ERRalpha)." *J Biol Chem* **278**(11): 9013-9018.
- Scorrano, L., M. Ashiya, et al. (2002). "A distinct pathway remodels mitochondrial cristae and mobilizes cytochrome c during apoptosis." *Dev Cell* **2**(1): 55-67.
- Sen, A., V. T. Damm, et al. (2013). "Drosophila clueless is highly expressed in larval neuroblasts, affects mitochondrial localization and suppresses mitochondrial oxidative damage." *PLoS One* **8**(1): 16.
- Shah, O. J., S. Ghosh, et al. (2003). "Mitotic Regulation of Ribosomal S6 Kinase 1 Involves Ser/Thr, Pro Phosphorylation of Consensus and Non-consensus Sites by Cdc2." *Journal of Biological Chemistry* **278**(18): 16433-16442.
- Sonoda, J. and R. P. Wharton (1999). "Recruitment of Nanos to hunchback mRNA by Pumilio." *Genes Dev* **13**(20): 2704-2712.
- Spassov, D. S. and R. Jurecic (2002). "Cloning and comparative sequence analysis of PUM1 and PUM2 genes, human members of the Pumilio family of RNA-binding proteins." *Gene* **299**(1-2): 195-204.
- Srivastava, S., F. Diaz, et al. (2009). "PGC-1alpha/beta induced expression partially compensates for respiratory chain defects in cells from patients with mitochondrial disorders." *Hum Mol Genet* **18**(10): 1805-1812.
- St Johnston, D., D. Beuchle, et al. (1991). "Staufen, a gene required to localize maternal RNAs in the Drosophila egg." *Cell* **66**(1): 51-63.
- Taylor, R. W. and D. M. Turnbull (2005). "Mitochondrial DNA mutations in human disease." *Nat Rev Genet* **6**(5): 389-402.
- Tenenbaum, A., M. Motro, et al. (2005). "Dual and pan-peroxisome proliferator-activated receptors (PPAR) co-agonism: the bezafibrate lessons." *Cardiovasc Diabetol* **4**: 14.
- Thedieck, K., B. Holzwarth, et al. (2013). "Inhibition of mTORC1 by Astrin and Stress Granules Prevents Apoptosis in Cancer Cells." *Cell* **154**(4): 859-874.
- Trapnell, C., B. A. Williams, et al. (2010). "Transcript assembly and quantification by RNA-Seq reveals unannotated transcripts and isoform switching during cell differentiation." *Nat Biotechnol* **28**(5): 511-515.
- Trifunovic, A., A. Wredenberg, et al. (2004). "Premature ageing in mice expressing defective mitochondrial DNA polymerase." *Nature* **429**(6990): 417-423.
- Tsai, N. P., J. Bi, et al. (2007). "The adaptor Grb7 links netrin-1 signaling to regulation of mRNA translation." *Embo j* **26**(6): 1522-1531.
- Valcarce, C., R. M. Navarrete, et al. (1988). "Postnatal development of rat liver mitochondrial functions. The roles of protein synthesis and of adenine nucleotides." *J Biol Chem* **263**(16): 7767-7775.

- Valente, E. M., P. M. Abou-Sleiman, et al. (2004). "Hereditary early-onset Parkinson's disease caused by mutations in PINK1." Science **304**(5674): 1158-1160.
- Valente, E. M., A. R. Bentivoglio, et al. (2001). "Localization of a novel locus for autosomal recessive early-onset parkinsonism, PARK6, on human chromosome 1p35-p36." Am J Hum Genet **68**(4): 895-900.
- van der Giezen, M. and J. Tovar (2005). "Degenerate mitochondria." EMBO Reports **6**(6): 525-530.
- Vega, R. B., J. M. Huss, et al. (2000). "The coactivator PGC-1 cooperates with peroxisome proliferator-activated receptor alpha in transcriptional control of nuclear genes encoding mitochondrial fatty acid oxidation enzymes." Mol Cell Biol **20**(5): 1868-1876.
- Vellosillo, T., V. Aguilera, et al. (2013). "Defense Activated by 9-Lipoxygenase-Derived Oxylipins Requires Specific Mitochondrial Proteins." Plant Physiology **161**(2): 617-627.
- Vornlocher, H.-P., P. Hanachi, et al. (1999). "A 110-Kilodalton Subunit of Translation Initiation Factor eIF3 and an Associated 135-kilodalton Protein Are Encoded by the *Saccharomyces cerevisiae* TIF32 and TIF31 Genes." Journal of Biological Chemistry **274**(24): 16802-16812.
- Wang, Y. and D. F. Bogenhagen (2006). "Human mitochondrial DNA nucleoids are linked to protein folding machinery and metabolic enzymes at the mitochondrial inner membrane." J Biol Chem **281**(35): 25791-25802.
- Wang, Y. X., C. H. Lee, et al. (2003). "Peroxisome-proliferator-activated receptor delta activates fat metabolism to prevent obesity." Cell **113**(2): 159-170.
- Weis, B. L., E. Schleiff, et al. (2013). "Protein targeting to subcellular organelles via mRNA localization." Biochimica et Biophysica Acta (BBA) - Molecular Cell Research **1833**(2): 260-273.
- Wickens, M., D. S. Bernstein, et al. (2002). "A PUF family portrait: 3'UTR regulation as a way of life." Trends Genet **18**(3): 150-157.
- Williams, B. A., R. P. Hirt, et al. (2002). "A mitochondrial remnant in the microsporidian *Trachipleistophora hominis*." Nature **418**(6900): 865-869.
- Wong, L. J. (2007). "Diagnostic challenges of mitochondrial DNA disorders." Mitochondrion **7**(1-2): 45-52.
- Wreden, C., A. C. Verrotti, et al. (1997). "Nanos and pumilio establish embryonic polarity in *Drosophila* by promoting posterior deadenylation of hunchback mRNA." Development **124**(15): 3015-3023.
- Wu, Z., P. Puigserver, et al. (1999). "Mechanisms Controlling Mitochondrial Biogenesis and Respiration through the Thermogenic Coactivator PGC-1." Cell **98**(1): 115-124.
- Xing, J., M. Chen, et al. (2008). "Mitochondrial DNA Content: Its Genetic Heritability and Association With Renal Cell Carcinoma." JNCI Journal of the National Cancer Institute **100**(15): 1104-1112.
- Xu, E. Y., R. Chang, et al. (2007). "A gene trap mutation of a murine homolog of the *Drosophila* stem cell factor Pumilio results in smaller testes but does not affect litter size or fertility." Mol Reprod Dev **74**(7): 912-921.
- Yamaguchi, R., L. Lartigue, et al. (2008). "Opa1-mediated cristae opening is Bax/Bak and BH3 dependent, required for apoptosis, and independent of Bak oligomerization." Mol Cell **31**(4): 557-569.
- Yamano, K. and R. J. Youle (2013). "PINK1 is degraded through the N-end rule pathway." Autophagy **9**(11): 1758-1769.

- Yoon, J. C., P. Puigserver, et al. (2001). "Control of hepatic gluconeogenesis through the transcriptional coactivator PGC-1." Nature **413**(6852): 131-138.
- Zamore, P. D., J. R. Williamson, et al. (1997). "The Pumilio protein binds RNA through a conserved domain that defines a new class of RNA-binding proteins." Rna **3**(12): 1421-1433.
- Zhang, B., M. Gallegos, et al. (1997). "A conserved RNA-binding protein that regulates sexual fates in the *C. elegans* hermaphrodite germ line." Nature **390**(6659): 477-484.
- Zhu, Q. and M. Clarke (1992). "Association of calmodulin and an unconventional myosin with the contractile vacuole complex of *Dictyostelium discoideum*." J Cell Biol **118**(2): 347-358.
- Zhu, Q., D. Hulen, et al. (1997). "The *cluA*- mutant of *Dictyostelium* identifies a novel class of proteins required for dispersion of mitochondria." Proc Natl Acad Sci U S A **94**(14): 7308-7313.
- Zipor, G., L. Haim-Vilmovsky, et al. (2009). "Localization of mRNAs coding for peroxisomal proteins in the yeast, *Saccharomyces cerevisiae*." Proc Natl Acad Sci U S A **106**(47): 19848-19853.
- Zivraj, K. H., Y. C. Tung, et al. (2010). "Subcellular profiling reveals distinct and developmentally regulated repertoire of growth cone mRNAs." J Neurosci **30**(46): 15464-15478.

Appendix

Table 16: Quality control from RNA sequencing

ID	Label	# Reads	#Aligned	Dupl Removed	MapQ \geq 30	Stranded	miRNA	rRNA	Other ncRNA	Ins Size
786	34_Input	55.0M	44.9M	27.3M	23.2M	0.0%	0.6M	2.9M	5.6M	630.3 \pm 935.4
787	34_L1	37.8M	30.3M	4.5M	3.5M	0.0%	0.6M	3.5M	4.4M	459.4 \pm 735.6
788	34_CLU	66.1M	55.2M	19.8M	14.2M	0.0%	0.4M	2.2M	5.9M	714.1 \pm 995.7
789	35_Input	59.6M	49.2M	32.2M	27.9M	0.0%	0.6M	2.4M	6.5M	619.6 \pm 931.9
790	35_L1	34.2M	27.6M	4.8M	3.9M	0.0%	0.6M	3.4M	3.9M	490.8 \pm 778.5
791	35_CLU	53.2M	44.3M	14.3M	10.5M	0.0%	0.4M	2.1M	4.8M	673.6 \pm 971.8
792	36_Input	68.8M	57.3M	38.8M	34.5M	0.0%	0.7M	1.8M	7.8M	642.5 \pm 956.1
793	36_L1	46.8M	38.3M	9.8M	7.9M	0.0%	0.9M	3.3M	4.8M	531.7 \pm 843.8
794	36_CLU	41.8M	34.5M	13.0M	10.1M	0.0%	0.6M	2.2M	3.7M	619.3 \pm 931.2

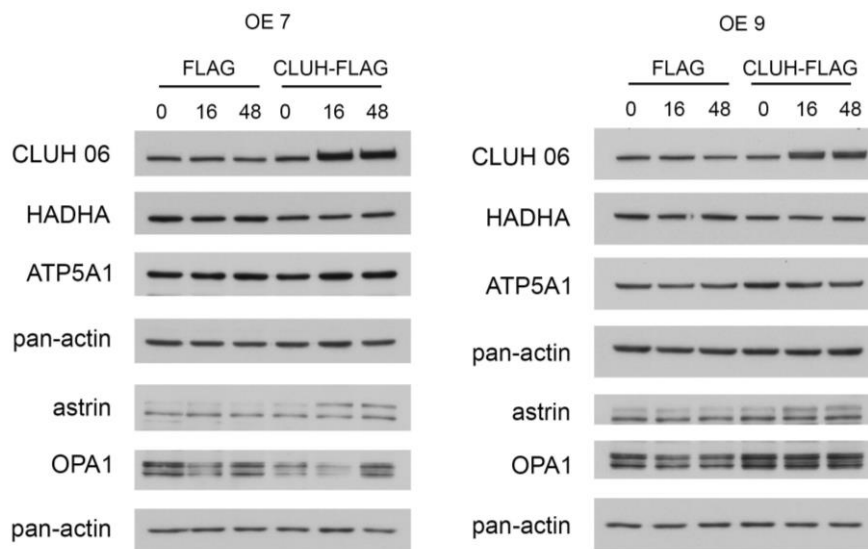


Figure 34 : CLUH overexpression induces different target responses. The two replicates of this experiment (Figure 20)

Table 17. The complete list of genes encoding for NEMPs that are bound by CLUH. Only gene enriched more than 5 times, P<0.01 were analysed

Symbol	FoldChange	pValue	Description
ABAT	13,71	0,000008	4-aminobutyrate aminotransferase
ABCB10	5,88	0,000001	ATP-binding cassette, sub-family B (MDR/TAP), member 10
ABCB7	25,24	0,000001	ATP-binding cassette, sub-family B (MDR/TAP), member 7
ABCB8	24,04	0,000001	ATP-binding cassette, sub-family B (MDR/TAP), member 8
ABHD10	9,94	0,000001	abhydrolase domain containing 10
ABHD11	12,4	0,000001	abhydrolase domain containing 11
ACAA2	9,79	0,000001	acetyl-CoA acyltransferase 2
ACAD10	9,61	0,000003	acyl-CoA dehydrogenase family, member 10
ACAD8	16,44	0,000001	acyl-CoA dehydrogenase family, member 8
ACAD9	5,41	0,000001	acyl-CoA dehydrogenase family, member 9
ACADL	21,07	0,000001	acyl-CoA dehydrogenase, long chain
ACADM	35,22	0,000001	acyl-CoA dehydrogenase, C-4 to C-12 straight chain
ACADS	21,69	0,000001	acyl-CoA dehydrogenase, C-2 to C-3 short chain
ACADSB	6,65	0,000001	acyl-CoA dehydrogenase, short/branched chain
ACADVL	6,15	0,000001	acyl-CoA dehydrogenase, very long chain
ACAT1	17,3	0,000001	acetyl-CoA acetyltransferase 1
ACO2	19,17	0,000001	aconitase 2, mitochondrial
ACOT2	9,34	0,000001	acyl-CoA thioesterase 2
ACSF2	32,86	0,000001	acyl-CoA synthetase family member 2
ACSF3	7,5	0,000001	acyl-CoA synthetase family member 3
ACSM3	16,8	0,000001	acyl-CoA synthetase medium-chain family member 3
ADCK5	7,08	0,000001	aarF domain containing kinase 5

AGK	10,69	0,000001	acylglycerol kinase
AGMAT	23,1	0,000001	agmatine ureohydrolase (agmatinase)
AIFM1	28,76	0,000001	apoptosis-inducing factor, mitochondrion-associated, 1
ALAS1	30,99	0,000001	aminolevulinate, delta-, synthase 1
ALDH18A1	34,22	0,000001	aldehyde dehydrogenase 18 family, member A1
ALDH1B1	11,16	0,000001	aldehyde dehydrogenase 1 family, member B1
ALDH1L2	17,73	0,000001	aldehyde dehydrogenase 1 family, member L2
ALDH2	20,13	0,000001	aldehyde dehydrogenase 2 family (mitochondrial)
ALDH4A1	9,91	0,000001	aldehyde dehydrogenase 4 family, member A1
ALDH5A1	20,95	0,000001	aldehyde dehydrogenase 5 family, member A1
ALDH6A1	42,97	0,000001	aldehyde dehydrogenase 6 family, member A1
ALDH7A1	25,98	0,000001	aldehyde dehydrogenase 7 family, member A1
ALDH9A1	13,55	0,000001	aldehyde dehydrogenase 9 family, member A1
AMACR	5,23	0,008462	alpha-methylacyl-CoA racemase
APEX2	7,26	0,000001	APEX nuclease (apurinic/apyrimidinic endonuclease) 2
APOO	5,65	0,000001	apolipoprotein O
ATP5A1	5,85	0,000001	ATP synthase, H ⁺ transporting, mitochondrial F1 complex, alpha subunit 1, cardiac muscle
ATPAF1	12,37	0,000001	ATP synthase mitochondrial F1 complex assembly factor 1
ATPAF2	37,6	0,000001	ATP synthase mitochondrial F1 complex assembly factor 2
AUH	13,62	0,000001	AU RNA binding protein/enoyl-CoA hydratase
AURKAIP1	7,43	0,000001	aurora kinase A interacting protein 1
BCAT2	16,52	0,000001	branched chain amino-acid transaminase 2, mitochondrial
BCKDHA	11,77	0,000036	branched chain keto acid dehydrogenase E1, alpha polypeptide

BCKDHB	7,93	0,000001	branched chain keto acid dehydrogenase E1, beta polypeptide
BCKDK	6,09	0,000001	branched chain ketoacid dehydrogenase kinase
BCO2	10,76	0,000001	beta-carotene oxygenase 2
BDH1	23,94	0,000001	3-hydroxybutyrate dehydrogenase, type 1
BPHL	5,12	0,000001	biphenyl hydrolase-like (serine hydrolase)
C10orf2	10,48	0,000001	chromosome 10 open reading frame 2
C1QBP	5,18	0,000001	complement component 1, q subcomponent binding protein
C2orf47	8,54	0,000001	chromosome 2 open reading frame 47
CARS2	17,23	0,000001	cysteinyl-tRNA synthetase 2, mitochondrial (putative)
CCDC109B	6,99	0,000001	coiled-coil domain containing 109B
CCDC51	9,31	0,000001	coiled-coil domain containing 51
CECR5	10,2	0,000001	cat eye syndrome chromosome region, candidate 5
CHDH	37,26	0,000001	choline dehydrogenase
CKMT1B;CKMT1A	24,81	0,000001	creatine kinase, mitochondrial 1A
CKMT1B;CKMT1A	17,04	0,000001	creatine kinase, mitochondrial 1B
CLPB ?	21,64	0,000001	ClpB caseinolytic peptidase B homolog (E. coli)
CLPP	6,57	0,000001	caseinolytic mitochondrial matrix peptidase proteolytic subunit
CLYBL	7,78	0,000066	citrate lyase beta like
COQ3	21,46	0,000001	coenzyme Q3 methyltransferase
COQ6;LOC1027238	19,96	0,000001	coenzyme Q6 monoxygenase
COX15	18,72	0,000001	cytochrome c oxidase assembly homolog 15 (yeast)
CPOX	9,5	0,000001	coproporphyrinogen oxidase
CPS1;LOC1027239	16,36	0,000001	carbamoyl-phosphate synthase 1, mitochondrial

CPT2	35,27	0,000001	carnitine palmitoyltransferase 2
CRAT	5,82	0,000001	carnitine O-acetyltransferase
D2HGDH	17,76	0,000001	D-2-hydroxyglutarate dehydrogenase
DARS2	38,23	0,000001	aspartyl-tRNA synthetase 2, mitochondrial
DBT	9,24	0,000001	dihydrolipoamide branched chain transacylase E2
DDX28	9,28	0,000001	DEAD (Asp-Glu-Ala-Asp) box polypeptide 28
DECR1	16,01	0,000001	2,4-dienoyl CoA reductase 1, mitochondrial
DHODH	5,73	0,000001	dihydroorotate dehydrogenase (quinone)
DHRS2	21,78	0,000001	dehydrogenase/reductase (SDR family) member 2
DHTKD1	7,37	0,000001	dehydrogenase E1 and transketolase domain containing 1
DLAT	36,76	0,000001	dihydrolipoamide S-acetyltransferase
DLD	24,28	0,000001	dihydrolipoamide dehydrogenase
DLST	16,2	0,000001	dihydrolipoamide S-succinyltransferase (E2 component of 2-oxo-glutarate complex)
DUS2	10,03	0,000001	dihydrouridine synthase 2
EARS2	5,8	0,000001	glutamyl-tRNA synthetase 2, mitochondrial
ECH1	5,46	0,000001	enoyl CoA hydratase 1, peroxisomal
ECHDC3	8,5	0,000001	enoyl CoA hydratase domain containing 3
ECHS1	23,53	0,000001	enoyl CoA hydratase, short chain, 1, mitochondrial
ELAC2	12,18	0,000001	elaC ribonuclease Z 2
ETFA	8,95	0,000001	electron-transfer-flavoprotein, alpha polypeptide
ETFDH	30,3	0,000001	electron-transferring-flavoprotein dehydrogenase
FAM210A	5,21	0,000001	family with sequence similarity 210, member A
FARS2	5,38	0,000001	phenylalanyl-tRNA synthetase 2, mitochondrial

FASTKD1	8,69	0,000001	FAST kinase domains 1
FASTKD5	6,28	0,000001	FAST kinase domains 5
FECH	9,11	0,000001	ferrochelatase
FH	17,81	0,000001	fumarate hydratase
FOXRED1	5,7	0,000001	FAD-dependent oxidoreductase domain containing 1
FTSJ2	6,76	0,000001	FtsJ RNA methyltransferase homolog 2 (E. coli)
FXN	10,58	0,000001	frataxin
GATB	11,02	0,000001	glutamyl-tRNA(Gln) amidotransferase, subunit B
GATM;102724493	17,68	0,000001	glycine amidinotransferase (L-arginine:glycine amidinotransferase)
GBAS	25,24	0,000001	glioblastoma amplified sequence
GFM1	57,35	0,000001	G elongation factor, mitochondrial 1
GFM2	21,65	0,000001	G elongation factor, mitochondrial 2
GHITM	37,78	0,000001	growth hormone inducible transmembrane protein
GLDC	22,19	0,000001	glycine dehydrogenase (decarboxylating)
GLRX2	5,33	0,000001	glutaredoxin 2
GLS	12,8	0,000001	glutaminase
GLUD1	9,55	0,000001	glutamate dehydrogenase 1
GPT2	11,75	0,000001	glutamic pyruvate transaminase (alanine aminotransferase) 2
GTPBP3	6,79	0,000001	GTP binding protein 3 (mitochondrial)
GUF1;LOC1027253	6,22	0,000001	GUF1 GTPase homolog (S. cerevisiae)
HADHA	21,13	0,000001	hydroxyacyl-CoA dehydrogenase/3-ketoacyl-CoA thiolase/enoyl-CoA hydratase (trifunctional protein), alpha subunit
HADHB	18,15	0,000001	hydroxyacyl-CoA dehydrogenase/3-ketoacyl-CoA thiolase/enoyl-CoA hydratase (trifunctional protein), beta subunit

HIBADH	43,97	0,000001	3-hydroxyisobutyrate dehydrogenase
HSCB	9,99	0,000001	HscB mitochondrial iron-sulfur cluster co-chaperone
HSPA9	37,77	0,000001	heat shock 70kDa protein 9 (mortalin)
HSPD1	14,84	0,000001	heat shock 60kDa protein 1 (chaperonin)
IARS2	31,17	0,000001	isoleucyl-tRNA synthetase 2, mitochondrial
IBA57	6,96	0,000001	IBA57, iron-sulfur cluster assembly homolog (<i>S. cerevisiae</i>)
IDH2	11,02	0,000001	isocitrate dehydrogenase 2 (NADP+), mitochondrial
IMMT	26,16	0,000001	inner membrane protein, mitochondrial
IVD	5,72	0,000001	isovaleryl-CoA dehydrogenase
KIAA0141	11,16	0,000001	KIAA0141
KIAA0391	8,43	0,000001	KIAA0391
L2HGDH	19,56	0,000001	L-2-hydroxyglutarate dehydrogenase
LACTB	41,1	0,000001	lactamase, beta
LACTB2	7,53	0,000001	lactamase, beta 2
LARS2	39,12	0,000001	leucyl-tRNA synthetase 2, mitochondrial
LDHD	11,61	0,000001	lactate dehydrogenase D
LETM1	10,78	0,000001	leucine zipper-EF-hand containing transmembrane protein 1
LONP1	22,66	0,000001	lon peptidase 1, mitochondrial
LRPPRC	26,04	0,000001	leucine-rich pentatricopeptide repeat containing
MACROD1	17,33	0,000001	MACRO domain containing 1
MCAT	9,09	0,000001	malonyl CoA:ACP acyltransferase (mitochondrial)
MCCC1	14,71	0,000001	methylcrotonoyl-CoA carboxylase 1 (alpha)
MCCC2	17,9	0,000001	methylcrotonoyl-CoA carboxylase 2 (beta)

MDH2	10,46	0,000001	malate dehydrogenase 2, NAD (mitochondrial)
ME2	11,09	0,000001	malic enzyme 2, NAD(+)-dependent, mitochondrial
ME3	7,06	0,000001	malic enzyme 3, NADP(+)-dependent, mitochondrial
MECR	7,04	0,000001	mitochondrial trans-2-enoyl-CoA reductase
METTL17	6,47	0,000001	methyltransferase like 17
MICU1	9,21	0,000001	mitochondrial calcium uptake 1
MIPEP	12,12	0,000001	mitochondrial intermediate peptidase
MMAA	8,54	0,000025	methylmalonic aciduria (cobalamin deficiency) cblA type
MRPL13	8,03	0,000001	mitochondrial ribosomal protein L13
MRPL16	33,05	0,000001	mitochondrial ribosomal protein L16
MRPL22	7,64	0,000001	mitochondrial ribosomal protein L22
MRPL30	12,85	0,000001	mitochondrial ribosomal protein L30
MRPL39	12,33	0,000001	mitochondrial ribosomal protein L39
MRPL4	5,91	0,000001	mitochondrial ribosomal protein L4
MRPL44	8,93	0,000001	mitochondrial ribosomal protein L44
MRPS11	5,7	0,000001	mitochondrial ribosomal protein S11
MRPS14	5,88	0,000001	mitochondrial ribosomal protein S14
MRPS15	7,23	0,000001	mitochondrial ribosomal protein S15
MRPS2	5	0,000001	mitochondrial ribosomal protein S2
MRPS26	5,78	0,000001	mitochondrial ribosomal protein S26
MTERF2	6,08	0,000001	mitochondrial transcription termination factor 2
MTERF3	6,7	0,000001	mitochondrial transcription termination factor 3
MUT	29,64	0,000001	methylmalonyl CoA mutase

NADK2	12,25	0,000001	NAD kinase 2, mitochondrial
NDUFA10	10,19	0,000001	NADH dehydrogenase (ubiquinone) 1 alpha subcomplex, 10, 42kDa
NDUFA9	8,05	0,000001	NADH dehydrogenase (ubiquinone) 1 alpha subcomplex, 9, 39kDa
NDUFAB1	20,76	0,000001	NADH dehydrogenase (ubiquinone) 1, alpha/beta subcomplex, 1, 8kDa
NDUFAF5	9,67	0,000001	NADH dehydrogenase (ubiquinone) complex I, assembly factor 5
NDUFAF7	7,12	0,000001	NADH dehydrogenase (ubiquinone) complex I, assembly factor 7
NDUFS1	17,96	0,000001	NADH dehydrogenase (ubiquinone) Fe-S protein 1, 75kDa (NADH-coenzyme Q reductase)
NDUFS2	11,62	0,000001	NADH dehydrogenase (ubiquinone) Fe-S protein 2, 49kDa (NADH-coenzyme Q reductase)
NDUFS7	6,23	0,000001	NADH dehydrogenase (ubiquinone) Fe-S protein 7, 20kDa (NADH-coenzyme Q reductase)
NDUFV1	17,6	0,000001	NADH dehydrogenase (ubiquinone) flavoprotein 1, 51kDa
NFS1	18,77	0,000001	NFS1 cysteine desulfurase
NIPSNAP1	5,64	0,000001	nipsnap homolog 1 (<i>C. elegans</i>)
NLRX1	5,89	0,000001	NLR family member X1
NNT	30,93	0,000001	nicotinamide nucleotide transhydrogenase
NUBPL	6,44	0,000001	nucleotide binding protein-like
NUDT13	5,38	0,000004	nudix (nucleoside diphosphate linked moiety X)-type motif 13
NUDT6	6,05	0,000176	nudix (nucleoside diphosphate linked moiety X)-type motif 6
OAT	8,86	0,000001	ornithine aminotransferase
OGDH	41,06	0,000001	oxoglutarate (alpha-ketoglutarate) dehydrogenase (lipoamide)
OGDHL	8,56	0,000001	oxoglutarate dehydrogenase-like
OMA1	19,09	0,000001	OMA1 zinc metallopeptidase
OPA1	23,49	0,000001	optic atrophy 1 (autosomal dominant)
OXA1L	5,53	0,000001	oxidase (cytochrome c) assembly 1-like

OXCT1	20,66	0,000001	3-oxoacid CoA transferase 1
PARS2	12,65	0,000001	prolyl-tRNA synthetase 2, mitochondrial (putative)
PC	41,85	0,000001	pyruvate carboxylase
PCCA	57,35	0,000001	propionyl CoA carboxylase, alpha polypeptide
PCCB	15,94	0,000001	propionyl CoA carboxylase, beta polypeptide
PCK2	16,37	0,000001	phosphoenolpyruvate carboxykinase 2 (mitochondrial)
PDE12	6,68	0,0016	phosphodiesterase 12
PDF	5,47	0,000001	peptide deformylase (mitochondrial)
PDHA1	13,67	0,000001	pyruvate dehydrogenase (lipoamide) alpha 1
PDHB	17	0,000001	pyruvate dehydrogenase (lipoamide) beta
PDHX	8,56	0,000001	pyruvate dehydrogenase complex, component X
PDSS2	22,06	0,000001	prenyl (decaprenyl) diphosphate synthase, subunit 2
PINK1	39,82	0,000001	PTEN induced putative kinase 1
PITRM1	26,94	0,000001	pitrilysin metallopeptidase 1
PMPCA	38,73	0,000001	peptidase (mitochondrial processing) alpha
PNPT1;LOC102723	11,75	0,000001	polyribonucleotide nucleotidyltransferase 1
POLDIP2	8,81	0,000001	polymerase (DNA-directed), delta interacting protein 2
PPA2	37,06	0,000001	pyrophosphatase (inorganic) 2
PPIF	10,34	0,000001	peptidylprolyl isomerase F
PPOX	5,29	0,000001	protoporphyrinogen oxidase
PRDX3	12,74	0,000001	peroxiredoxin 3
PUS1	5,84	0,000001	pseudouridylate synthase 1
PYROXD2	10,5	0,000001	pyridine nucleotide-disulphide oxidoreductase domain 2

RNMTL1	7,67	0,000001	RNA methyltransferase like 1
SCO1	8,15	0,000001	SCO1 cytochrome c oxidase assembly protein
SDHA	31,02	0,000001	succinate dehydrogenase complex, subunit A, flavoprotein (Fp)
SDHB	6,9	0,000001	succinate dehydrogenase complex, subunit B, iron sulfur (Ip)
SDHC	5,03	0,000001	succinate dehydrogenase complex, subunit C, integral membrane protein, 15kDa
SDHD	6,41	0,000001	succinate dehydrogenase complex, subunit D, integral membrane protein
SPG7	8,07	0,000001	spastic paraplegia 7 (pure and complicated autosomal recessive)
SPRYD4	7,96	0,000001	SPRY domain containing 4
SUGCT	19,55	0,000001	succinyl-CoA:glutarate-CoA transferase
SUOX	9,7	0,000001	sulfite oxidase
TARS2;MIR6878	11,85	0,000001	threonyl-tRNA synthetase 2, mitochondrial (putative)
TFAM	6,14	0,000001	transcription factor A, mitochondrial
TFB2M	6,39	0,000001	transcription factor B2, mitochondrial
THNSL1	20,72	0,000001	threonine synthase-like 1 (<i>S. cerevisiae</i>)
TIMM21	8,03	0,000001	translocase of inner mitochondrial membrane 21 homolog (yeast)
TK2	5,52	0,000001	thymidine kinase 2, mitochondrial
TMEM143	9,11	0,000001	transmembrane protein 143
TMEM177	5,65	0,000001	transmembrane protein 177
TMEM186	9,62	0,000001	transmembrane protein 186
TMEM70	6,74	0,000001	transmembrane protein 70
TMLHE	13,09	0,000001	trimethyllysine hydroxylase, epsilon
TRMT10C	17,21	0,000001	tRNA methyltransferase 10 homolog C (<i>S. cerevisiae</i>)
TRNT1	6,96	0,000001	tRNA nucleotidyl transferase, CCA-adding, 1

TRUB2	15,49	0,000001	TruB pseudouridine (psi) synthase family member 2
TSMF	10,9	0,000001	Ts translation elongation factor, mitochondrial
TST	6,35	0,000001	thiosulfate sulfurtransferase (rhodanese)
TXNRD2	20,87	0,000001	thioredoxin reductase 2
UNG	5,22	0,000001	uracil-DNA glycosylase
UQCRC2	5,29	0,000001	ubiquinol-cytochrome c reductase core protein II
UQCRFS1	8,03	0,000001	ubiquinol-cytochrome c reductase, Rieske iron-sulfur polypeptide 1
VWA8	11,64	0,000001	von Willebrand factor A domain containing 8
WBSCR16	19,77	0,000001	Williams-Beuren syndrome chromosome region 16
XPNPEP3	5,61	0,000001	X-prolyl aminopeptidase (aminopeptidase P) 3, putative
ZADH2	8,7	0,000001	zinc binding alcohol dehydrogenase domain containing 2

List of Abbreviations

Abbreviation	Full name
μCi	Microcurie
Afg3l1	ATPase family gene-3 like-1
AHA	L-Azidohomoalanine
ATP	Adenine-5'-triphosphate
CHX	Cycloheximide
CLIP	Crosslinking immunoprecipitation
CLUH	Clustered mitochondria (cluA/CLU1) homolog
DMEM	Dulbecco's Modified Eagle's medium
DMSO	Dimethyl sulfoxide
DPBS	Dulbecco's Phosphate-Buffered Saline
g	earth gravitational acceleration
HEK	Human embryonal kidney cell
kDa	Kilo dalton
M	Molar
mA	Miliampere
MEF	Mouse Embryonic Fibroblast
mg	Miligram
Min	Minutes
mM	Milimolar
mtDNA	Mitochondrial DNA
NEMP	Nuclear encoded mitochondrial protein
nM	Nanomolar
OPA1	Optic Atrophy 1
OXPHOS	Oxidative Phosphorylation
PBS	Phosphate buffer saline
PINK1	PTEN Induced Putative kinase
PNK	Polynucleotide Kinase
RIPA buffer	Radioimmunoprecipitation assay buffer
RNP	Ribonucleoprotein
RT	Room temperature
s	Second
siRNA	Small interfering RNA
TCA	Trichloroacetic Acid
WT	Wildtype

Acknowledgement

First of all, I would like to express my gratitude to Prof. Elena Rugarli, Prof. Aleksandra Trifunovic and Prof. Matthias Hammerschmidt for agreeing to be on my thesis committee. My special thank goes to Prof. Elena Rugarli for accepting me in her lab and letting me work on this super fantastic CLUH project.

Now, this is to all my dear colleagues who are really my friends. We worked together and shared so many moments of tears, laughter and excitement. We helped each other scientifically without any reservation and gave each other comfort during testing times. These are especially true for my CLUH gals Desi and Jette. You were never stingy in giving hugs, care and most importantly, scientific discussions over our beloved CLUH. To Shuaiyu and Nimesha, who are my “home” gals. We always went home together, shared jokes and occasionally went to a random restaurant just because “why not”. I thank for your support too, whenever I felt angry, weak or weary you are always there. And Shuaiyu, I thank you so much for always being patient with me and helping me with the mouse work, Apotome and discussion of mAAAs. And dear Anja, our little lab baby, you are always willing to help and support scientifically and personally. To Esther, thank you for always being there to support my work. Simon, almost all the time you managed to fool me with your pranks, but I think that you are really funny and I really enjoyed to work with you and shared the same office. Lastly, I would like to extend my immense gratitude to all the other current and past lab members namely Sara, Tania, Julie, David, Valentin, Arun, Eva, Paola and Guisse for being a part of this whole 4-year journey and helping me at all times. To Antonella, our new member of the lab, I am so lucky to have shared the office with you during the writing up time, thanks for your support!

Last but not least, I want to thank my dear parents, you gave me life, raised me up, supported me through all of these years without any reservation. I owe you so much and I really hope one day we could live together and I could see you and care for you more often. Pierre, my husband, I still remember when I told you that I will come to Cologne for PhD, you replied that there was a direct flight from Stansted to Cologne and that we

can make it. Thank you for always being there with me and always try to make me laugh. Like what I always say, you made me a better person.

亲爱的爸爸妈妈，感谢你们赐予我生命，守护我成长，这么多年来对我毫无保留的支持与呵护。我希望在不久的将来，我们可以住的很近，我可以像你们照顾我一般的照顾你们，关怀你们。

Eidesstattliche Erklärung

Ich versichere, dass ich die von mir vorgelegte Dissertation selbständig angefertigt, die benutzen Quellen und Hilfsmittel vollständig angegeben und die Stellen der Arbeit – einschließlich der Tabellen, Karten und Abbildungen –, die anderen Werken im Wortlaut oder dem Sinn nach entnommen sind, in jedem Einzelfall als Entlehnung kenntlich gemacht habe; dass diese Dissertation noch keiner anderen Fakultät oder Universität zur Prüfung vorgelegen hat; dass sie – abgesehen von unten angegebenen Teilpublikationen – noch nicht veröffentlicht worden ist sowie, dass ich eine solche Veröffentlichung vor Abschluss des Promotionsverfahrens nicht vornehmen werde. Die Bestimmungen der Promotionsordnung sind mir bekannt. Die von mir vorgelegte Dissertation von Professorin Dr. Elena Rugarli betreut worden.

Ort, Datum

Jie (Jane) Gao

Curriculum Vitae

PERSÖNLICHE DATEN

Name Jie (Jane) Gao

Geburtsdatum und -ort 20.10.1984 in Xinxiang, Henan, China

AUSBILDUNG UND BERUFLICHER WERDEGANG

June 2011 - Present

Ph.D

University of Cologne, Germany

2008 - 2011

Research Assistant

Medical Research Council, Mitochondrial Biology. Cambridge

2007 - 2008

M.Sc. Applied Molecular Technology

University of Nottingham

2003 - 2007

B.Sc. Biochemistry

University of Bath

PUBLIKATION

J. Gao, D. Schatton, P. Martinelli, H. Hansen, D. Pla-Martin, E. Barth, C. Becker, J. Altmueller, P. Frommolt, M. Sardiello, E. I. Rugarli. *J Cell Biol* 2014 Oct 27;207(2):213-23 **CLUH regulates mitochondrial biogenesis by binding mRNAs of nuclear-encoded mitochondrial proteins.**